UNIVERSITÄT PADERBORN
Die Universität der Informationsgesellschaft

FAKULTÄT FÜR
ELEKTROTECHNIK,
INFORMATIK UND
MATHEMATIK

Ein neuartiges autonomes Echtzeit-Lastüberwachungs- und -steuerungssystem in Mikronetzen auf der Grundlage von Fuzzy-Logik-Steuerung und drahtloser LoRa-Kommunikation

Von der Fakultät für Elektrotechnik, Informatik und Mathematik
der Universität Paderborn

zur Erlangung des akademischen Grades

Doktor der Ingenieurwissenschaften (Dr.-Ing.)

genehmigte Dissertation

von

Ibrahim Abdallah Mwammenywa, M.Sc.

Erster Gutachter: Prof. Dr.-Ing. Ulrich Hilleringmann
Zweiter Gutachter: Prof. Dr.-Ing. habil. Stefan Krauter

Tag der mündlichen Prüfung: 23 Mai 2024

Paderborn, 2024

Diss. EIM-E/381

UNIVERSITÄT PADERBORN
Die Universität der Informationsgesellschaft

FACULTY OF
ELECTRICAL ENGINEERING,
COMPUTER SCIENCE AND
MATHEMATICS

A Novel Autonomous and Real-time Load Monitoring and Control System in Microgrids based on Fuzzy Logic Control and LoRa Wireless Communication

From the Faculty of Electrical Engineering, Computer Science and Mathematics
Paderborn University

for obtaining the academic degree

Doctor of Engineering (Dr.-Ing.)

approved dissertation

from

Ibrahim Abdallah Mwammenywa, M.Sc.

First reviewer: Prof. Dr.-Ing. Ulrich Hilleringmann
Second reviewer: Prof. Dr.-Ing. habil. Stefan Krauter

Day of the oral exam: May 23, 2024

Paderborn, 2024

Diss. EIM-E/381

Paderborn University
Faculty of Electrical Engineering, Computer Science and Mathematics
Department of Sensor Technology

A NOVEL AUTONOMOUS AND REAL-TIME LOAD MONITORING AND CONTROL SYSTEM IN MICROGRIDS BASED ON FUZZY LOGIC CONTROL AND LORA WIRELESS COMMUNICATION

A Doctoral Dissertation Submitted in Fulfillment of the Requirements for the Degree of Doctor of Engineering in Electrical Engineering (*Dr.-Ing.*) of the Paderborn University

Ibrahim A. Mwammenywa

Paderborn, Germany

May 2024

ABSTRACT

The distributed microgrids based on Renewable Energy Sources (RES) offer a solution to the massive electricity shortage in Sub-Saharan Africa (SSA), especially in remote regions that are not connected to national grids. Nevertheless, RES-based microgrids suffer some reliability issues and experience frequent blackouts mainly due to microgrid instability. This is due to the intermittent nature of RES. Lack of proper load monitoring and control leads to loss of reliability and frequent power outages. To address this problem, the microgrids must be real-time monitored at distributed locations by cost-effective, high-accuracy, responsive systems to respond quickly to generation-consumption imbalances. Advancements in wireless sensor networks, particularly Long-Range Wide Area Networks (LoRaWAN), are leveraged to design an affordable and bidirectional wireless sensory network. This research work proposes a novel real-time load monitoring and control sensor system in microgrids. The system is based on Fuzzy Logic Controller (FLC) technique and Long-Range (LoRa) wireless communication technology. It manages imbalances between power generation and energy demand by setting a loading limit to a microgrid, based on the instant PV generation and State of Charge (SoC) of the battery energy storage system. The proposed system comprises a wireless low-power, a low-maintenance network of distributed power sensory modules for demand-side load monitoring and management. This study developed the prototypes of the system, and deployed it in a solar PV microgrid, in Silale village in Dodoma, Tanzania. The findings after the implementation of the developed system in the microgrid show that it is evidently possible to use a FLC-based traffic light for the load control to ensure a proper and achieve a real-time DSM, to avoid overloading in the microgrids. However, this research has also shown that some people would not willingly cooperate with this DSM technique. In further studies, the financial incentives and penalties should be considered and added to this developed FLC-based traffic light DSM technique so as to make more people conscious of following and responding to the traffic light signals. Furthermore, future studies should focus in integrating other monitoring and control systems such as weather forecasting, and load forecasting systems to this system in order to deliver a more reliable and robust solution.

Keywords: *Microgrid, LoRa network, LPWAN, Wireless Sensory System (WSS), Fuzzy Logic Control (FLC), Demand-side Management (DSM), power management*

Kurzfassung *(Abstract in German)*

Die dezentralen Mikronetze auf der Grundlage erneuerbarer Energiequellen (EE) bieten eine Lösung für den massiven Strommangel in den afrikanischen Ländern südlich der Sahara (SSA), insbesondere in abgelegenen Regionen, die nicht an die nationalen Stromnetze angeschlossen sind. Die auf erneuerbaren Energien basierenden Microgrids leiden jedoch unter Zuverlässigkeitsproblemen und häufigen Stromausfällen, die meist auf die Instabilität der Microgrids zurückzuführen sind. Dies resultiert aus der intermittierenden Natur der genutzten erneuerbaren Energiequellen. Das Fehlen einer angemessenen Lastüberwachung und -steuerung führt zu einem Verlust an Zuverlässigkeit und zu häufigen Stromausfällen. Um dieses Problem zu lösen, müssen die Mikronetze an dezentralen Standorten durch kosteneffiziente, hochpräzise und reaktionsfähige Systeme in Echtzeit überwacht werden, um schnell auf Ungleichgewichte zwischen Erzeugung und Verbrauch reagieren zu können. Fortschritte bei drahtlosen Sensornetzwerken, insbesondere Long-Range Wide Area Networks (LoRaWAN), werden genutzt, um ein kostengünstiges und bidirektionales drahtloses Sensornetzwerk zu entwickeln. In dieser Forschungsarbeit wird ein neuartiges sensorisches Echtzeit-Lastüberwachungs- und -steuerungssystem für Mikronetze vorgeschlagen. Das System basiert auf der Fuzzy-Logic-Controller-Technik (FLC) und der drahtlosen Long-Range-Kommunikationstechnologie (LoRa). Es verwaltet Ungleichgewichte zwischen Stromerzeugung und Energiebedarf, indem es auf der Grundlage der momentanen PV-Erzeugung und des Ladezustands des Batteriespeichersystems eine Belastungsgrenze für ein Mikronetz festlegt. Das vorgeschlagene System besteht aus einem drahtlosen, wartungsarmen Netzwerk verteilter Energiesensormodule zur Überwachung und Steuerung der Last auf der Nachfrageseite. In dieser Studie wurden die Prototypen des Systems entwickelt und in einem Solar-PV-Mikronetz im Dorf Silale in Dodoma, Tansania, eingesetzt. Die Ergebnisse nach der Implementierung des entwickelten Systems im Mikronetz zeigen, dass es offensichtlich möglich ist, eine FLC-basierte Ampel für die Laststeuerung zu verwenden, um ein ordnungsgemäßes und echtzeitfähiges DSM zu gewährleisten, um eine Überlastung in den Mikronetzen zu vermeiden. Diese Forschung hat jedoch auch gezeigt, dass es einige Personen gibt, die nicht bereit sind, mit dieser DSM-Technik zu kooperieren. In zukünftigen Studien sollten finanzielle Anreize und Strafen in Betracht gezogen und zu dieser entwickelten FLC-basierten Ampel-DSM-Technik hinzugefügt werden, um mehr Menschen dazu zu bringen, den Ampelsignalen zu folgen und auf sie zu reagieren. Darüber hinaus sollten sich künftige Studien auf die Integration anderer Überwachungs- und Kontrollsysteme wie Wettervorhersage- und Lastvorhersagesysteme in dieses System konzentrieren, um eine zuverlässigere und robustere Lösung zu bieten.

Schlüsselwörter: *Microgrid, LoRa-Netzwerk, LPWAN, Wireless Sensory System (WSS), Fuzzy Logic Control (FLC), Demand-side Management (DSM), Energiemanagement*

Ikisiri *(Abstract in Swahili)*

Maikrogridi zilizosambazwa na kujitegemea zinazotumia Vyanzo vya Nishati Mbadala (VNM) huleta suluhisho la uhaba mkubwa wa umeme, Kusini mwa Jangwa la Sahara (KJS), hasa katika maeneo yaliyoko mbali ambayo hayajaunganishwa na gridi ya taifa. Hata hivyo, maikrogridi zenye msingi wa KJS zinakabiliwa na changamoto kadhaa ikiwemo kukatika mara kwa mara kwa umeme hasa kutokana na kuyumba kwa uzalishaji umeme kwenye maikrogridi. Hii ni kutokana na asili ya vipindi vya VNM. Ukosefu wa ufuatiliaji na udhibiti sahihi wa mzigo husababisha kupoteza uaminifu na kukatika mara kwa mara kwa umeme. Ili kushughulikia tatizo hili, maikrogridi lazima zifuatiliwe kwa wakati sahihi katika maeneo ziliposambazwa kwa gharama nafuu, umakini wa hali ya juu, mifumo inayopokea ili kukidhi usawa katika matumizi ya kizazi cha sasa. Maendeleo katika mitandao ya kung'amua isiyo na waya, hususani Mitandao ya Maeneo Makubwa na Masafa Marefu (LoRaWAN) hutumiwa kubuni mtandao usiotumia waya wa bei nafuu na unaoelekea pande mbili. Kazi hii ya utafiti inapendekeza ufuatiliaji wa upakiaji kwa wakati mwafaka na udhibiti wa mfumo unaotumia mawimbi katika maikrogridi. Mfumo huu unatokana na mbinu ya Kidhibiti Mantiki cha Fuzzy (FLC) na teknolojia ya mawasiliano isiyotumia waya ya Masafa Mrefu (LoRa). Inadhibiti usawa kati ya uzalishaji wa nishati na mahitaji ya nishati kwa kuweka ukomo wa matumizi ya nishati kwa kuzingazia uzalishaji wa umeme jua na kiwango cha nishati kilichohifadhiwa kwenye mfumo wa betri. Mfumo unaopendekezwa unajumuisha mtandao usiotumia waya, nishati ndogo, matengenezo nafuu chini ya moduli-hisi za nguvu zinazosambazwa kwa ufuatiliaji na usimamizi wa upakiaji kulingana na mahitaji. Utafiti huu ulitengeneza mifano ya mfumo na kuusambaza katika gridi ya jua ya PV, katika kijiji cha Silale kilichoko Dodoma, Tanzania. Baada ya mfumo huu kutekelezwa na kuwekwa kijijini, matokeo yanaonyesha kuwa ni dhahiri na inawezekana kutumia taa ya trafiki yenye msingi wa FLC kwa udhibiti wa mzigo wa umeme kwenye maikrogridi, na unahakikisha kuwa ni njia ya wakati halisi ifaayo ya kuzuia upakiaji mwingi wa mzigo kwenye maikrogridi. Hata hivyo, utafiti huu pia umeonyesha kuwa kuna baadhi ya watu ambao hawatashirikiana kwa hiari na mbinu hii. Katika tafiti za baadaye, motisha na adhabu za kifedha zinapaswa kuzingatiwa na kuongezwa kwa mbinu hii iliyotengenezwa ya taa ya trafiki yenye msingi wa FLC ili kuwafanya watu wengi kufahamu kufuata na kuitikia mawimbi ya mwanga wa trafiki. Zaidi ya hayo, tafiti za siku zijazo zinapaswa kuzingatia kuunganisha mifumo mingine ya ufuatiliaji na udhibiti kama vile utabiri wa hali ya hewa, na kupakia mifumo ya utabiri kwa mfumo huu ili kutoa suluhisho la kuaminika na thabiti zaidi.

Maneno muhimu: *Mikrogridi, mtandao wa LoRa, LPWAN, Mfumo wa Kung'amua Usio na Waya (WSS), Udhibiti wa Mantiki wa Fuzzy (FLC), Usimamizi wa Mahitaji (DSM) na usimamizi wa nishati.*

DECLARATION

I, **Ibrahim A. Mwammenywa,** do hereby declare to the Senate of the Paderborn University that this dissertation is my original work and that it has neither been submitted nor is concurrently submitted for degree award in any other institution. I have completed this doctoral dissertation titled "*A Novel Autonomous and Real-time Load Monitoring and Control System in Microgrids based on Fuzzy Logic Control and LoRa Wireless Communication*" independently and only with the aid of the designated tools. All parts of the work, which are taken from other printed works or works available on the Internet, either in wording or in spirit, have been identified by precise reference to the source.

Ibrahim A. Mwammenywa

Paderborn, 27.05.2024

Place and Date

ACKNOWLEDGEMENT

First and foremost, I would like to show gratitude to my God almighty for giving me this wonderful opportunity to undertake this research work to completion by providing me with the right people and resources at the right time. All is due to His sufficient grace in my life. To God be all the glory!

I deeply thank my family, especially my wife, Florah, and our children, Rehoboth-Ruth and Caleb-Isaac. My gratitude is extended to my parents as well, my father, Abdallah Mwammenywa, and my mothers, Eligrace Korosso and Joyce Bogwe for their encouragement and prayers without ceasing.

Despite this dissertation carrying a single author name, the successful completion of this work involves a combination of dedicated efforts of several parties and individuals. I would also like to express my sincere appreciation and gratitude to the following for their support, help, and valuable contribution during the whole research period.

Prof. Dr.-Ing. Ulrich Hilleringmann, for an opportunity to recruit me in his research group, the Sensorik department at Paderborn University. He diligently and closely worked with me from the very beginning of this research work, starting from the research proposal development, throughout the research work, and lastly in the production of this dissertation. My gratitude is extended to all other staff members of the Sensorik department (Dmitry Petrov, Dennis Drude, Mark Kagarura, Joseph Sisala and Sabine Schleghuber), and Masters students and assistants (Phillip Holle, Oscar Elysee, Nisha Shilpakar and Asif Iqbal) for their participation in improving my work through their constructive comments, support, and criticism where required.

The University of Dar es Salaam (UDSM), and the government of the United Republic of Tanzania for granting me a 3-year study-leave that enabled me to pursue my Ph.D. studies in a foreign country, Germany. The study-leave enabled me to easily undertake my research work and complete it within the required time.

The German Federal Ministry of Education and Research (BMBF) for adequate financial support through the project (Grant: 03SF0607B A:RT-D Grids). The finances were very important to cover both my living costs in Germany and research costs during the designing, prototype development, and field deployment of modules during the data collection. The entire project team worked with me hand-to-hand in every phase of the project which positively

contributed to the completion of this dissertation work. Thanks to Prof. Dr.-Ing. Stefan Krauter, Prof. Dr.-Ing. Katrin Temmen, Prof. Dr.-Ing. Joachim Böcker, Prof. Dr. Christine Freitag, Prof. Dr. Burkhard Hehenkamp, Henrik Bode, Teddy Mangeni, Donna Nammuju, Godiana Philipo, Josephine Kakande, Henrietta Acquah, Irene Ngoti, Paul Bogere, Henry Asiimwe, and the project coordinator, Mr. Tobias Klaus.

Lastly, the leadership and people of Silale village in Dodoma Tanzania, for allowing this research to use their microgrid as the case study. They allowed the installation of consumer modules in their houses and supported this research work. The technicians, David Job, Bernard Semango, and Amos Marandu who were always present hand-to-hand at the microgrid and in the village entirely.

May my almighty God bless you all with both heavenly and earthly abundant blessings!

Ibrahim A. Mwammenywa
Paderborn, May 25, 2024

DEDICATION

This work is entirely dedicated to the Kingdom of God, through Christ Jesus, and to my family. Moreover, my children, Rehoboth-Ruth and Caleb-Isaac should use this work as an inspiration to exploit and achieve even bigger targets than a Doctoral degree.

TABLE OF CONTENTS

LIST OF TABLES

LIST OF FIGURES

LIST OF APPENDICES

LIST OF ABBREVIATIONS

ACRONYM	DEFINITION
ADC	Analog-Digital Converter
AfDB	African Development Bank
AI	Artificial Intelligence
AMI	Advanced Metering Infrastructure
ANN	Artificial Neural Network
BS	Base Station
BW	Bandwidth
CC	Coulombs Counting
CF	Carrier Frequency
CMP	Capacity Market Program
CR	Coding Rate
CSS	Chirp Spread Spectrum
DLC	Direct Load Control
DoD	Depth of Discharge
DR	Demand Response
DSM	Demand-side Management
DSR	Design Science Research
EDA	Electronic Design Automation
EDR	Emergency Demand Response
EE	Energy Efficiency
EMU	Energy Management Unit
EU	Europe Union
EWURA	Energy and Water Utilities Regulatory Authority
FIS	Fuzzy Inference System
FLC	Fuzzy Logic Controller

GPRS	General Packet Radio Service
GSM	Global System for Mobile Communication
GUI	Graphical User Interface
HEMS	Home Energy Management System
HSPA	High-Speed Packet Access
I2C	Inter-Integrated Circuit
IC	Integrated Circuit
ICSP	In-Circuit Serial Programming
IDE	Integrated Development Environment
IEA	International Energy Agency
IMS	Intelligent Metering System
IO	Input/Output
IoT	Internet of Things
IRP	Integrated Resources Planning
ISM	Industrial, Scientific and Medical
ISP	Internet Service Providers
ITU	International Telecommunication Union
JSON	JavaScript Object Notation
LCD	Liquid Crystal Display
LED	Light Emitting Diode
LoRa	Long-Range
LoRaWAN	Long-Range Wide Area Network
LPWAN	Low-Power Wide Area
LS	Load Shifting
LTE	Long-Term Evolution
MAC	Media Access Control
MCU	Microcontroller Unit
MDMS	Meter Data Management Systems
ML	Machine Learning

MNOs	Mobile Network Operators
MPPT	Maximum-Power-Point-Tracking
NB-LTE	Narrow Band Long-Term Evolution
OCV	Open Circuit Voltage
OS	Operating System
PC	Personal Computer
PCB	Printed Circuit Board
PHP	Hypertext Preprocessor
PLC	Power Line Communication
PMIC	Power Management Integrated Circuit
PTP	Peak Time Pricing
PU	Processing Unit
PV	Photovoltaic
RDBMS	Relational Database Management System
REA	Rural Energy Agency
REP	Rural Electrification Program
RESs	Renewable Energy Sources
RF	Radio Frequency
RTP	Real-Time Pricing
SDGs	Sustainable Development Goals
SF	Spreading Factor
SG	Smart Grid
SLG	Strategic Load Growth
SM	Smart Meter
SMS	Short-Messages Service
SMT	Surface-mount Technology
SNR	Signal-to-Noise Ratio
SoC	State of Charge
SPI	Serial Peripheral Interface

SPP	Small Power Producers
SQL	Structured Query Language
SSA	Sub-Saharan African
TANESCO	Tanzania Electric Supply Company
THT	Through-hole Technology
ToU	Time-of-Use
TP	Transmission Power
USB	Universal Serial Bus
VAS	Value-Added-Service
VSPP	Very Small Power Producers
Wi-Fi	Wireless-Fidelity
WSN	Wireless Sensor Network
XAMPP	Cross-platform, Apache, MySQL, PHP and Perl

CHAPTER ONE

INTRODUCTION

1.1 Background of Study

Electricity is a precious commodity that has become the key driver of economic and technological development; without it, most technologies are limited or unusable [1, 2]. It is no different in Africa, as electricity has been so essential for its gradual development. However, it is an open secret that there is a day-to-day increase in electricity demand in Africa, particularly in Tanzania. It is due to the massive growth in population and industrialization which is currently taking place. The International Energy Agency (IEA) report 2018 stated an average annual global power demand increase of 4% over the past five years [3].

Conventional power grids have been massively employed for electrification in almost all Sub-Saharan African (SSA) countries, including Tanzania. However, more than 90% of people in SSA still do not have a reliable access to electricity, as shown in Fig. 1 [3]. For instance, in Tanzania, only 40% of the households are electrified, of which 75% are connected to the national grid, and the rest primarily depend on diesel engines and solar power [4]. Many households in rural areas are far from the national electric grid; thus, they cannot afford the electricity connection cost, which is unbearable.

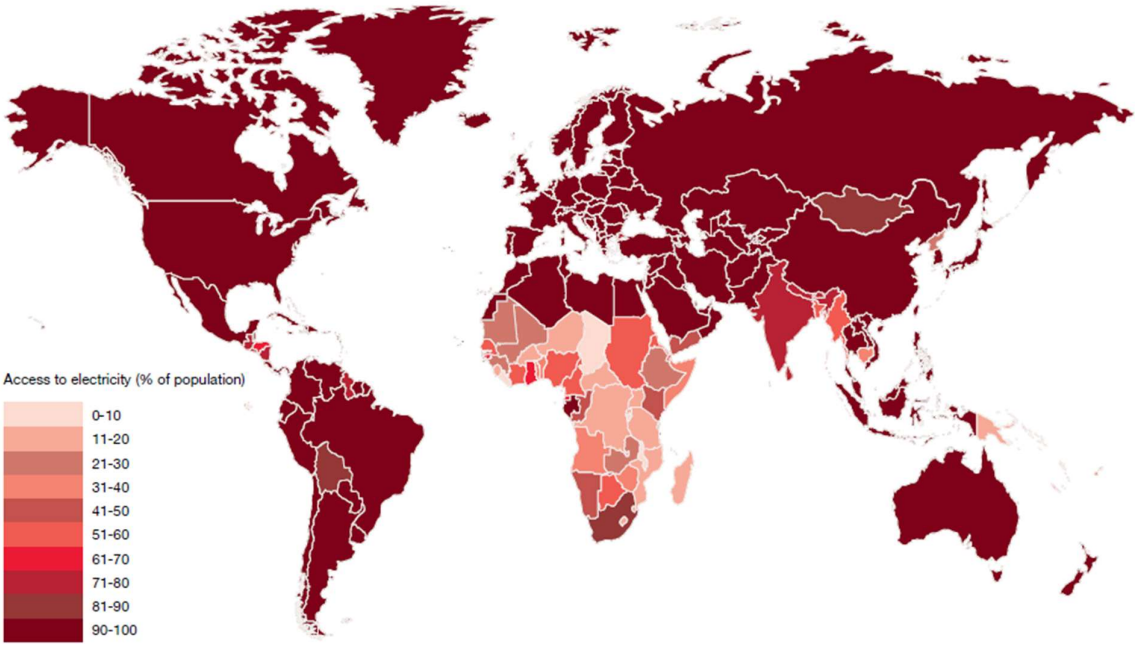

Fig. 1: Electrification world map [5]

In 2015, the United Nations General Assembly set the global Sustainable Development Goals (SDGs), with goal number 7 being to ensure access to affordable, reliable, sustainable modern energy for all [6]. To achieve this goal, the governments in the SSA region deliberate increasing the energy access rate as among the significant goals. The objective is to attain a higher energy access rate via the deployments of communities' mini-grids, especially those based on Renewable Energy Sources (RESs), such as solar, wind, biomass, and hydropower [7].

Recent advancements in telecommunications, such as the Internet of Things (IoT), and electric power generation technologies, especially with RESs, have led to new electric infrastructures; the smart electric grids [8]. This development has included information technologies into independently distributed microgrids made up RESs such as solar PV. These microgrids have emerged as an alternative, viable, and affordable electrification solution in remote and rural areas [9, 10]. For instance, in Tanzania, the deployment of microgrids has been accelerated by the government's political will to electrify the country from 36% in 2014 to 50% in 2025 and at least 75% of households by 2035 [11]. The government's target has been a result of policy changes, as well as the introduction of the Small Power Producers (SPP) framework, the Rural Energy Agency (REA) for rural electrification, and the ambitious plan to enhance power generation significantly over the next two decades [12, 13]. By using the mini- and microgrids, the government can attain that goal. It was projected by the International Energy Agency in 2014 that about 40% of the new and cost-effective electrical power connections would be of microgrids to achieve universal electrification in Africa [3]. With these distributed independent microgrids, most households in rural areas now have the luxury of accessing electricity.

However, microgrid-based electricity supply in rural areas is characterized by frequent blackouts and unreliability due to the intermittent nature and the stochastic behaviour of RES [14]. Lack of adequate real-time monitoring and controlling mechanisms to nullify the effects of the intermittent nature of RES leads to microgrids experiencing many imbalances and power outages [7, 14, 15]. This lack of reliability has contributed to the low performance of these microgrids as faults are not arrested in real-time, contributing to microgrid system failures [7].

This research aims at employing the advancements in IoT and wireless communication technologies to develop a robust, autonomous, and low-cost wireless sensor system for load monitoring and controlling the power utilization in microgrids. The developed system of consumer modules is based on Long-Range Wide Area Network (LoRaWAN), which monitors each consumer's load and sends the readings to a host computer of the microgrid using a distributed wireless sensor architecture. The system ensures proper and real-time demand-side

management (DSM) to avoid overloading in the microgrid. It may be integrated with other monitoring and control systems to provide a reliable microgrid operation.

1.2 Problem Statement

The monitoring of electrical networks in rural microgrids has been an enormous challenge. Most distributed private-owned microgrids in SSA, particularly in Tanzania, do not have a reliable system for monitoring the power quality parameters such as current, voltage, phase, and frequency. They do not control the load demand and power consumption [16]. Due to the lack of such monitoring and control systems, the microgrids frequently face operation failures, as maintenance is only limited to corrective measures [7]. The lack of intelligent and effective systems for monitoring power quality parameters and load control has led to unstable and unreliable microgrids. Frequent blackouts characterize these microgrids with low-quality power supply showing varying electrical parameters such as frequency and voltage (i.e. over-voltage and/or under-voltage).

Moreover, overloading is another critical problem in rural microgrids in SSA. Load-generation imbalances primarily cause overloading due to a lack of coordination between the actual power generated with the overall power demand. The load-generation imbalances are due to rural microgrids' lack of load monitoring and control systems [17]. The load-generation mismatch leads to frequent power outages, resulting in an unreliable power supply in microgrids. Without the load-demand management and control system, the microgrids are not properly and optimally utilized [18]. Therefore, to attain the load-generation balance for a reliable electricity supply in microgrids, there is a need to monitor the load demand from all connected consumers individually in real-time and to control the total load in microgrids [19, 20].

Furthermore, without load monitoring and control systems, electric power consumers are unaware of their load demand and power utilization [21]. This situation leads to some complaints in bill payments and the implementation of different tariffs. For example, some of the microgrids' customers are charged flat-rate tariffs, which has accounted for complaints from customers as they feel they consume power differently from each other [18]. In conclusion, a system for monitoring power consumption is lacking. Additionally, communication with the customers on their consumption behaviour is missing.

1.3 Proposed Solution: System Architecture

This research study proposes a wireless sensory system comprising consumer modules and a host computer, as shown in Fig. 2. The consumer modules will be installed for all consumers for load monitoring, control, and tariff management. The host computer manages the load demand versus available microgrid power (both, generated and stored energy).

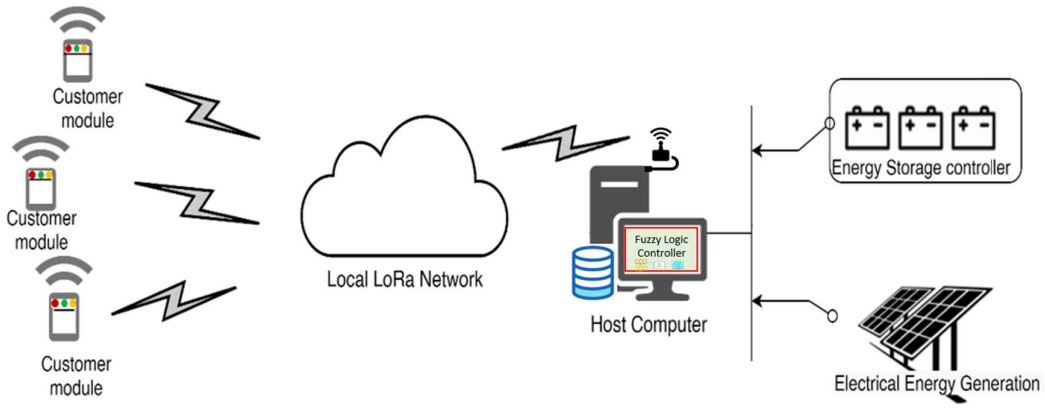

Fig. 2: Proposed system architecture

Fig. 3 explains the proposed system architecture in the block diagram. The consumer modules measure and wirelessly transmit a load of each consumer to the host computer. The host computer sums the total load from all the consumer units and compares it with the total power generated and stored in batteries as State of Charge (SoC) in real-time. From the actual status of the available power, the host computer wirelessly broadcasts a control signal to all consumers to advise on power consumption, providing real-time usage control. The Long-Range (LoRa) wireless communication technology, which provides a Low Power Wide Area Network (LPWAN) wireless communication, is proposed in this research study for data communication between consumers and the host computer.

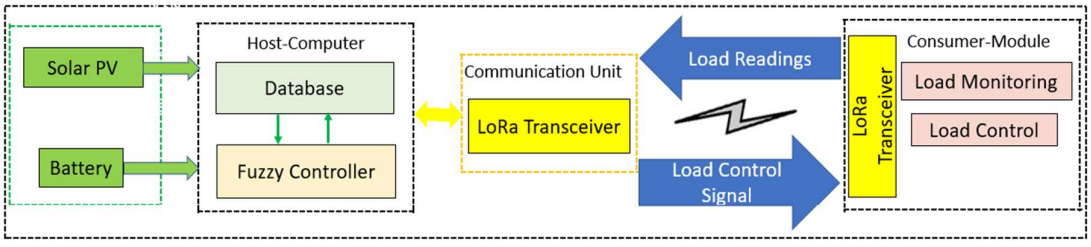

Fig. 3: Proposed system block diagram

The power usage control signal is associated with a tariff, such that the consumer is charged higher during the time of low-power generation compared to the charges during the high-power generation time. The real-time comparison of the load demand to the power generation and energy stored is essential for avoiding load-generation imbalance and therefore thwart any overloading of the microgrid. The system works on the real-time pricing (RTP) principle based on tariff-based Demand-Side Management (DSM) to avoid microgrid overloading and, subsequently, the possibility of power blackouts.

1.4 Research Objectives

1.4.1 General Objective

The main objective of this research is to design and develop a real-time load monitoring and control system in a microgrid based on Fuzzy Logic Controller (FLC) and LoRa Wireless Communication. The system is robust and autonomous, with a low-cost communication technique for load monitoring and controlling the power utilization in a microgrid. This system should ensure proper and real-time demand-side management (DSM) to avoid overloading in the microgrids. The system should be capable of data transmission within a range of 1 km to 2 km, which is the typical radius of rural villages.

1.4.2 Specific Objectives

The specific objectives of this research are;

(i) To analyse the actual state of need of the load monitoring and control system.

(ii) To identify and establish the requirements for the wireless sensor system for load monitoring and control in microgrids.

(iii) To design and develop a sensory unit for load monitoring for each consumer.

(iv) To design and develop a low-power, long-range radio transmission system for bidirectional data transmission between the consumer-modules and the host computer of a microgrid.

(v) To design and develop a load control mechanism based on real-time PV generation and SoC.

(vi) To deploy, validate and analyse the performance of the developed wireless sensor system in monitoring and load control in a microgrid (using a real existing microgrid).

1.5 Research Design

The research design involves all the approaches and methodological structures employed during the studies. These approaches are applied to find the answers to research questions and achieve the research objectives. Research design outlines everything that must be done, starting with formulating research questions (or problem statements) through the methodological implementation of the research study to the final analysis of the results that provide the solution to the research problem [22].

This research study uses the Design Science Research (DSR) approach. DSR approach is considered suitable for engineering research with socio-implication and applications involving the scientific knowledge base [23]. Fig. 4 details the SDR approach as explained by [23]. This research study is based mainly on the central design cycle; nonetheless, it covers the whole DSR approach, from Relevance Cycle, through Design Cycle to Rigor Cycle.

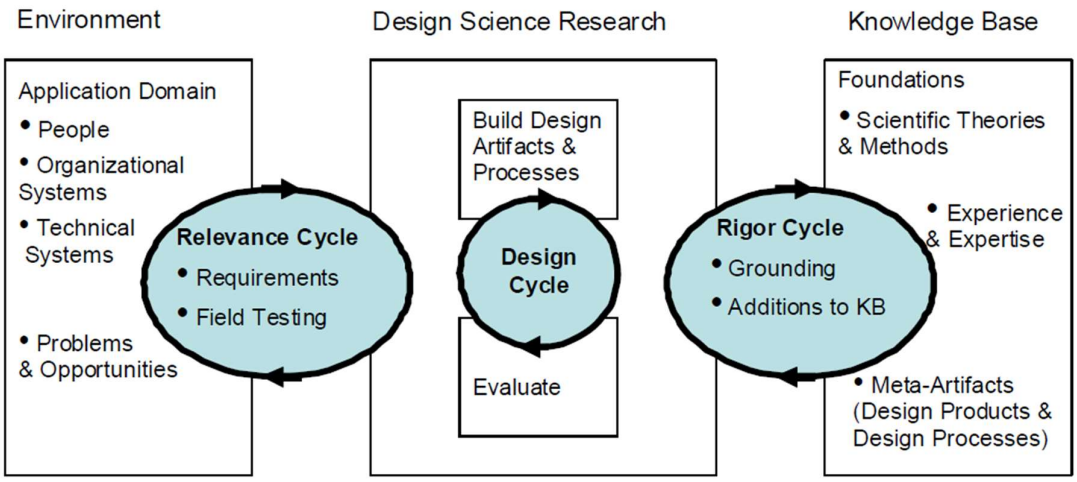

Fig. 4: Design Science Research (DSR) cycles [23]

The Design Cycle is a tight loop of designing and building prototypes concerning the research questions and objectives. Furthermore, in this cycle, the designed and developed prototypes are tested and evaluated to find different gaps and ways to perfect the solution before being drafted into the natural working environment. The prototype development and lab tests were carried out in the Sensorik-Laboratories at the Paderborn University in Germany in this research work.

This study uses the Relevance Cycle approach to collect input requirements from the contextual environment, such as an existing microgrid network and its operations. Moreover, after the completion of the prototype design and development, the Silale Community Microgrid in Tanzania was used as the field-testing ground.

The Rigor Cycle offers the background knowledge, previous scientific methodologies, and findings used as a foundation or stepping-stone while conducting this research study. Moreover, with the successful completion of this study, this research would add to the growing knowledge of electrical engineering, especially in the area of applications of wireless sensor technologies in electric grids.

Fig. 5 shows the delineation of all steps taken in this research study. Different methodological steps were employed in this study, starting from the literature review, field data collection, prototype designing, development, and testing to the final commissioning of the developed system.

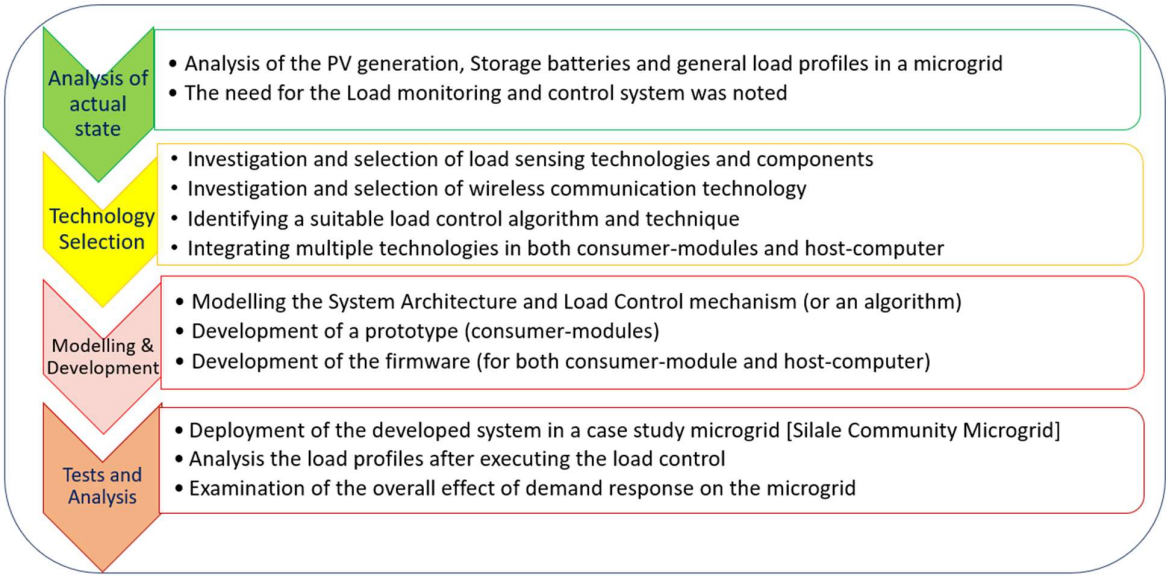

Fig. 5: Research framework

1.6 Rationale of Study

There is an increasing interest in deploying electric microgrids in Africa, particularly in Tanzania. It is caused by microgrids' potential for achieving a flexible, reliable, and efficient electricity supply to off-grid communities, among other economic benefits. Having multiple microgrids has caught the attention of researchers to develop different solutions to different challenges facing the microgrids as well as optimizing the cost and efficiency. One area which has been looked upon is the ability of microgrids to self-monitor and control load.

This research employs a Wireless Sensor Network system as a robust, autonomous, and cost-effective solution to control and monitor the grid parameters. Wireless sensor network technology has been actively and extensively applied in environmental monitoring, smart control of domestic appliances, wildfire detection, health monitoring, and precision agriculture areas, to name a few. The applications mentioned give the confidence that the Wireless Sensor Network technology can also be used to monitor and control the microgrids' load. This is also fuelled by the ability of wireless sensors to standalone operations (i.e. operate without a need for human intervention) for years [24].

1.7 Significance of Study

The monitoring and control systems in microgrids play an important role in ensuring the power system functions effectively and efficiently [25]. It helps minimise unexpected power outages, whereas the monitoring system provides the platform to facilitate the detection and troubleshooting of any technical problem in the microgrid. Therefore, with the load monitoring and control system proposed in this study, the microgrid will have enhanced reliability by enabling the service vendors to maintain the quality of electricity based on the balance between generation and load demand to avoid blackouts. With this proposed system, even power theft and/or overload can easily be detected before it affects the sustainability of the microgrid.

Microgrid utility companies can use the information the monitoring system collects to plan the current situation and future grid expansions at low investment costs. With the real-time monitoring data, the utility company can as well improve the billing and revenue collection and realize the profit of running the microgrid [26]. Moreover, not only the microgrid utility companies will benefit from such a system, but also the government can use the same data while planning and expanding the national grid and/or integrating the microgrids into the national grid.

The bidirectional flow of information can also help shape the customers' power-usage behaviour. The customers will become aware of how they consume electricity. It eventually helps them to use electricity based on necessary needs and economic status. In total, it can help customers economically [27, 28]. Furthermore, this system can be used as the catalyst in cultivating utility-customer collaboration in properly utilising electrical energy resources for socio-economic development [15]. These can be considered as the Value-Added-Service (VAS) from the microgrid utility companies to their customers [16, 29].

Additionally, the study will contribute to the fields of smart-grid and wireless sensor network systems. This research will provide another building block for applying sensors to control and monitor electric grids smartly. Despite much research in the electric grid and wireless sensor networks and technologies, this research will add more knowledge to the academic community. The knowledge can be helpful in the electrical engineering arena for both academic researchers and field engineers.

1.8 Chapter Summary

This chapter sets the tone for this dissertation. It provides a general introduction to the research study. The introduction to this dissertation has opened up the research problem statement, research-specific objectives, and the general significance of this research study. The subsequent chapters will explain in-depth the literature involved in this research and the methods and materials used in designing and implementing the wireless sensor network system for load monitoring and controlling the microgrid. Furthermore, this dissertation will give an in-depth discussion of the results obtained from the research, together with a conclusion and recommendations.

CHAPTER TWO

LITERATURE REVIEW

2.1 Introduction

This chapter analyzes literature related to this research study. This literature has been collected from different sources such as books, journal and conference articles, and official reports. The literature has given a detailed explanation of the meaning and structure of the microgrid, as well as examining the role of microgrids in SSA by taking the case of Tanzanian. Furthermore, wireless sensor technologies, wireless communication systems, and different Demand Side Management (DMS) techniques have been studied and evaluated concerning the objectives of this research study. Lastly, similar projects were also studied to have building blocks in implementing this research study and close the technological gaps left behind in those studies.

2.2 Microgrid Concept

2.2.1 Definition of Microgrid

The term 'Microgrid' has been defined in various ways by scholars working in electrical engineering fields, with all of them defining the microgrid as a smaller version of the electric power grid [7]. For the context of this study, Microgrid is defined as the arrangement of the electrical system made up of electrical energy source(s) and the loads, whether being connected in the existing grid (the on-grid connection mode) or as the stand-alone grid system (off-grid connection mode) [7]. This interconnection of electrical loads and distributed electrical energy sources must be confined to a defined electrical boundary [30].

Fig. 6 explains the simple schematic of a solar/wind hybrid microgrid. Solar and wind are renewable energy sources converted to electric energy using solar PV cells and wind turbines, respectively. The microgrid also has a battery power bank for energy storage. The energy stored in the battery is usually used when there is insufficient power generation from solar PV and wind turbines. Moreover, the microgrid can have a diesel generator for backup power generation during times without enough sunlight and wind speed to generate sufficient electrical energy.

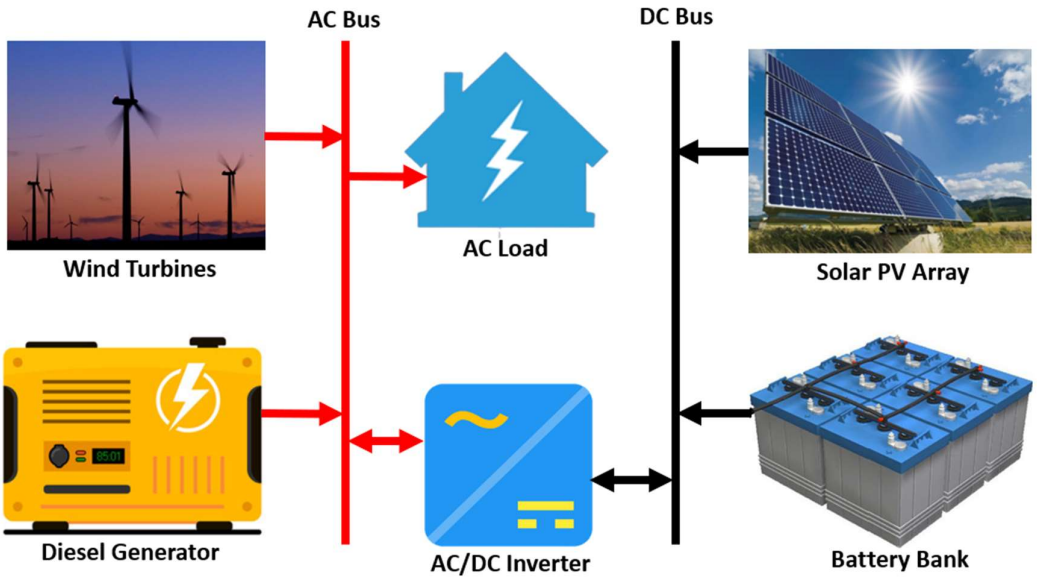

Fig. 6: Decentralized solar-wind hybrid microgrid

Microgrids are classified based on the size of the power generated. They are categorized into scales such as mini, small, medium, and large grids with generated electric power capacities of 0.001–0.005 MW, 0.005–5 MW, 5–50 MW, and 50–300 MW, respectively [31, 32]. [33] reviewed different studies to define the microgrid as a decentralized power plant with an independent generation system and a local distribution network of about 2 MW in capacity. It utilizes one or multiple energy sources such as solar, biomass, hydro, wind, and diesel generators.

A microgrid can be made of either conventional energy sources (such as fossils, i.e. combustible fuels and gases) or the RESs (such as solar, wind, thermal, biomass, and hydro energies sources) [34]. The application of RES-based microgrids has attracted growing interest worldwide due to its potential for realizing flexible, efficient, and smart electrical grid systems. Currently, there is advocacy towards the employment of RESs due to their low carbon emission, which is environment-friendly. Reducing carbon emissions is the 13th global Sustainable Development Goal (SDG) [35]. Therefore, RES-based microgrids are proving to be an electricity generation option for now and future as the advocate for an environmentally-friend low-carbon future.

Furthermore, RES-based microgrids lead to access to cheap and affordable electricity compared to fossil sources. Almost all RESs are free, inexhaustible, non-perishable, and environmentally pollution-free [36]. With RES-based microgrids, the goal of supplying electricity to off-grid and rural villages, together with its economic benefits, a once-distant

dream is becoming a reality [37]. This has well resulted in socioeconomic development in rural communities [38].

For low and medium-sized loads, such as rural and local households, using electricity from the microgrids provides a more viable option than the main grid extension. For instance, decentralized microgrids can be easily monitored, controlled, and managed without using complex systems. Compared to the central main grid, microgrids can operate 24/7 by offering a power capacity suitable for their rated loads and applications [39]. These potentials have impressed stakeholders such as policy-makers in governments and producers, making the mini-grids promising electrical systems for the present and future [7, 40].

Nevertheless, the employment of RESs in electrical grids poses a natural challenge. The RESs are intermittent in nature and hence unreliable. The RESs depend on the variation in weather conditions [41, 42]. Yet, with all the challenges of using RESs in electricity generation, the RESs are seen as the way forward for global electrification towards equal access to affordable and clean energy for all. Different research studies and developments have been carried out and are ongoing to fully realize and utilize the potential of using RES for electric power generation. Researches focus on monitoring and managing the microgrids to improve the reliability and efficiency of accessing electrical energy. [43] emphasized the role of having monitoring systems for microgrids to attain their full potential and avoid failures.

2.2.2 Role of Microgrids in Rural Electrification: Case of Tanzania

According to Tanzania's[1] Power System Master Plan 2020, the national electric grid only supplied 1,120 MW in 2019 compared to the short-term need capacity of 3,971.4 MW [44]. Fig. 7 depicts the national grid map for Tanzania. The map shows the existing connected regions (with the solid line, with each line colour having a different capacity). More than 50% of the country is not connected to the national grid, even with the connections just projected (the dotted lines) with a long-term plan of up to the year 2044 [44].

About 64% of the power generated and fed into the national grid is due to hydropower plants [45]. The generation was sorely dependent on the amount of rain and failed to reach its total capacity during the dry seasons. Therefore, in 2006, the Tanzanian government, through its utility company, Tanzania Electric Supply Company (TANESCO), went for the deployment of

[1] The United Republic of Tanzania (herein referred to as Tanzania), is situated in the East-Africa region. Tanzania has an approximate population of more than 60 million people, covering an area size of 945,087 square kilometers.

natural gas and diesel (i.e., heavy fuel oil) as other sources for electricity generation [36]. However, these sources are not sustainable, expensive and economically hinder the expansion of the grid into the country, going to the rural areas. With the current national grid network, the rural areas have been left behind without any supply of clean energy sources, particularly electrical energy.

With more than 70% of the Tanzanian population living in rural areas and having no access to the national electric grid, there is a huge need for rural electrification. Currently, the primary energy source in rural areas is biomass, for about 88%, in the form of firewood and charcoal [46].

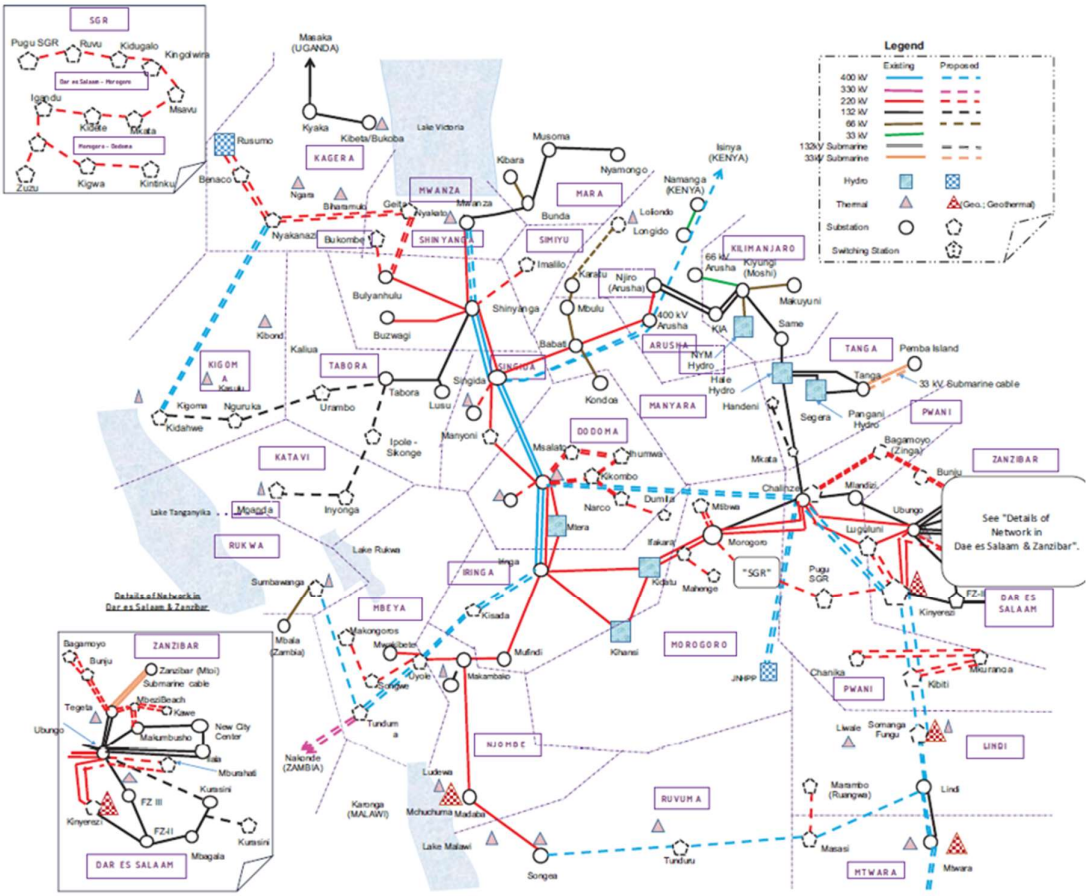

Fig. 7: Tanzania's national grid map [44].

However, the government of Tanzania set the Rural Electrification Program (REP) of 2013-2022. The goal of REP is to ensure an increase in rural electrification, such that access to electricity should increase to at least 75% of the rural population by 2033 [47]. The attention has been turned to establishing decentralised RES-based microgrids fully supported by government policies and frameworks [12, 45] to achieve the goal.

Currently, there is a massively growing interest in deploying microgrids in different communities in Tanzania, especially in rural areas. The interest is due to the microgrids' potential of employing RESs in supplying electrical energy to off-grid communities for their socio-economic development. Due to its geographical position, Tanzania is blessed with the potential of untapped RESs such as solar, wind, biomass, and hydro sources. The Energy and Water Utilities Regulatory Authority (EWURA) in Tanzania reported that by 2017, there were at least 109 registered microgrids in Tanzania, as shown in Fig. 8 [48]. These microgrids have a rated capacity of 248.64 MW while serving more than 184,000 customers (including households). The installed capacity of 245.439 MW comes from licensees who generate electricity for their own use, such as in the manufacturing and mining industries. In comparison, only a capacity of about 3.2 MW comes from Very Small Power Producers (VSPP) for rural communities through mini and microgrids. Fig. 9 below shows the geographical distribution of the microgrids in Tanzania.

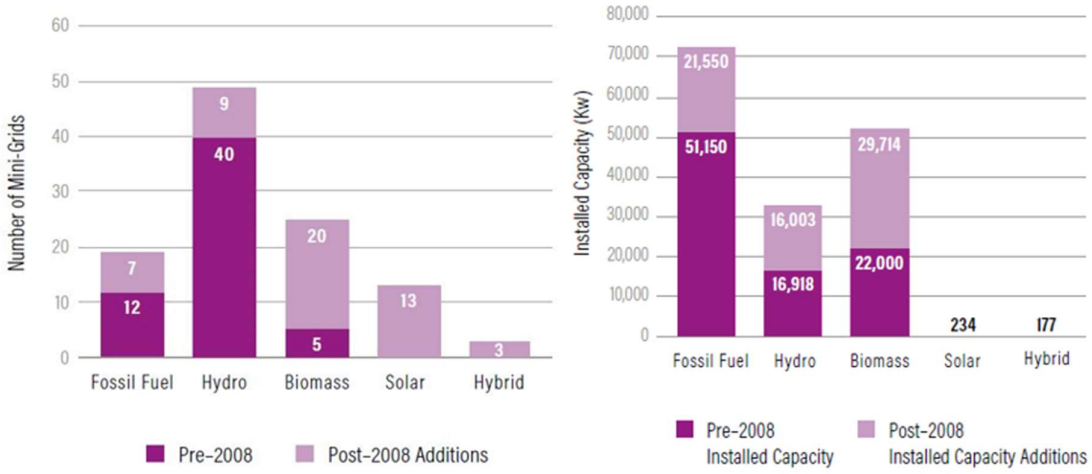

Fig. 8: Number of registered microgrids by 2017 [48].

Different local and international programs have supported multiple microgrid projects, such as the GMG MDP initiative by S4All implemented through African Development Bank (AfDB), the Sida and DfID joint support, iTEC, and others [16, 18]. There are also some reputable microgrid operators such as Power-Gen, Devergy, ELICO foundation, Jumeme Electrical, and Ensol, whose projects connect many rural households in Tanzania [49]. The availability of these microgrids has contributed strongly to socio-economic activities such as fostering the milling, welding, carpentry, and other small businesses in rural areas hence the rural development [18].

However, like other microgrid systems, these systems in Tanzania face similar challenges like their incapability to ensure reliability due to their dependence on the weather conditions and the ever-intermittent nature of RESs. It has resulted in unnecessary power blackouts due to power demand and supply imbalances in some microgrids in Tanzania [18]. This research works on developing such a load monitoring and control system for solar-based microgrids in Tanzania.

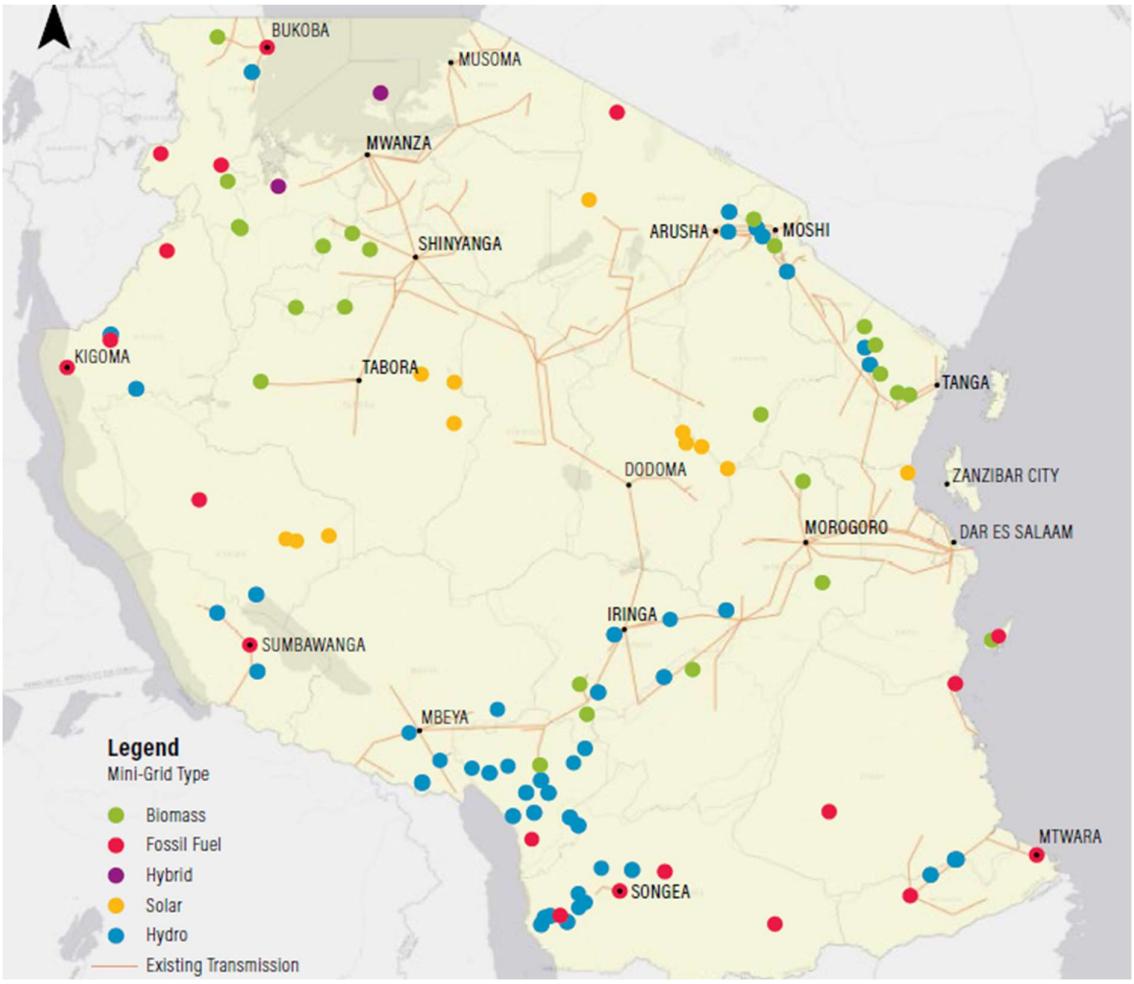

Fig. 9: Registered microgrids centers in Tanzania [4]

2.3 Demand-Side Management and Demand Response

Electrical power systems face continually changing power consumption requirements with a constant need for a satisfactory level of reliability, quality, and environmental friendliness. It is estimated that the global electricity demand will increase by more than 50% of the present

demand by 2030 [50]. Nonetheless, overcoming this challenge is becoming increasingly tough owing to increased electricity demands due to population and industrial growth. The rate at which electricity demand is growing does not match the growth in electricity supply or the pace of investing in new electricity generation. The ever-growing electricity demand has forced most microgrid utilities to invest more in increasing the generation capacities, which has proved to be more expensive and unsustainable in most cases [51]. The problems associated with the overloading of the electric grid and the unbearable costs of expanding the generation capacities have opened the space for researchers and utilities to rethink alternative ways of organizing and managing the electric grids, including employing DSM techniques [52, 53]. In order to avoid overloading and maintain the balance between generation and load, the DSM must be integrated into an electric grid. Deploying the proper DSM technique can benefit sustainable load management in an electric grid.

DSM is the totality of the process, which involves a range of energy management functions related to directing and controlling demand-side activities. This process includes planning, implementation, monitoring, and evaluation. In other words, DSM refers to reducing unimportant loads and/or shifting the electric energy consumption to achieve the balance between load and generation in an electric grid [54]. A successful DSM technique forces the customers to reduce unnecessary loads during the peak demand and shift the consumption to off-peak demand duration relative to the power generation in the electric grid. Therefore, DSM employs techniques that enable electric grid utilities to maintain the load demand profile balancing with the generation capacity.

DSM is, therefore, a broad concept of having a Strategic Load Growth (SLG), ensuring the Energy Efficiency (EE) in usage and encompassing the Demand Response (DR) measures on the customers' side, as shown in Fig. 10. Successful DSM techniques and approaches involve proper load monitoring and control.

Strategic Load Growth (SLG) is a process of gradually increasing the electrical load commonly induced using utilities that can use and store electricity during off-peak times and keep functioning during peak times without being connected to the power grid [55]. SLG is usually used in modern power systems such as with electric vehicles (batteries are charged during off-peak times and can continue being driven even during peak times) and thermal storage (thermal energy is stored during off-peak times for use during on-peak times) in cold regions.

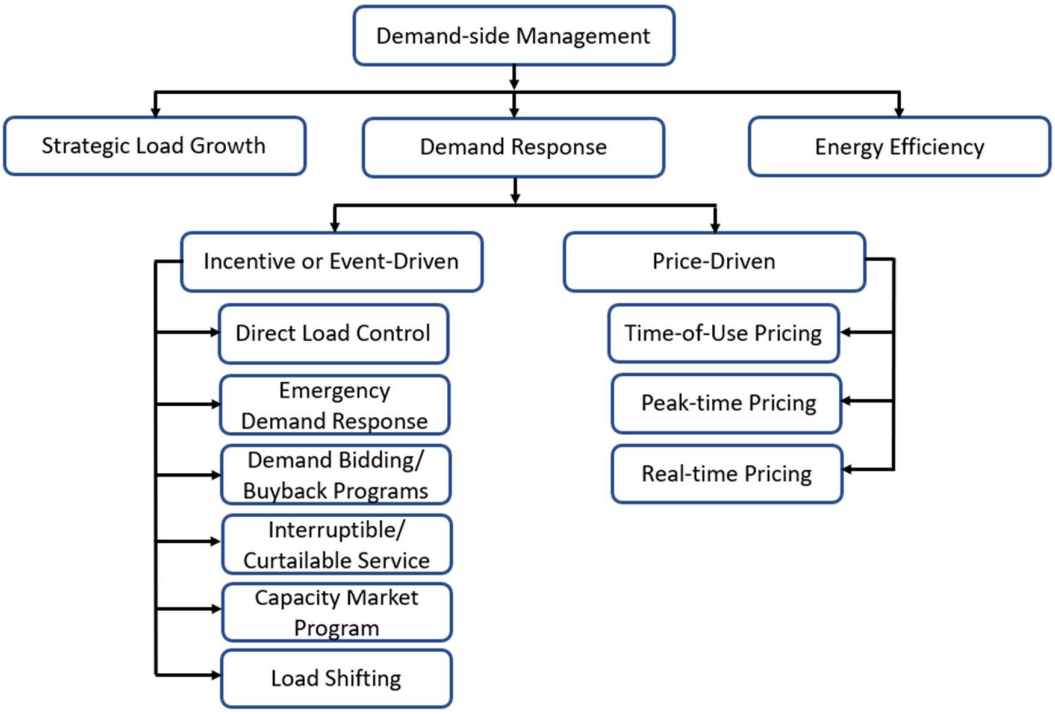

Fig. 10: Various DSM techniques

Energy Efficiency (EE) is defined as a reduction in the total energy used for a given activity (or service) without affecting the level of energy supplied to the end-user service [56]. EE is achieved by using energy-saving appliances which serve the same purpose as the previous services, hence, enjoying the same services and activities at lower energy consumption.

Demand Response (DR) refers to how the end-user customers change their power consumption pattern corresponding to the electric utility's request to properly match the available and generated power to the load demand. DR involves altering the electrical energy consumption, including the load capacity and time of use [57]. The change in the consumption pattern can be influenced by different mechanisms and approaches, including financial incentives and penalties to customers [58]. Fig. 10 portrays the broad classification of DR schemes, incentive-based DR schemes and price-driven DR schemes.

In incentive-based DR schemes, customers are motivated to change their consumption patterns, expecting that a change in consumption patterns will result in an overall change in the load profile. The consumption pattern change leads to energy cost reduction and enhanced energy utilization efficiency. These schemes are either executed at the utility side, such as Direct Load Control (DLC) and emergency programs, or at the customer side. The following are some incentive-driven schemes:

- *Direct Load Control (DLC):* The utility has direct access to the customer's appliances. Thus, the utility can control the load by switching off some appliances during peak demand. The customers are incentivized by participating in this scheme and receive the token of incentives whenever their loads are switched off [59].
- *Load Shifting (LS):* This scheme involves shifting loads from peak to off-peak times. Customers are incentivized by low charges during off-peak times, hence having low electricity bills. This scheme does not necessarily change the total energy consumed; it shifts the excess load from peak to off-peak times to maintain the balance between supply and demand.
- *Emergency Demand Response (EDR):* This scheme provides a mechanism where the demand should be reduced on short notice or without notice during emergencies. Customers can opt for an agreement with the utility to remove the customer load from the grid. In this scheme, the customer is paid for the hours the service was interrupted or cut from accessing the electricity.
- *Interruptible/Curtailable Services:* In this DR scheme, customers on interruptible/curtailable service agreements receive a price discount in exchange for agreeing to reduce load during the electric grid system contingencies. Interruptible/curtailable tariffs differ from the EDR as it is an optionally implemented service [60].
- *Demand Bidding Program:* This scheme allows the electricity customer to bid for voluntary load reduction during high load periods. If a customer bids for this scheme and delivers a load reduction, he/she can earn incentives in the form of generous payment. In this scheme, there is no penalty if a customer fails to deliver the load reduction.
- *Capacity Market Program (CM)*: In this scheme, individuals are encouraged to invest in power generation and be able to supply to the utilities when there is a shortage of power or during high-load peak periods. The plants in the capacity agreement are paid extra capacity payments on top of the regular earnings they would get by selling electricity to the market.

In price-driven schemes, the customers are offered time-varying price rates (tariffs), which attract them to follow a particular trend and reschedule their consumption patterns. The rescheduling of their consumption pattern is reflected by the cost of the electricity at a particular time to save money on the electricity bills. The following are some price-driven schemes:

- *Time-of-Use (ToU) Pricing:* The electricity unit price varies during the daytime. Typically, the high price is set during peak hours (times with expected high demand) and low during off-peak hours. These prices are normally fixed at particular times based on historical data and not on the usage at the instant time.
- *Peak Time Pricing:* This scheme has a fixed base price for electricity usage. However, the prices are inflated during peak demand. The customer is needed to pay an additional fee to access the electricity during peak hours
- *Real-time Pricing (RTP):* This is a dynamic pricing scheme. It works similarly to ToU. However, the prices are not set with the pre-defined times. In this scheme, the price changes as the demand changes concerning the available power at the utility.

With a proper DR scheme, better power generation and utilization matching are realized while increasing the plant capacity utilization factor [61]. The DR scheme is successful if it motivates the consumer to change the energy consumption pattern, which improves the overall electric grid system efficiency and reliability.

Therefore, with the employment of DSM in an electric grid, the utility can shape the load profile curve to match the power generation best and maximize the efficiency and reliability of the power supply. Fig. 11 shows different load profile shapes which can be achieved by employing DSM techniques;

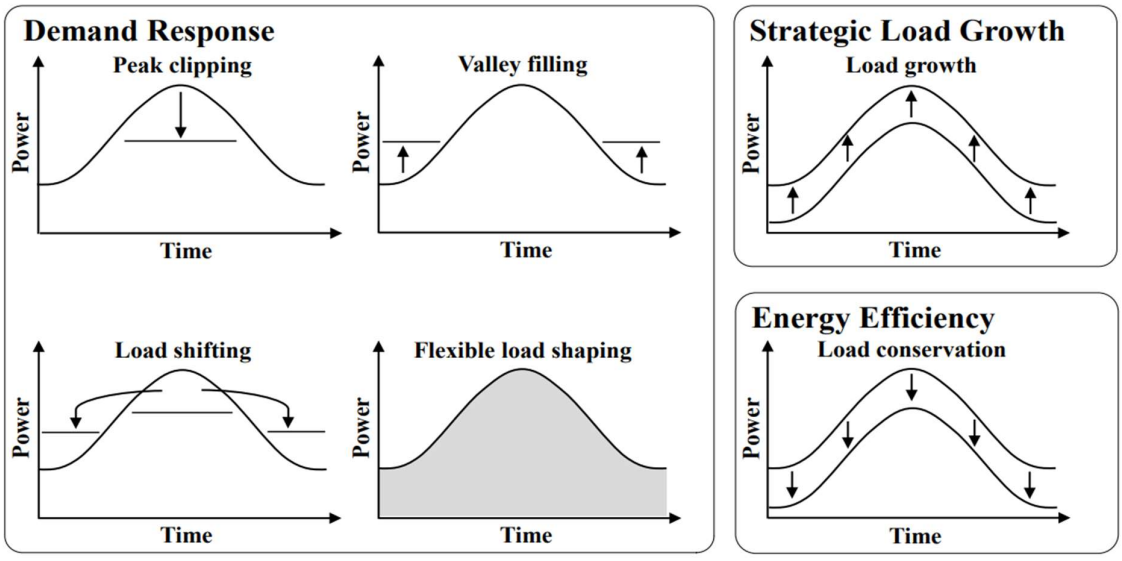

Fig. 11: Load profile changes with different DSM techniques [55]

2.3.1 Demand-side Management: Architecture and Components

The fundamental design and implementation of DSM are made up of basic components such as a power plant with power generators, for example, the solar PV plant, the connected consumer (electric load), smart meters for automatic monitoring and remotely controlling the power consumption, together with the Energy Management Unit (EMU). The sensor-based monitoring devices should be able to communicate with the EMU to provide the intended control as specified by the DSM policy in use. Fig. 12 shows the simplified DSM architectural components.

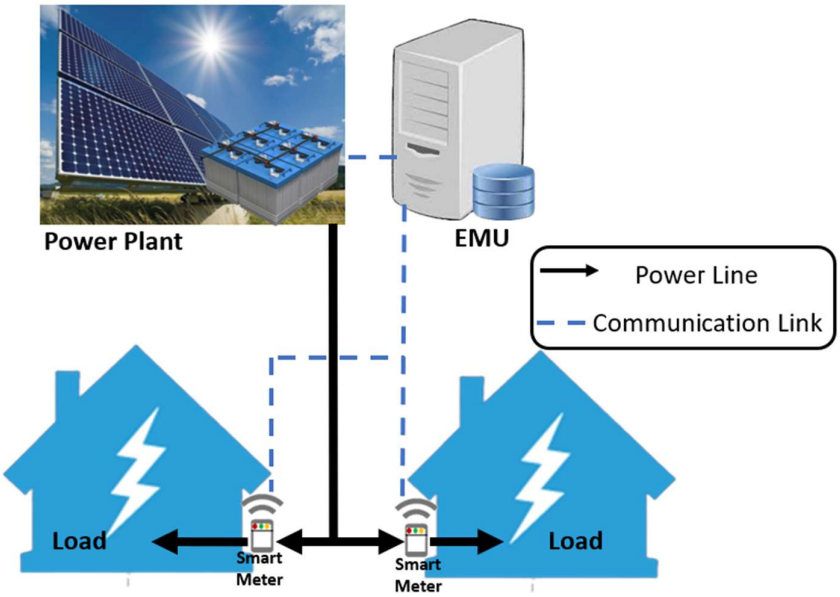

Fig. 12: DSM architectural components

The technological development in the fields of IoT and wireless communication between electricity utilities and users, together with an increased deployment of Advanced Metering Infrastructure (AMI) and smart meters, have made it possible to deploy different DSM techniques, making the electric grids smarter [61]. Smart meters are important tools for detailed and precise customer load monitoring and control in electric grids.

However, less research has been conducted in Africa on deploying DSM in electric grids, especially the decentralized microgrids in rural areas, compared to Europe and North America [62]. Furthermore, the DSM approaches are not fully utilized in implementing microgrids in developing countries of SSA [63, 64]. This research study aims at bridging this gap by employing the hybrid of direct load control (DLC) and real-time pricing (RTP) or tariff-based DSM techniques for overload control in a decentralized microgrid in Tanzania, Africa.

2.3.2 Advantages of Demand-side Management

The implementation of DSM in an electric grid comes with many benefits. The benefits of employing DSM policies in electric grids, such as a decentralized microgrid, can be divided into economic, market-based, social, and technical benefits, as articulated in Fig.13.

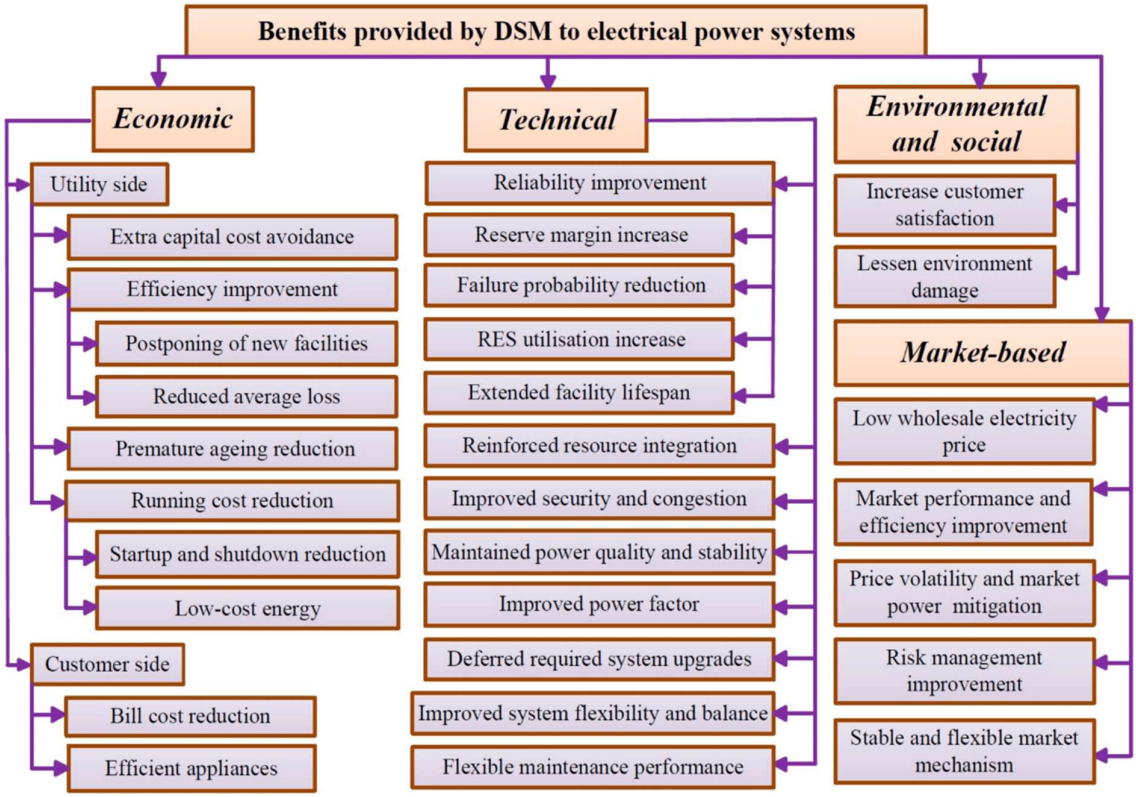

Fig. 13: The summarized benefits of employing DSM in a microgrid [52].

DSM has proved to be economically beneficial for both consumers and utilities. Consumers regularly enjoy the economic benefits through the incentive payments from participating in various DSM programs and reduced electricity bills. Studies show that DSM allows consumers to reduce up to 33% of their electricity bills by altering their use time and behavioural changes [65].

Furthermore, the utilities also gain economic benefits due to DSM. Usually, the economic gains are reduced operating costs, decreased load losses, and increased system efficiency [52]. With increased system efficiency, the system's reliability is increased, reducing the need for new investment in power generation facilities. The peak-demand period happens roughly 5% - 10% of the load cycle and is estimated to consume majority of the total system energy. Hence, investing in building a new generation facility to satisfy this need is uneconomical. With DSM

in place, peak-time generation demands can be accommodated and efficiently resolve the problem of investing in new generation facilities [66].

With the DSM in place, there is a decrease in energy production, especially for fossil-based power plants, which reduces greenhouse gas emissions. Reduction of greenhouse gas emissions attenuates environmental damage. In the case of RES-based power plants, greenhouse gas emissions reduction can be achieved by ensuring the optimal balance of the load and power generation. The proper balance between load and power generation reduces the risk of running the backup diesel generators.

DSM also positively impacts the technical aspects of power plant operations. DSM has been proven to help maintain voltage stability in all power lines as well as frequency stability [67, 68]. Moreover, DSM has been useful in integrating multiple RESs for maximizing plant capacity and reliability. By employing DR, a the uncertainty caused by wind and solar power generation in a solar-wind hybrid microgrid can be compensated and power reliability can be attained [69].

2.3.3 Application of Demand-side Management in Microgrids: Related Works

Different scholars have researched the application of the DSM in smart electric grids, particularly in microgrids. The studies have focused on the different DSM approaches applied to the microgrids, together with the observed findings on the operational improvements in the particular microgrids. The following are some related research works and their success and challenges, which other scholars have done. The research findings associated with these works are the stepping stones for conducting this study.

A recent study of integrating the DR into a Home Energy Management System (HEMS) in Western Australia has shown that up to 2.95 kWh of energy can be shifted to low-demand periods, resulting in a total daily energy savings of 3%. By integrating the DR with HEMS, the optimal scheduling and coordination of various smart appliances could be achieved, leading to significant energy efficiency and cost savings [70]. The study revealed that it was possible to have an opportunity to save much more energy with or without HEMS in a microgrid, based on the results presented for a solar-wind hybrid (and a backup diesel generator) microgrid serving 100 households.

In a study conducted at the National Institute of Technology (NIT) Patna in India, Load Shifting (LS) was implemented as a DSM technique. The campus grid is supplied with solar energy and

smart meters. With LS implemented for flexible loads, daily peak demand was significantly reduced. LS smoothens the load profile curve, significantly reducing power consumption from the main grid and subsequent electricity bills [71].

A microgrid system in Shanghai, China, contains various load types, totalling 221 kW with a maximum of 50 kW controllable by DSM. The grid had maximum generation limits of 100 kW and 33 kW for solar PV and wind turbines, respectively. A diesel generator typically supplies the extra load. By implementing an Integrated Resources Planning (IRP) with a direct load control (DLC) as the DSM technique, a microgrid could manage to reduce the fuel costs by 2%, hence reducing the total operation cost [72].

Moreover, other studies have focused on various algorithms which can be implemented to achieve the DSM approaches. Among the approaches is the activities planning approach, which does not need EMU infrastructure to perform DSM. In the study done in the Antarctic communities, the DSM was implemented using the combination of multiple activities involving load control [73]. A linear programming algorithm was implemented for load scheduling in microgrids in India to replace the complicated approach of non-linear frameworks [74].

Furthermore, some research works have proposed more intelligent and complex frameworks and algorithms to implement DSM in microgrids. These algorithms include the Artificial Bee Colony algorithm and quasi-static technique, which provided about 8.33%, 11.11%, and 11.11% in cost reduction, peak reduction, and load-factor improvement, respectively [75]. Another study used an Artificial Neural Network (ANN) to optimise the load shifting and peak clipping DSM on the data from the East African microgrid. The simulation results exhibited that the load profile better matched the PV-based power generation due to the change in the power usage pattern by load shifting to hours with more power generation [76].

2.4 Fuzzy Logic Control

2.4.1 Understanding of Fuzzy Logic

Fuzzy logic is an extension of classical set theory and logic extensively used in the fields of Artificial Intelligence (AI) in computer science and engineering [77]. It resembles the human decision-making methodology by oversimplifying real-world problems and is based on degrees of truth rather than usual true or false logic. Fuzzy Inference Systems (FISs) can widely deal with vague concepts, uncertainties, and linking a human language to numerical data [78]. FIS

has allowed fuzzy logic to be successfully implemented in different data sciences and engineering contexts, such as in knowledge-driven or data-driven applications, decision-making cases, system modelling, classification and control, and regression problems [79]. When FLC is compared to other conventional controllers, FLC has an advantage as it does not require any complex mathematical modelling in developing a controller [80].

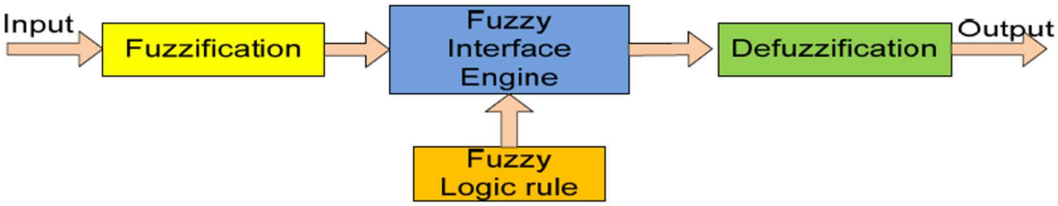

Fig. 14: Basic FLC model [81]

The Fuzzy Logic Controller (FLC) consists of five components, as shown in Fig. 14.

- *Input:* The crisp value that is applied to the FLC model.
- *Fuzzification:* The process of transforming the crisp input value into a linguistic variable. All real-valued input data is firstly fuzzified with membership functions. A membership function allocates a truth value between 0 and 1 to each point in the fuzzy set's domain. A linguistic variable is a word or a sentence in a natural language.
- *Inference engine (Rules):* The decision-making unit. It uses the "IF…THEN" rules along with connectors (operators) such as "NOT", "OR", and "AND" for drawing essential decision rules. The rules are based on the prior knowledge of the outside world and specify how to react to input signals as well. This provides a natural framework that includes expert knowledge in the form of linguistic rules. The fuzzy operators "NOT", "OR", and "AND" are defined in equations (1), (2), and (3) below:

$$NOT\ x\ =\ 1 - x \tag{1}$$

$$x\ OR\ y\ =\ max(x, y) \tag{2}$$

$$x\ AND\ y\ =\ min(x, y) \tag{3}$$

- *Defuzzification:* The process of reducing or converting a fuzzy set into a crisp set (value) or converting a fuzzy member into a crisp member. It rounds off the value of a linguistic variable to a crisp result (output). The result expresses the level of activation acquired from the rule database. The most common methods used for perfecting the final results are calculating the Maximum, Center of Area, and/or Centre of Gravity method [82].

- *Output:* The crisp value that is obtained from the FLC model.

Fig. 15 illustrates how the FLC model works based on the Mamdani FIS. The model has two fuzzy inputs x_0 and y_0, with a degree of truth ranging in [0, 1] in membership functions A and B respectively. The FIS is made up of the following two rules:

$$\text{IF } (x_0 \text{ is } A^1) \text{ AND } (y_0 \text{ is } B^1) \text{ THEN } (Z_1 \text{ is } C^1) \quad (4)$$

$$\text{IF } (x_0 \text{ is } A^2) \text{ AND } (y_0 \text{ is } B^2) \text{ THEN } (Z_2 \text{ is } C^2) \quad (5)$$

The two fuzzy inputs are fuzzified using the intersection of crisp input value with the input membership function. The two fuzzified inputs are combined using Mamdani FIS based on the rules in equations (4) and (5).

The output shape is found by employing a fuzzy operator "and" by clipping the output membership function in accordance with the rules' strength. The output z^* is obtained by defuzzification of the combined fuzzified outputs z_1 and z_2 of each rule, respectively. The most common method is the "Sugeno Centroid Defuzzification" method, mathematically expressed in equation (6).

$$z^* = \frac{\sum_0^i z_i \int C^i \, dz}{\sum_0^i \int C^i \, dz} \quad (i = 1, 2, \dots) \quad (6)$$

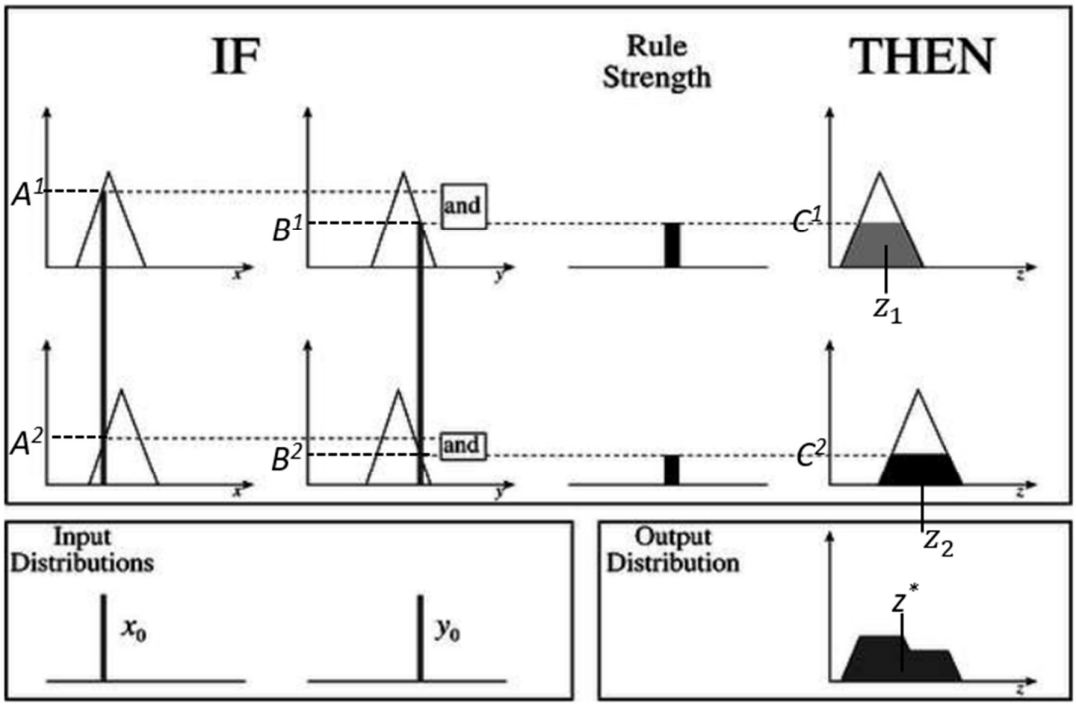

Fig. 15: A two fuzzy inputs and two rules-based Mamdani inference system

2.4.2 Fuzzy Logic Control for Demand-side Management: Related Works

Smart-grid implementation involves different computational techniques, including swarm intelligence, evolutionary algorithms, and fuzzy logic [83]. Different studies have shown that results obtained from fuzzy logic are considered steady and efficient [84]. In the context of DSM, fuzzy logic is applied as an artificial intelligence technique normally used in load control systems in such a way it can lead to either reduce, control or modify power consumption. The load control is achieved based on the set of rules set within the system. These rules stipulate when and how the electric energy should be consumed relative to other parameters such as electric power generation, time of use, state of energy storage, and classification of loads (i.e. vital and non-vital loads).

Researchers have employed the FLC algorithm in DSM systems, particularly in the electricity market. Further research has shown that it is possible to flatten the load profile by using FLC within a DSM technique. In their studies, DSM has used the FLC to maximise economic benefits and energy serving while considering factors such as demand, comfort, and energy cost. Therefore, the FLC is among the tested and proven approaches for optimising the utilization of the available energy sources.

The FLC has been used as a practical algorithm for load shifting and has given valuable results in flattening the load demand curve [85]. [85] describes a fuzzy logic-based DSM for shifting the peaks of the mean residential electric water heater power demand from high-demand hours for electricity to off-peak hours.

FLC has also been employed in developing energy management and cost control for standalone distributed renewable energy systems used in buildings [86]. In the paper presented by [86], a flexible energy allocation strategy based on a two-stage FLC has been developed to give special attention to managing stored energy and emergency resource. The results show that an FLC is more accurate in real-time energy management with less cost.

In other studies, the FLC was used for peak-clipping by shutting off some loads during peak hours, considering vital and non-vital loads [87, 88]. [88] gives a design based on FLC for load management during peak hours by controlling the usage of domestic loads by considering both peak and off-peak hours, aiming to reduce the gap between the demand and the supply of electrical energy.

Employing the FLC technique can benefit the microgrid by ensuring the sustainability of microgrids by maximizing the utilization of RESs and reducing the overall energy costs. Thus,

other researchers have employed FLC as an algorithm for DSM, such as in peak shifting and valley filing. However, no research has given the freedom to a customer to respond to the control signal. This work aims to use FLC to implement a real-time control and load response in a solar PV microgrid while considering a current energy demand versus the current PV power generation and state of the battery energy storage.

2.5 Wireless Sensor Network

2.5.1 Understanding of Wireless Sensor Network

Over many years, the field of wireless communication technologies has been evolving. The Wireless Sensor Network (WSN) is among the application of wireless communication. WSN refers to a group of spatially distributed static or mobile sensor nodes deployed randomly, predetermined, and wirelessly interconnected [89]. The primary purpose of the WSN sensor nodes is to form a self-organized system and collaborate to detect, process, and transmit the monitoring information of a particular object or parameter in an area of WSN coverage [90]. Fig. 16 shows an example of a WSN in which a target node is remotely accessed via the Internet.

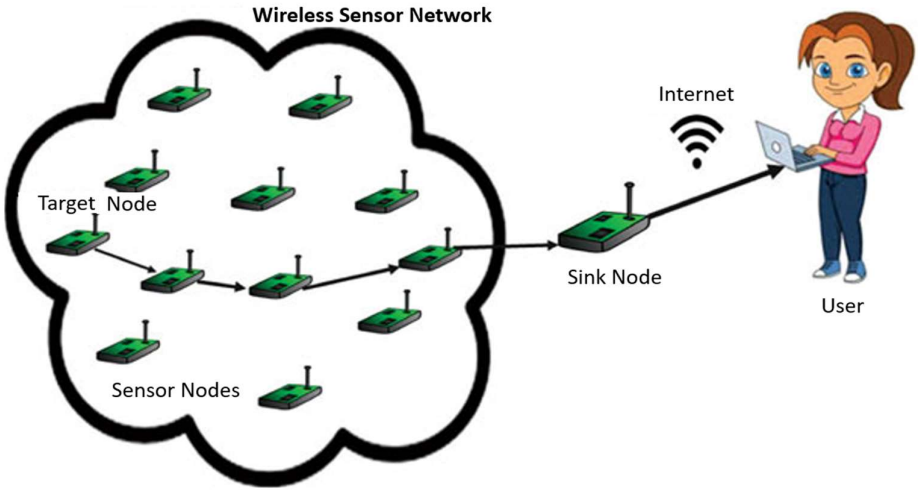

Fig. 16: A Wireless Sensor Network (WSN) [91].

WSNs are among the most swiftly growing technological domains, thanks to rapid technological developments in the wireless communication domain and the numerous benefits that WSNs provide. In the past few years, WSN technologies have been widely applied in multiple areas of monitoring and controlling different parameters such as security-surveillance systems, environmental monitoring, intrusion detection and others [92]. These WSN systems

are becoming valuable tools and are frequently deployed in harsh environments or inaccessible areas. Consequently, since WSN came into use today, WSN has had a continuously growing range of applications. Among the applications of WSN are forest fire detection, air pollution monitoring, water quality monitoring, health applications, automotive applications, military applications, smart home/office – automation, and smart grids.

Among the merits of deploying the WSN monitoring systems is the ability of WSN nodes to auto-configure themselves and operate without human intervention for years. The nodes are capable of real-time sensing, data collection from remote sites, and communicating with the control centre [24].

2.5.2 Sensor Node

The sensing node is the fundamental component of WSN as it acts as a monitoring agent. Sensing nodes are application specific, meaning that a sensing node can only monitor specific parameters it is designed to monitor [93]. Fig. 17 shows the block structure of a sensing node. The sensing node is fundamentally made up of four basic units: the sensing unit, the processing unit, the communication unit, and the power unit.

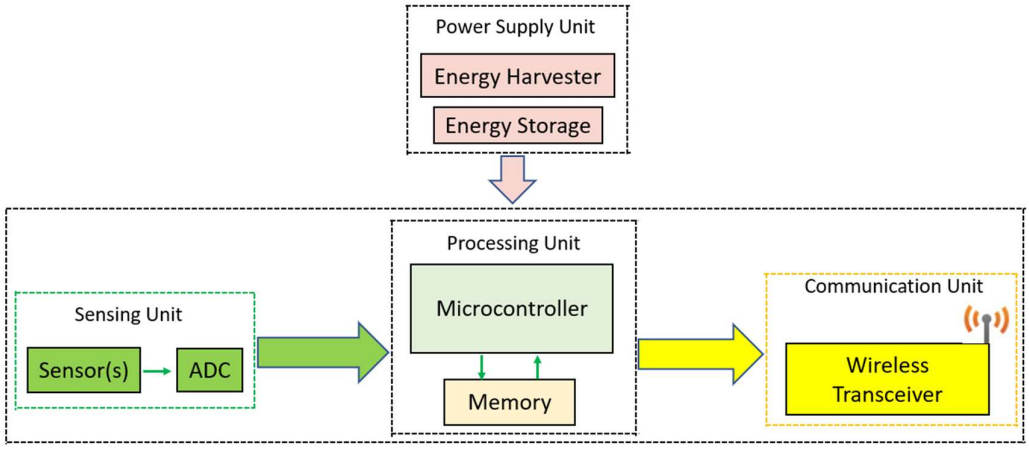

Fig. 17: The typical structure of the sensing node

Sensory Unit

The sensing unit comprises the chosen sensors and the Analog-Digital Converters (ADCs). The sensors are responsible for measuring the actual physical state of the monitored parameter; it can be electrical current, environmental temperature, pressure, and others, depending on the monitoring objective. The sensed and measured parameters are converted from analogue to

digital values using ADCs. The digital values are transferred to the processor. Every WSN application has a suitable set of sensors.

Processing Unit

The processing unit (PU) is the brain of the sensing node. In this unit, it is where all the sensing operations are controlled. The sensor values are manipulated, temporarily stored, and/or transferred to the communication unit as binary information. All the control and data manipulations in the processing unit are digital to enhance accuracy and efficiency.

The processing activity in a sensor node is carried out using a microcontroller unit (MCU). The microcontroller is a tiny computer fabricated in a single-circuit architecture. MCUs are considered suitable for sensor nodes due to their small sizes and low prices, essential requirements for making portable IoT devices. Many microcontrollers exist, such as ATmega, Raspberry Pi, and others. The selection of a suitable MCU is mainly based on the core function of the sensor node. However, other factors such as power consumption, processing speed, number of input/output (AO) pins, and costs should also be considered.

Wireless Communication Unit

The node wirelessly transmits the data its processor produces to other nodes or/and to a selected sink point, also known as the Base Station (BS). The communication unit consists of the transceiver or radio frequency (RF) modules, which are responsible for transmitting and/or receiving digital information from other remote devices, such as the gateway or directly to the central system controller. It comprises wireless communication components such as a radio antenna for radio communication. BS can be configured to perform the supervisory control on the WSN and transmit data to other remote systems over other networks, such as the Internet, for other analytics. Different wireless communications technologies such as Bluetooth, Wi-Fi, GSM/GPRS, and others can be selected and used within a sensor node depending on other factors such as transmission power, range of transmission, and location of the sensor nodes.

Power Supply Unit

The components of the sensor node must be electrically powered to operate. However, sensor nodes are always constrained by an extremely strict power supply. Ensuring a reliable power supply is a challenge since the sensing nodes are designed to work either in remote areas or harsh environments, away from traditional electric power grids. Some WSN designs use

batteries, but the battery life has been challenging, especially in measuring energy conservation and power consumption [24, 94]. Nevertheless, changing or recharging the batteries becomes practically more complicated when the sensor nodes are placed in a remote and harsh environment [93, 95, 96]. Some designs propose using both battery (primary or rechargeable) and a direct power line to ensure power availability on the sensing node. However, this works for accessible sensor nodes in urban areas with an extensive electric grid network. Fig. 18 illustrates the options for power supply to the sensor nodes.

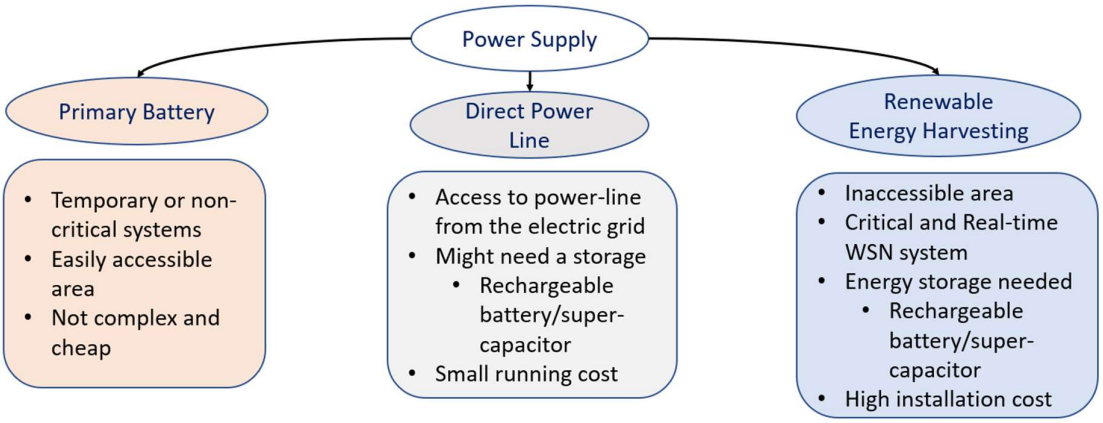

Fig. 18: Options for power supply to the sensor node

In recent years, energy harvesting for wireless sensing nodes in WSN has gained much attention due to the increasing demand for independent, reliable, and robust sensor nodes. The current studies have touted the development of sensor nodes embedded with energy harvesters and higher life-span energy storage devices such as super-capacitors [97]. Energy harvesting or scavenging refers to converting available energy from the environment to usable electrical energy. The environment is typically enriched with various natural or RES and man-made energy sources such as light, heat and electromagnetic effects. Fig. 19 describes the energy harvesting process for power supply to a sensor node. With the energy harvested from the RESs, the sensor node is ensured with a cheap, efficient, and reliable power supply, even if placed in an inaccessible environment.

Data transmission consumes the most energy among the tasks of a sensor node. The sensor nodes must be designed to operate intelligently in energy-serving schemes to minimize power supply costs in sensor nodes. Different research studies have proposed different energy

conservation schemes, such as using the sleeping mode when there is no scheduled data transmission activity and employing energy-efficient routing protocols [89].

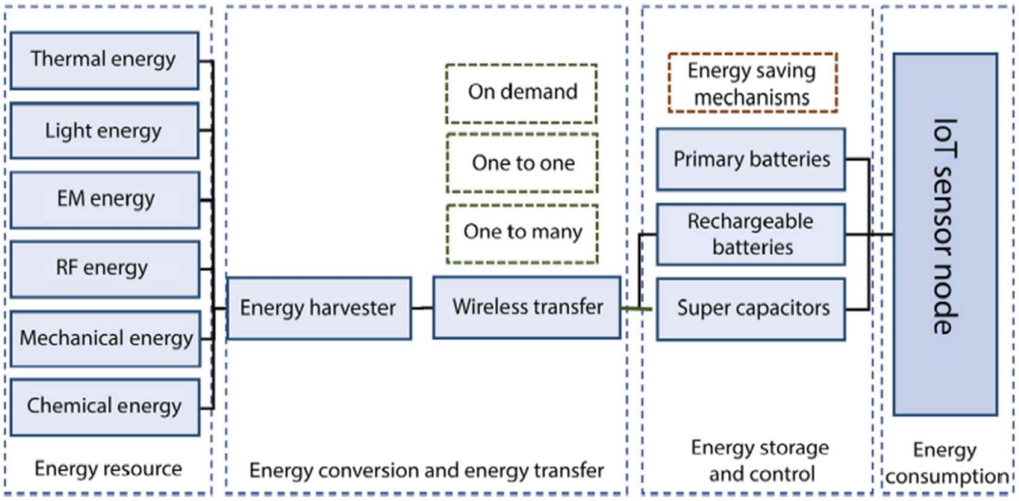

Fig. 19: Typical energy harvesting process for a sensor node [98].

2.6 Wireless Communication Technologies

A wireless communication system refers to a type of data communication system that wirelessly (by using radio frequencies) transfers data from one point to another point. A wireless communication system can be made of either long-range or short-range communication technology. There have been different areas of improvement, such as increasing data rate, lowering transmission power, and increasing the coverage area (transmission range). For the sensor nodes in WSN, parameters such as power consumption and transmission range are essential.

There have been different wireless communication technologies, both commercial and non-commercial. The commercial technologies involve licensed radio frequencies to the Mobile Network Operators (MNOs), through which the WSN uses the existing commercial infrastructures for data communication. Non-commercial technologies use unlicensed radio frequencies, such as those allocated for Industrial, Scientific, and Medical purposes (ISM), for data transmission in WSN.

An ever-going advancement in wireless communication has resulted in different wireless communication technologies. These technologies have different characteristics, even though advanced technologies are proving to provide better data transfer rates and larger area coverage. Commercial data transmission has been evolving from Global System for Mobile

Communication (GSM) which uses short-messages service (SMS) for transferring data, to General Packet Radio Service (GPRS), which is a packet-oriented mobile communication technology providing Internet connectivity over the GSM infrastructure [99]. Over recent years, the speed of mobile Internet communication has been improved due to an ongoing improvement in GPRS technologies. It involves the evolution from 3G to High-Speed Packet Access (HSPA) to Long-Term Evolution (LTE). There have been many developments in the LTE technological family, such as the 4G, the introduction of 5G, and even the usage of Narrow Band LTE (NB-LTE). However, some of these characteristics come with operating costs (in the case of commercial technologies) and high-power consumption, as shown in Table 1.

Low Power – Wide Area Network (LPWAN) technologies have been studied to solve the high-power consumption problem in commercial wireless communication technologies [100]. Studies [101] have shown that LPWAN technologies such as LoRa are suitable for a more efficient, reliable, and robust battery-powered WSN system for applications in remote or easily inaccessible areas. Moreover, [102] suggested that designing transceivers to the ultra-high frequency range will cause a trade-off with antenna efficiency and power consumption.

Table 1: Comparison of the currently wireless communication technologies used in WSN [101]

Technology	Data Rate	Transmit Power	Coverage	Remarks
3G-HSPA and 4G	2 – 20 Mbps	560 mW	MNO/Cellular Communication	‣ Costful: Running expenses ‣ Robust in urban areas
NB-LTE (NB-IoT and LTE-M)	100kbps to 1Mbps	300 mW	MNO/Cellular Communication	‣ Costful: Running expenses ‣ Robust in urban areas
ZigBee	Upto 250kbps	40 mW	Upto 100 m	‣ Depends on Line of sight ‣ Complex routing for reliability
LoRa	27-50 kbps	100 mW	Typical around 5-10 km in rural area	‣ Network Scallability ‣ Low data rate and message capacity

2.6.1 Low Power – Wide Area Network (LPWAN)

The trade-off between the transmission range and power consumption has challenged realising different IoT and WSN applications. Achieving a more extended transmission range and even remote access to the WSN requires commercial mobile communication from Internet service

providers (ISPs), which comes with extra cost for every transmitted data. Recent studies have been done on Low Power – Wide Area Network (LPWAN) technologies to provide a costless, long-range wireless communication in WSN applications [103]. LPWAN has used very little power compared to other communication technologies in data transmission over a long distance [104]. However, the LPWAN focuses on attaining the greatest possible range on comparatively low energy consumption at the expense of data throughput, the transmission's bi-directionality, and, in some cases, end-to-end reliability.

LPWAN technologies are categorized into ISP-based and unlicensed-based technologies. ISP-based technologies such as Long-Term Evolution for Machines (LTE-M), Sigfox, and Narrowband-IoT (NB-IoT) are commercial technologies that charge per connected node and amount of data transferred. The unlicensed radio frequency (RF) LPWAN technologies are compared in Table 2. Table 3 lists several unlicensed frequency bands for Industrial, Scientific, and Medical (ISM) applications in different countries/regions. LPWAN technologies complement other wireless communication technologies, such as cellular networks, and they can work in hybrid mode with cellular networks or ISP-based LPWAN technologies when there is a need for remote access or data transmission.

Table 2: Comparison of different LPWAN technologies [105]

Feature	**LoRa**	**ZigBee**	**Wi-Fi**	**Bluetooth**
IEEE Standard	802.15.4g	802.15.4	802.15.1	802.11
Modulation	Chirp Spread Spectrum (CSS)	Direct Sequence Spread Spectrum (DSSS)	Quadrature Phase Shift Keying (QPSK)	Frequency Hopping Spread Spectrum (FHSS)
Frequency	ISM bands	ISM bands and 2.4GHz	2.4GHz	2.4G
Network Topology	Star	Mesh	Tree	Tree
Coverage Range	To 10 Km (in rural areas)	75 - 100 m	To 70 m indoor; 100 m outdoor	To 10 m
Battery Life	Long (to years)	Long (to years)	Less than week	About a week
Cost	Low	Low	Moderate	Low

Table 3: ISM radio frequency bands [106]

ISM band	Frequency Range	Central Frequency	ITU Region
433 MHz	433.050–434.790 MHz	433.92 MHz	Reg. 1 (Europe)
868 MHz	863–870 MHz	868 MHz	Reg. 1 (Europe and Africa)
915 MHz	902–928 MHz	915 MHz	Reg. 3 (AUS/NZ), and Reg. 2 (USA/CAN)
2.4 GHz	2.4–2.425 GHz	2.4125 GHz	Reg. 1, 2, and 3 (Worldwide)

Long Range (LoRa) communication technology is among the popular LPWAN, implemented in many IoT-based embedded systems and even sought communication in smart electric grids. LoRa has an edge over license-free wireless technologies such as Bluetooth and Wi-Fi. LoRa can span to a considerably higher distance and still transmit data at low power, hence, cost-effectiveness [107]. ZigBee is another LPWAN technology for WSN systems. Unlike LoRa, ZigBee is short-range and energy-efficient but with a low data rate, based on IEEE 802.15.4 standard [108]. ZigBee might be energy efficient but unsuitable for applications such as monitoring microgrids, which cover a radius of up to a few kilometres.

In this research study, LoRa wireless communication technology was selected as it ticks many requirements criteria of this particular research design. This research involves the development of the load monitoring and control system for microgrids in rural (remote) villages in SSA. Among other criteria for research design were low energy consumption, low acquisition and operating costs, autonomous network (working independently of Internet connection), and covering a range of 1 km to 2 km.

2.6.2 LoRa Wireless Communication

The Long-Range (LoRa) wireless radio frequency technology is extensively adopted for long-range and low-power solutions for IoT systems. LoRa wireless technology functions in license-free usable frequencies which are part of the ISM bands [109]. LoRa technology is made on the Chirp Spread Spectrum (CSS) modulation technique, which permits the trade-off of data rate for sensitivity and long-range at a low power transmission [110]. The Chirp (which stands for 'Compressed High-Intensity Radar Pulse) is a modulation technique in which a signal frequency increases or decreases with time, maintaining a constant amplitude while using the whole bandwidth in a linear or non-linear way from a transmitter to a receiver [103]. A chirp

is a signal whose frequency increases (up-chirp) or decreases (down-chirp) over time [111]. Changing frequencies helps in long-range signal transmission and resisting the effect of doppler shift/effect [112].

Furthermore, LoRa provides other essential useful features such as end-to-end security with AES128 encryption technique, mobile communication for moving IoT devices, and standardized interoperability with other LoRaWAN devices for data transmission [105]. With LoRa wireless communication technology, the WSN-based IoT systems can assimilate features that result in low-power consumption, hence less cost on energy to power the sensor nodes [105]. LoRa offers high-link budgets and low-power consumption; subsequently, it is becoming predominantly suitable for remote wireless sensor systems [113].

LoRa and LoRaWAN are commonly used synonymously. However, LoRaWAN is the Media Access Control (MAC) layer protocol in the open networking structure, as shown in Fig. 20. When LoRa nodes are networked with other IoT devices and/or the Internet, the MAC protocol, LoRaWAN is used for further configurations. LoRaWAN is responsible for bidirectional communication within the network and the security of the LoRa gateway and nodes [114].

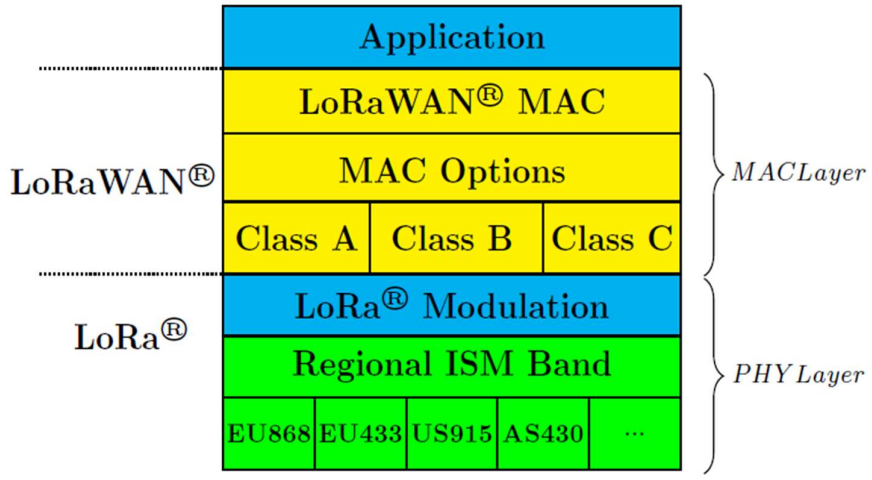

Fig. 20: LoRaWAN networking protocol stack [115]

LoRa has five configurable transmission parameters, namely, Transmission Power (TP), Spreading Factor (SF), Bandwidth (BW), Coding Rate (CR), and Carrier Frequency (CF).

- *Transmission Power (TP)* is the power the transmitter needs to correctly and efficiently transmit the signal. It usually ranges between -4 dBm to 20 dBm for the LoRa transmitters [116]. The TP value affects the transmission range and the battery life in the sensor node. The higher is TP, the more extended range it can transfer, but it's the shorter battery life.

- *Spreading Factor (SF)* measures how the chirps are spread out, or the number of the chirps contained in each symbol. Chirps are the individual bits of the code sequences. The SF is important in controlling noise interference during signal transmission, as shown in Fig. 21. The higher the SF, the higher the signal-to-noise ratio (SNR).

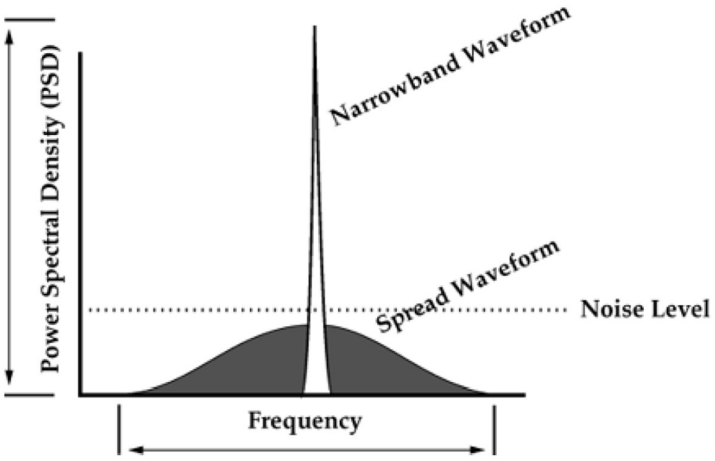

Fig. 21: Comparison of Spread signal and Narrowband signal against noise interference [117].

The relationship between SF, bandwidth (BW), chirp duration (T_s), bit rate (R_b), and symbol rate (R_s) are given by the formula in equations (7) to (9) below [118]. Table 4 illustrates how the SF affects signal transmission parameters such as data rate, transmission range, transmission time/Time-on-Air (ToA), and transmission power.

$$2^{SF} = BW * T_s \; [chips/symbol] \tag{7}$$

$$R_b = SF * \frac{1}{T_s} = SF * \frac{1}{\frac{2^{SF}}{BW}} = SF * \frac{BW}{2^{SF}} \; [bits/sec] \tag{8}$$

$$R_s = \frac{1}{T_s} = \frac{BW}{2^{SF}} \; [symbols/sec] \tag{9}$$

Table 4: Effects of Spread Factor on the other transmission parameters [115]

Transmission Parameter	Spreading Factor (SF)	
	Lower SF	**Higher SF**
Transmission range	Longer	Shorter
Data rate	Higher	Lower
Receiver sensitivity	Lower	Higher
Transmission Power	Lower	Higher
Transmission time	Shorter	Longer

- *Bandwidth (BW)* indicates the frequency range for signal transmission. Over this range, the LoRa's chirps are spread. BW determines the chirp rate for a given SF. Consequently, BW is proportional to the data rate. Thus, the higher the BW, the higher the data rate, but the lower the sensitivity of the LoRa receiver.
- *Carrier Frequency (CF)* is the frequency over which the signal is transmitted in the radio band domain. For a LoRa transmission, CF can be any value within the ISM bands corresponding to the particular geographical region, as explained in Table 3.
- *Coding Rate (CR)*: When the LoRaWAN modem is used, the CR refers to the modem's forward error correction (FEC) rate, which protects the signal transmitted against interference [119]. The CR offers protection at the expense of power consumption and increases in ToA during signal transmission. For LoRa transmission, the CR value is usually between 0 and 4, and no FEC is applied if CR = 0. With CR, the formula in equation (8) can be modified to get the nominal bit rate (Rb) as;

$$R_b = SF * \frac{\frac{4}{4+CR}}{\frac{2^{SF}}{BW}} [bits/sec] \qquad (10)$$

Currently, LoRa and LoRaWAN technologies are extensively used in various IoT and WSN applications to address different challenges in developing smart technologies for smart cities, transportation, energy management, health monitoring, pollution control, and smart farming [115]. In this research study, LoRa technology is employed in DSM in microgrids, and it is used for wireless communication between the load monitoring and control nodes at customers and the host computer at the microgrid power plant.

2.7 Load Monitoring and Control: Advanced Metering Infrastructure and Smart Meters

2.7.1 Advanced Metering Infrastructure

An Advanced Metering Infrastructure (AMI) is not a single unified technology but a configured infrastructure comprising various integrated technologies [120]. AMI as an infrastructure in the smart grid (SG) comprises smart meters (at the consumer end), Meter Data Management Systems (MDMS) at the management centre (at the utility point), and the communication networks for data and signal transfer between the two ends. AMI refers to a set-up containing

systems and networks, which are responsible for collecting and analysing data received from customers using smart meters and other sensors. The modern electric grids, smart grids, deploy AMI with sensing devices to detect any operational malfunctions. In case of any failure, the signal is sent from the sensors to the control centre. The meters (with sensors) transmit the collected data to MDMS for analysis, which results in helpful information for the utility in managing the electric grid.

Recently, AMI has been attracting the serious attention of researchers as it is considered a crucial component in the smart grids which increase reliability and efficiency in modern and next-generation power systems [121]. Current research studies advocate for developing AMI with bi-directional capability (read and write to smart meters) that enhances the data collection and analysis from smart meters and provides controls to the grid's connected loads [122]. With bidirectional communication, AMI becomes more important in implementing control and command signals for essential control actions such as DSM. Furthermore, AMI decreases the operation cost due to manual meter readings, as it can generate an automated bill for customers based on readings from smart meters [123].

2.7.2 Smart Meters and Related Works

Smart Meters (SMs) are end-user devices made up of state-of-the-art electronic hardware and software capable of taking load measurements and collecting data in desired time intervals. SMs are located at customers' premises to read and collect power consumption data. The SMs typically show how the electricity is used, billing and pricing (tariff setting), and automated circuit breaking in case of any circuit problem [124].

Multiple scholars have researched the area of deployment of smart meters in modernizing electric grids. In developed countries such as European Union (EU) and Northern America, the rollout of smart meters is moving rapidly. For example, research shows that the EU had committed to roll out about 200 million smart meters by 2020 for about 72% of electricity customers [125].

Smart meters have also attracted the interest of microgrid developers in different areas. Different studies show that smart meters have been used to monitor the grid, such as power consumption monitoring and power quality, using different methodologies and technologies. The following are some related works, together with their success and challenges, building the foundation of this study.

Different studies used GSM-based monitoring systems. These systems use GSM technologies for data transfer from the sensing node (i.e., smart meters) to the utility companies' servers. [126, 127] proposed the usage of a GSM modem to relay meter reading data to the utility central systems via SMSs. In another study by [128], an automatic meter reading system based on the GSM data transfer to the servers of the utility company. The utility company would have a web portal to generate and manage customer bills. With this system, the customer could pay and get the total units to balance over the SMS. [129] worked on improving this study by employing cloud servers for data storage and manipulation. The system was enhanced in security as the meter could disconnect if tempering is detected.

[130] used the ZigBee wireless communication technology for the area covered in the microgrid system. The solution seems viable only for the microgrid confined to a small area such as a hospital, a school campus, etc.

In a recent study by [131], the electricity usage monitoring system was developed based on the combination of LoRaWAN and GPRS. The system architecture included smart meters with LoRaWAN gateway modules to transmit data to a local monitoring centre and a GPRS gateway for data transmission from the local monitoring centre to the cloud server. Another study proposed using a LoRa-PLC combination for data transmission in microgrids. [132] presented a LoRa-PLC hybrid, with LoRa as the outdoor communication technology and PLC for indoor communication. These were implemented to improve energy metering. The study realized that the increased distance and obstacles posed challenges for LoRa in an outdoor environment.

Regrettably, most smart meters presented in different research are simple electronic meters (e-meters) with the objective of automated meter reading. The above similar developed systems were only capable of determining the power usage units (energy smart metering) and alerting the customer, as well as providing the utility with the ability to switch the connection on and off. However, the proposed systems are not intelligent enough to perform DSM and inform the customer on the load-power generation relationship to control load and avoid overloading in a microgrid. Furthermore, the traditional smart meter does not include data analysis, as it only provides communication abilities and load measurement [133].

A plausible solution for the abovementioned challenge is to have a sensitive smart grid that uses DSM via an Intelligent Metering System (IMS). It should be able to administer real-time load monitoring and control within the grid. Generally, several studies, as discussed above, the majority done outside Africa, have come out with multiple different solutions but with some limitations in the current need for microgrid setup in SSA, especially in Tanzania [49]. The

solutions which have been proposed are reasonable but not practical when adopted. Some solutions are incompatible with the African environment and/or technology, and some cannot be afforded by local people [16]. Some scholars even proposed improvements to their works by offering monitoring power quality, detection of power theft, and abnormal event alarming systems to be integrated into the microgrid's infrastructure [131]. Therefore, this study aims to develop a robust, autonomous, low-cost wireless sensor system for load monitoring and controlling power consumption to maintain the balance between load and power generated in microgrids.

2.8 Chapter Summary

This chapter has given a detailed review of the concept and the technologies essential in fulfilling this research study's primary objective. The main aim of this research is to design and develop a robust, autonomous and low-cost wireless sensor system for loading and controlling the power utilization; to ensure proper and real-time demand-side management (DSM) by using FLC to avoid overloading in the solar PV microgrids. This chapter has defined a microgrid and explained the role of microgrids in rural electrification in SSA. Moreover, the technical concept and technologies such as WSN, DSM, FLC, and AMI have been explained. Finally, the study also looked at similar research works done by other scholars in the field of load monitoring and control.

CHAPTER THREE

HARDWARE DESIGNING AND IMPLEMENTATION

3.1 Introduction

The previous chapter discussed the basic understanding and detailed explanation of different technologies used in this study. Nonetheless, the main objective of this research is to design and implement a wireless sensory system for load monitoring and control in microgrids in SSA. This chapter proposes the wireless sensory system with a sensory module attached to each connected customer, as shown in Fig. 22. The conceptualized system is designed and implemented into a working prototype in this chapter.

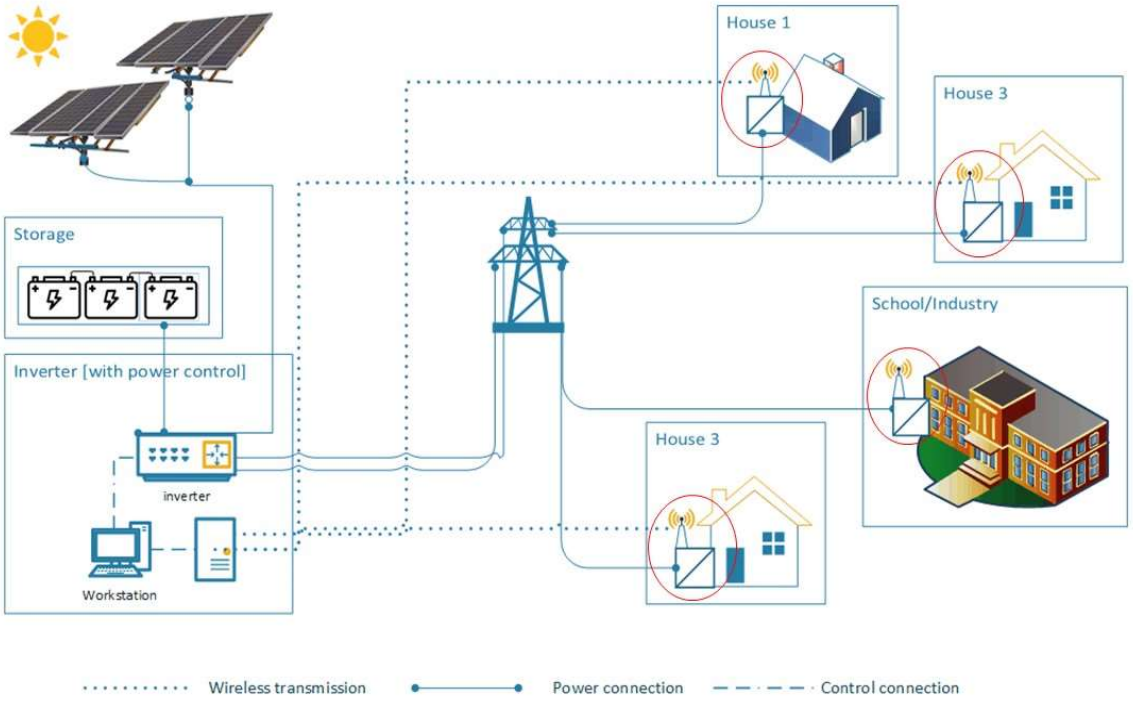

Fig. 22: Conceptual monitoring and control system[2] [134]

[2] This concept is published in paper: U. Hilleringmann, D. Petrov, I. Mwammenywa and G. M. Kagarura, "Local Power Control using Wireless Sensor System for Microgrids in Africa," *2021 IEEE AFRICON*, Arusha, Tanzania, 2021, pp. 1-5, doi: 10.1109/AFRICON51333.2021.9570970.

3.2 System Designing

The design of this system was built from the conceptual block diagram given in Fig. 23. There is a wireless sensory system on the customer's side that is wirelessly communicating with the grid's control unit. The bidirectional communication is such a way that the sensory system at the customer sends the power consumption (i.e., load) information to the mini-grid control unit. The mini-grid's controller compares the total load from the customers with the real power generated and available in battery storage, and sends the feedback to the customers. The feedback sent to the customers advises them on load control and change of the electric-power tariff.

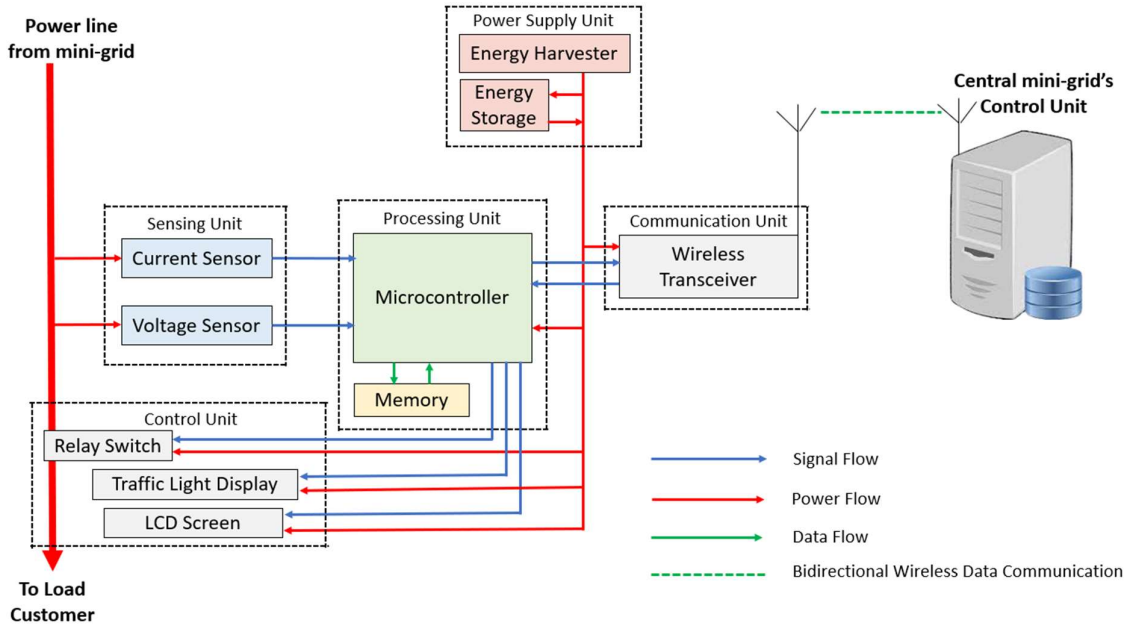

Fig. 23: Design - conceptual block diagram

The conceptual design block diagram in Fig. 23 comprises five blocks/units. These units are the power supply unit, sensing unit, processing unit, communication unit, and display unit. Each of the units is elaborated below.

3.2.1 Sensing Unit

The sensing unit is designed to monitor the load at each customer based on real-time measurement of both current and voltage as shown in Fig. 23. Electric power consumed by the electric load is the function of the voltage across the load and instant current passing through

it, as shown in the equation (11). The current and voltage sensors have been used in this system to accurately calculate the real-time power consumption, as shown in Fig. 24.

$$Power = Voltage\ x\ Current \tag{11}$$

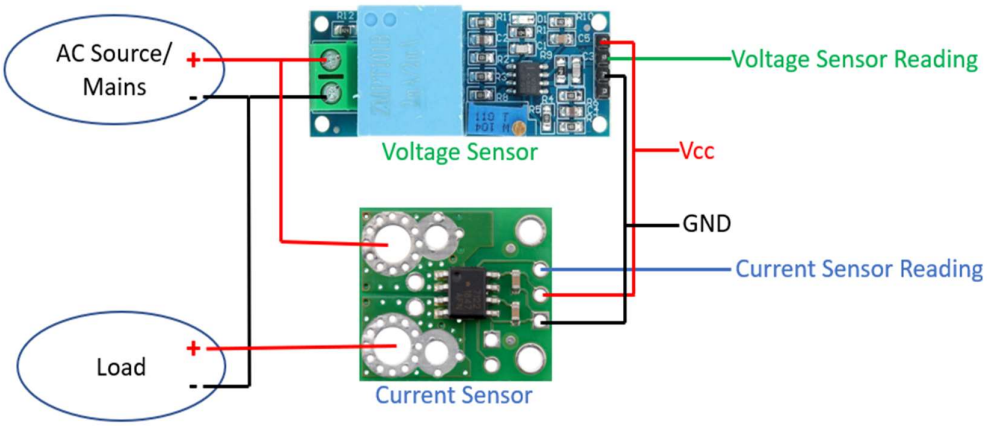

Fig. 24: The current and voltage sensing

Current Sensor

In this study, the Hall effect-based linear current sensor, ACHS-7122 has been used. A Hall-effect sensor detects the presence and magnitude of a changing magnetic field surrounding the current-carrying conductor. The sensor delivers an output voltage which is directly proportional to the strength of the field, which is also proportional to the magnitude of the current passing through a conductor [135].

The ACHS-7122 current sensor has a relatively wide measurement range, from -20A to +20A, which is the typical range for households in rural areas. It is made of a low-resistance (~0.7mΩ) current path with electrical isolation of up to 3kV RMS. It is a relatively high-resolution reading of 100mV/A when supplied with Vcc of 5V-dc and a low relative error of ±1.5% [136].

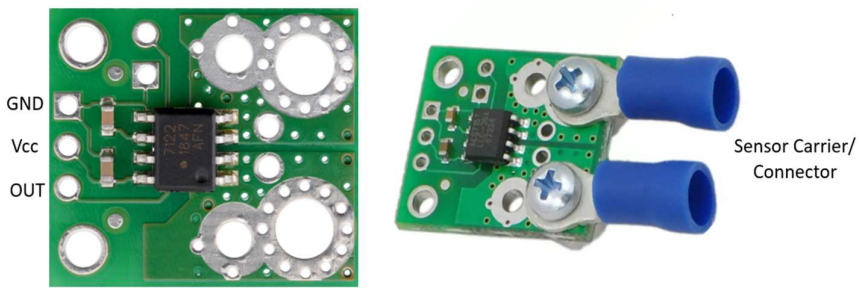

Fig. 25: Current sensor, ACHS-7122

Voltage Sensor

This study uses a single-phase voltage (or potential) transformer as a voltage sensor. The voltage transformer works under the principle of electromagnetic induction. Fig. 26 explains how the primary coil induces voltage to the secondary coil using the magnetic core. The sensor's output is read at the transformer's secondary coil, which is always proportional to the voltage across the primary coil.

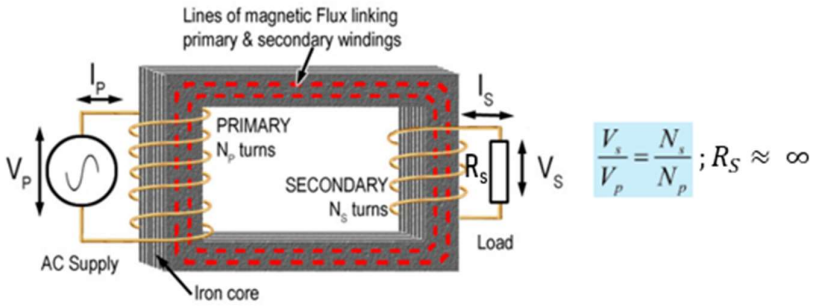

Fig. 26: Working principle of potential transformer

This study uses a potential transformer, ZMPT101B, as a voltage sensor. It measures up to 250V AC voltage, with an accuracy in the linearity of less than 2%. ZMPT101B was designated due to its high accuracy, enhanced with a built-in trim potentiometer for fine-tuning the ADC output [137].

Fig. 27: ZMPT potential transformer (voltage sensor) [138]

3.2.2 Communication Unit

Wireless communication between the developed module and the microgrid's central server is achieved through LoRa transceivers. The LoRa transceivers create a low-power, long-range transmission network between the consumer modules and local servers (computers) at the microgrid's centre. These LoRa modules used in this research have been designed and developed in the Sensorik Laboratory at Paderborn University [139]. It provides a transmission span of about 2 km, which is the typical radius of microgrids in sub-Saharan Africa.

LoRa modules use work at license-free frequency bands of 433 and 868 MHz [109, 140]. For this project, the frequency band of 868 MHz is used. The license-free band allows the creation of the private Low Power Wide Area Network (LPWAN), which covers the whole area connected to the microgrid.

The RFM96 transceiver is the LoRa module used for this application, giving high immunity [141]. The RFM95TW model of LoRa is used as it offers a matching network and a clock source, as well as simplicity in creating the transceiver [139, 142]. The complete transceiver used in this study is given in Fig. 28.

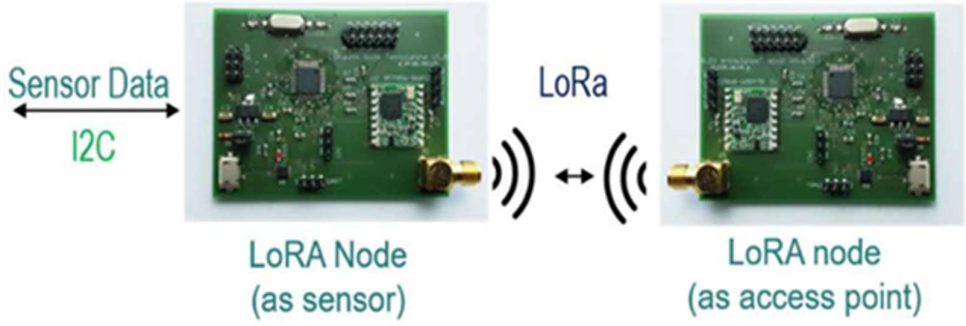

Fig. 28: LoRa transceiver with bidirectional data communication [143]

The LoRa transceiver given in Fig. 28 operates at the 3.3V supply voltage. It also has a load switch which allows the power supply to be turned off, and therefore, it reduces the inactive current of the transceiver during the idle state, which in turn, it saves energy. This module allows using a carrier frequency range of 862MHz to 1020MHz, which allows a greater bandwidth for uplink and downlink without signal interferences. It is recommended to have at least 1.5 times the channel bandwidth as a frequency gap between uplink and downlink frequencies [144]. The transceiver transmits at the power range of 2dB to 20 dB and a total power consumption of 156 mA, which may rise to the pick value of 204 mA when other accessories, such as LEDs and buzzers, operate.

3.2.3 Power Supply Unit

Power Requirement

The power consumption of the LoRa transceiver was measured as a function of the electric current passing through it when connected with a stable power supply of 5V-dc. In his thesis [139], using “Otii Arc" from the company Qoitech as the measuring device [145], the total

transmission power together with the associated LEDs and buzzer for notification was averaged at 193mA with a peak value of 204mA when transmitting at 20dB. Moreover, during the active state, the total power consumption is increased to 265mA when the sensory unit with the current sensor, voltage sensor and relay switches to the addition of the LoRa Transceiver. The power consumption of LoRa transceiver together with the associated LEDs and buzzer drops to 24mA in an inactive state (without transmitting or receiving data), bringing the total consumption down to 85mA with the sensory unit with the current sensor, voltage sensor and relay switches on. The active and inactive states implemented in this system are essential in optimising energy saving in the power supply unit, which saves the battery energy and prolongs battery life.

Table 5: Maximum current consumption

Module Component	Active Mode Current [mA]	Inactive Mode Current [mA]
LoRa Transceiver	204	24
Voltage Sensor	2	2
Current Sensor	15	15
Relay Switch 1	22	22
Relay Switch 2	22	22
Total	**265**	**85**

The module actively transmits and/or receives data on average after every 210s while actively operating for about 1s. The average required current is 85.85mA, as seen in equation (12) below.

$$Average\ Required\ Current = \frac{Current_{(Active)}\ x\ Time_{(Active)}\ + Current_{(Sleeping)}\ x\ Time_{(Sleeping)}}{Time\ period} \quad (12)$$

$$Average\ Required\ Current = \frac{265\ mA\ x\ 1s\ + 85mA\ x\ 210s}{211s} = 85.85mA$$

Thus, to operate this wireless sensing module with a 5V supply, a total power of 429.25mW is required, as shown in equation (13) below.

$$Power\ Required = Voltage\ x\ Current\ = 5V\ x\ 85.85mA = 429.25mW \quad (13)$$

Energy Source

For the module to provide precise data transmission, it must operate with a stable power supply. The developed wireless sensory module has a standalone, stable, and reliable power supply independent of the microgrid. An independent power supply ensures the module functions even when a faulty or blackout is in the mini-grid. This system's power supply unit can harvest solar energy or use electricity from the power-line.

Photovoltaic (PV) - Energy Harvester

Solar energy harvester comprises a solar cell and a rechargeable battery for energy storage and backup. It harvests energy during the daylight period and will use the energy stored in the rechargeable batteries during night-time. Fig. 29 below stipulates how the power unit for this system harvests energy and supply to the system loads.

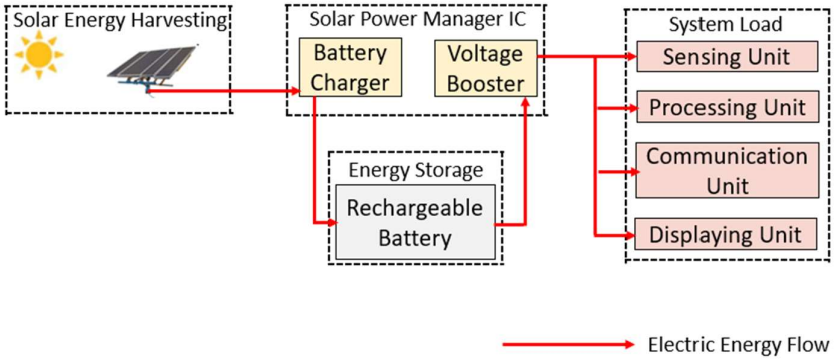

Fig. 29: Solar energy harvesting for powering the system

This research study uses a high-efficiency monocrystalline-Silicon solar panel to develop prototypes. The panel has a size of 133 x 73 mm. It generates a maximum power of 1.25W with an open-circuit voltage of 6V and a short-circuit current of 210mA. The panel can be illuminated even with an indoor light source (around 200 lux), giving an open-circuit voltage of about 5.2V. The panel output current of 210mA is sufficient to power the sensory module and charge the storage battery simultaneously. Therefore, the PV energy harvester module can supply enough energy for this LoRa-based sensory module at illumination conditions as low as 200 lux.

Fig. 30: Monocrystalline-silicon photovoltaic panel

Power-line - Energy Harvester

In this energy harvester, the electrical energy is tapped from the AC power line, bringing electricity to the particular consumer. Fig. 31 shows a block diagram of a power line energy harvester. It consists of an AC-DC converter which gives out a 5V-dc for powering the prototype system.

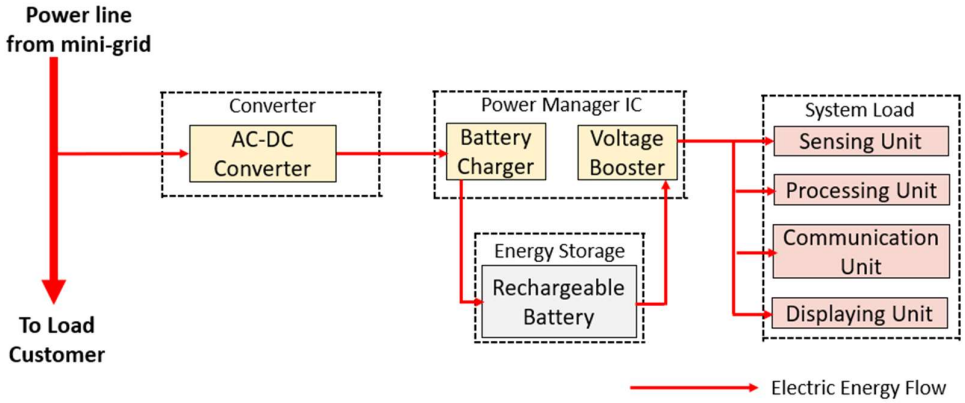

Fig. 31: Energy harvesting from AC power-line

Energy Storage

With solar PV, the sensor module can be powered with enough illumination during the daytime. However, a different energy source is required at night to power the LoRa-based sensory module. Nonetheless, the energy harvested in day time can be stored and utilized at night or during dark times.

There are different ways of implementing electric energy storage, such as rechargeable batteries and super-capacitors, for powering low-power sensory devices. In the development of this system, various parameters have been considered in storage selection, as summarized in Table 6.

Table 6: Comparison between super-capacitor and Li-ion batteries for energy storage

	Super-Capacitor	Battery (Lithium/ Lead Acid)
Energy Density [J/Kg]	Low	High
Power Density [W/Kg]	Higher	Very low
Cell voltage	High cell voltage up to 5.5V	Cell voltage up to 3.7V
Discharge voltage factor	• Decreasing voltage output during discharging (need boost converter) • Self-discharge rate is higher (not suitable for long-term storage)	• Relative constant output voltage • Low self-discharge rate
Charging Time	Fast charging	Relative slow charging
Risk factor	Can be damaged if charged with more than rated voltage.	Can explode if overcharged or charged with higher than rated current
Cost	About 10 times higher than Li/Pb Batteries [High cost per Watt-hour]	Relatively cheaper [low cost per Watt-hour]
Life span	High	Low
Remarks	Suitable for high energy – short time applications	Low energy – long time applications

Based on the comparison in Table 6 above, the Li-ion battery shown in Fig. 32 is used for this project. The Li-ion battery is used as it provides higher energy density and relative constant output voltage with a low self-discharge rate. A prolongation of the battery's life span can be achieved by the implementation of the power management circuit (as explained in the following section). Moreover, the batteries are cheaper and more suitable for low-economy countries in Africa, where the project is intended to be deployed.

Fig. 32: LiPo rechargeable battery

With the 1500mAh, and voltage supply of 3.7V, the battery is theoretically capable of providing 5,550 mWh as shown in equation (14).

$$Energy\ Stored\ =\ Voltage\ x\ Current\ x\ Time\ = 3.7V\ x\ 1500mAh = 5550mWh \qquad (14)$$

The LoRa-based module developed requires an average power of 429.25mW for its operations (as calculated in equation (13) above), equivalent to 13 hours, as shown by equation (15).

$$Storage\ Usage\ Time = \frac{Power\ Stored}{Instant\ Power\ Required} = \frac{5550mWh}{429.25mW} = 13\ hours \qquad (15)$$

The usage time of 13 hours theoretically shows that the consumer module can work during the night hours when there is no sunlight.

Power Management IC

A Power Management Integrated Circuit (IC) has been deployed in this module to maximize the usage of the harvested energy from PV or AC power line. The IC is used to manage the charging and discharging of the battery, which protects and prolongs the battery's lifetime. The IC contains the boost circuit, which ensures the constant supply of 5V to the system load. Fig. 33 shows the Power Management IC used in this system.

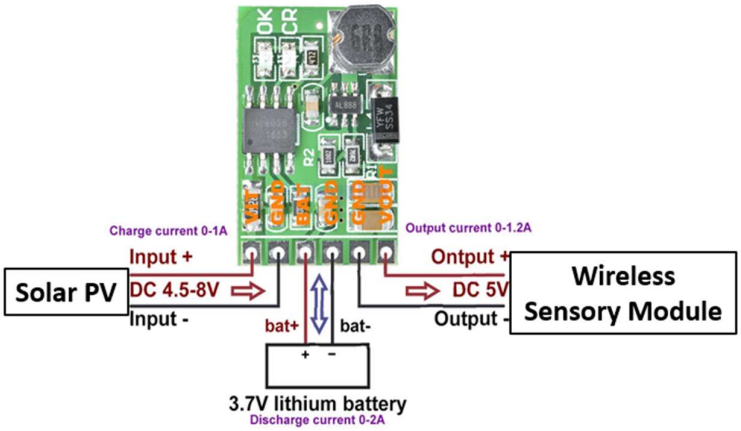

Fig. 33: Power Management IC with connection to solar PV, rechargeable battery and LoRa sensory module [146]

3.2.4 Control (Demand-Response) Unit

The main goal of this study is to manage the demand side so that the power consumption does not exceed the generation, hence attaining sustainability of the microgrid by preventing overloading. The system will advise the client to reduce power consumption based on the total available energy to achieve this primary goal. Two levels of control have been employed in this study for demand-side management, as explained below:

Traffic Lights Display

Consumers will be advised to switch on and/or off some loads based on the analysis of both the currently generated and available stored energy to avoid microgrid overloading,. The host computer does this analysis; then, the host computer sends a controlling signal to the consumer unit. The controlling signal from the host computer is received and processed by the consumer module, and the information will be displayed to notify the customer of a change in tariff (electricity price).

The display system has three states displayed by switching on a red, yellow, or green light-emitting diode for peak, off-peak, and low power consumption times, respectively, as shown in Fig. 34. This information is sufficient for the user to decide on the power use. As the user is trained to the meaning of the colours, they will know that the red light indicates high costs for electricity, whereas the green light means low prices [147].

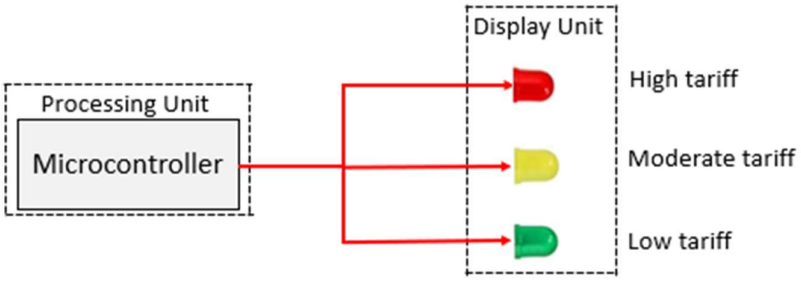

Fig. 34: Traffic-light display unit

Moreover, the piezoelectric buzzer, shown in Fig. 35, has been used to catch the consumers' attention while notifying them of the tariff change based on their power consumption.

Fig. 35: Piezoelectric buzzer

Furthermore, a Liquid Crystal Display (LCD) screen, shown in Fig. 36, is implemented within this system. It displays the real-time power units available for a particular customer and his/her current tariff type. The visual presentation helps a consumer to understand and plan better on his/her electricity usage pattern. The display uses an I2C serial communication bus for data communication from the MCU.

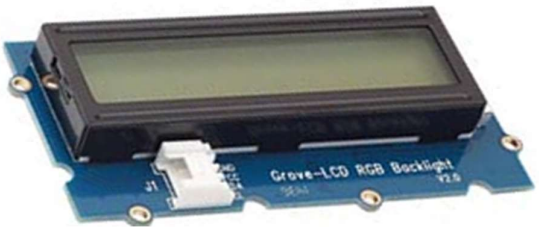

Fig. 36: LCD 16-by-2 screen

Direct Load Control

The tariff-based demand-side management proves to be useful for financially sensitive people. However, some people may ignore the control signal as they can pay for electricity at a higher tariff. To avoid the overloading and, subsequently the blackouts, this study has employed Direct Load Control (DLC) as another DSM technique together with the tariff-based DSM. DLC allows the microgrid utility company to directly control the total load from different consumers, and it is convenient when the consumers' behaviour to price sensitivity differs significantly [148].

In this study, the DLC is activated when there is a prolonged time (in this prototype, it is set to be 30 minutes) of the usage of red (high) tariff by the consumer, which might risk the sustainability of the whole microgrid. DLC is implemented using an electronically driven relay switch, a flip-flop latch relay. The relay is configured to defaultly connect the Common (COM) input to the 'Normally-Closed' (NC) output, and therefore, it allows the electricity flow, as shown in Fig. 37(b). However, when the usage is red-state, and there is a danger of overloading the microgrid, the microcontroller will send a signal to the relay to switch-off power to the subsequent load/consumer. When the relay receives the switching signal to switch off the load, it triples and connects to the 'Normally-Open (NO) state. Fig. 38 explains how the connection and disconnection of the load happen in this system.

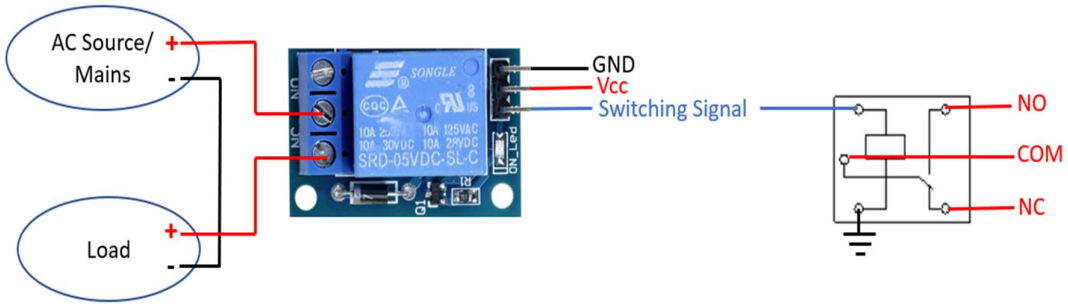

(a) (b)

Fig. 37: (a) The relay switch connection between power supply and load; (b) Internal structure of the relay switch

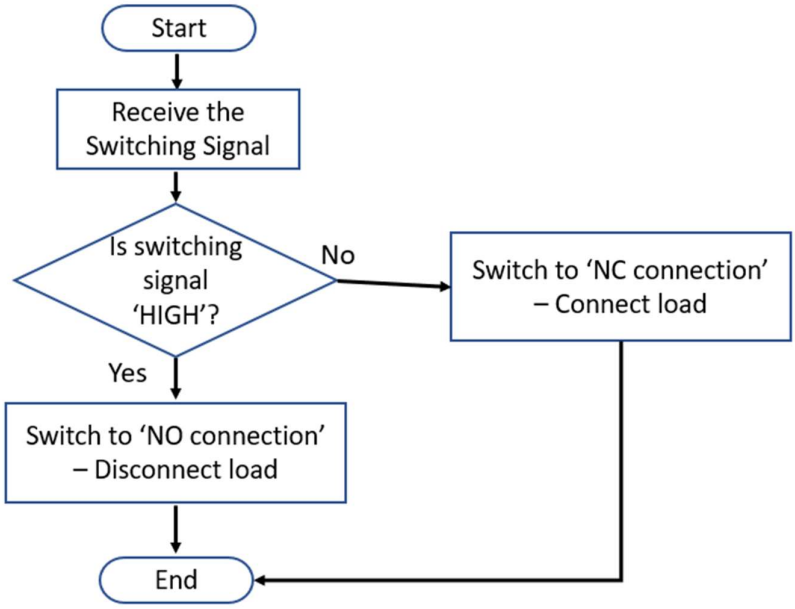

Fig. 38: The flowchart operation of the DLC technique using the Relay-switch

3.2.5 Processing Unit

The PU is used as the brain of this sensor module. The microcontroller governs all operations of this module. An Arduino 8-bit ATmega328p microcontroller has been employed in this system. The ATmega328p microcontroller provides various functions and development options with Arduino development boards and fundamental programming languages such as C and C++ [149]. Arduino-based ATmega328 also provides a large number of 28 pins of input/outputs; among them 6 pins are for analog input with built-in ADCs at the speed of up to 8MHz, and 12 pins are for digital input/output working by the voltage level of 0-5V [150].

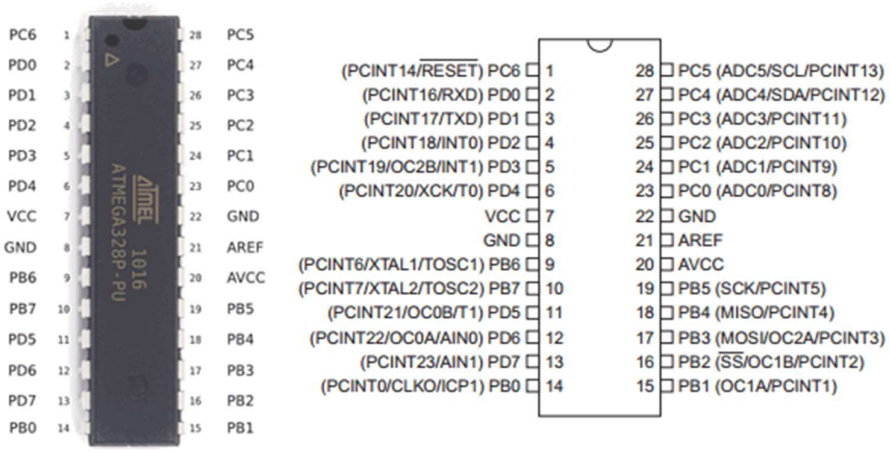

Fig. 39: ATmega328P microcontroller with pin-mapping

This microcontroller-based sensory module has been designed to carry out the following functions; real-time customer load monitoring, wirelessly communicating to the host computer, and provision of demand-side response and billing. The microcontroller operations are explained below;

Electricity Metering (Load Monitoring)

The microcontroller activates the current and voltage sensors, explained in section 3.2.1, to take the current and voltage measurements. The measured analogue values are converted into digital values by the microcontroller's ADCs. The digital values can be manipulated to obtain different desired results.

Based on the current and voltage values, the consumed load is computed. Then microcontroller activates the wireless transceiver and sends the calculated load value to a host computer. Fig. 40 explains the load monitoring process. Moreover, the sensory module will send any abnormal voltage and/or current reading to the host computer as an alert for power quality control in the mini-grid.

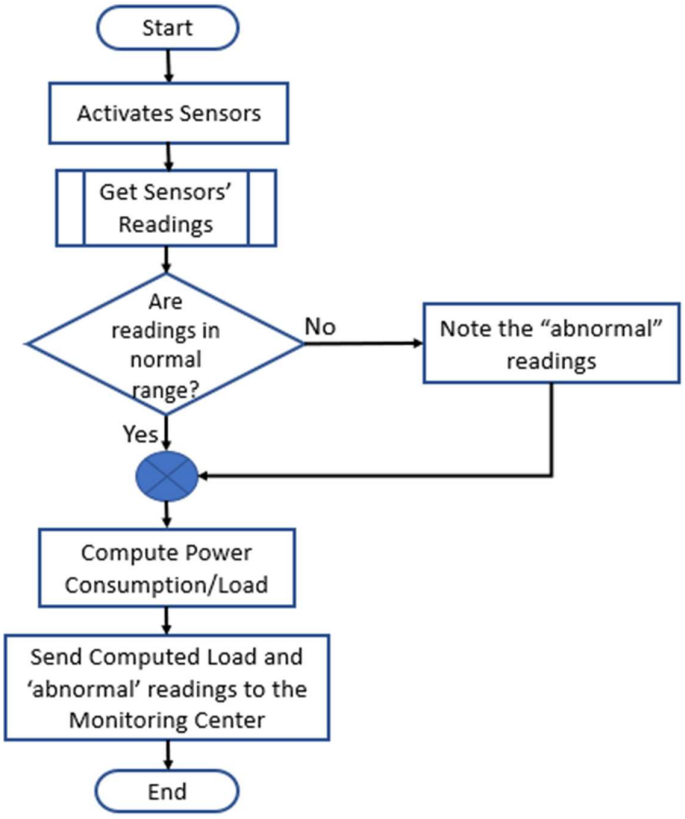

Fig. 40: The process flow for load monitoring and power measurement

LoRa-based Bidirectional Wireless Communication

The microcontroller unit (MCU) switches on the RFM95 of the LoRa module to initiate the data transfer and/or data receiving operations. MCU also initializes the Serial Peripheral Interface (SPI) as the communication with the LoRa module takes place via the SPI interface

To achieve bidirectional communication, the MCU is programmed to set to different frequencies, i.e. 868.1 MHz and 886.1 MHz are used in this study; for uplink (data transmission) and downlink (data reception), respectively. Fig. 41 explains how the uplink and downlink operation is achieved.

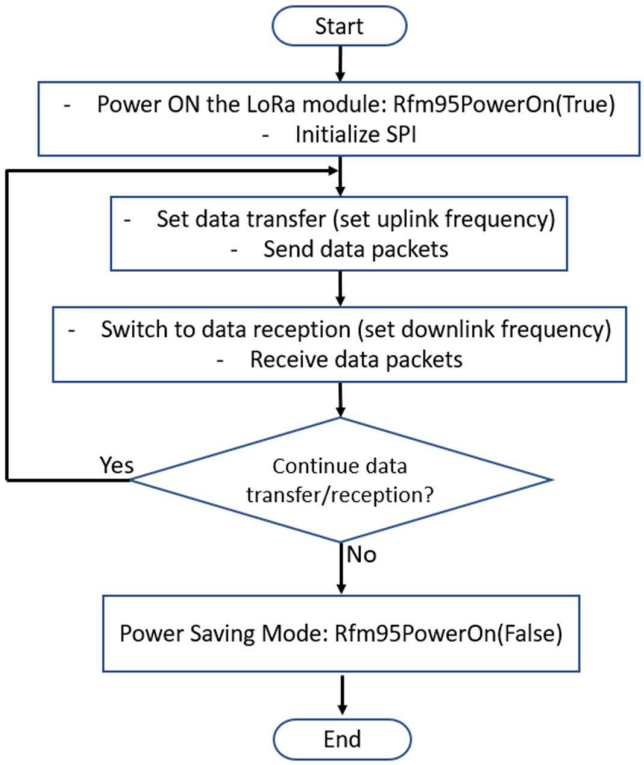

Fig. 41: Process flow for bidirectional communication (uplink and downlink)

Demand Response Control

The microcontroller compares the actual computed load with the power consumption limit received from the host computer. With the comparison, if the consumer load is below the limit, the microcontroller will send a signal to the display unit to light on the green LED. Similarly, if the load is around the limit or greater than the limit, the microcontroller will send a signal to the display for yellow LED or red LED, respectively. Fig. 42 gives the logical flow of lighting the green, yellow, and red LEDs for demand response control.

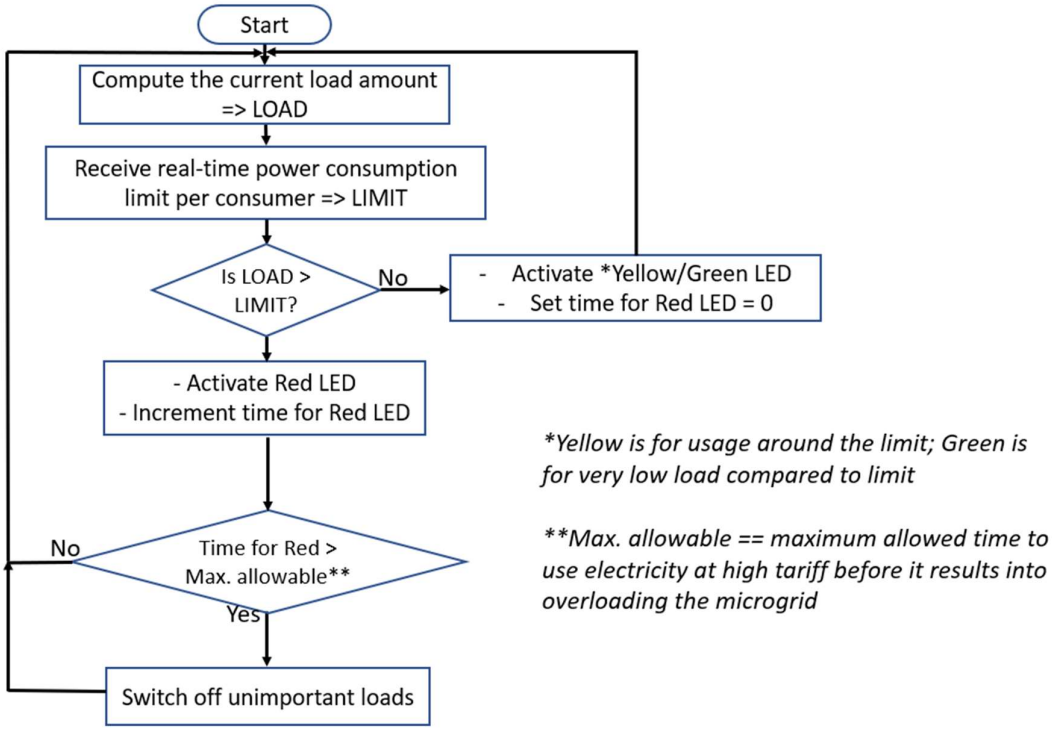

Fig. 42: Flowchart for demand response and load management

Moreover, the microcontroller is configured to evaluate the consumer reaction to the red LED indication. Suppose the consumer uses electricity at red LED for a long time. In that case, the microcontroller will send a signal to trigger the relay (as explained in section 3.2.4) and switches off the electricity supply to some loads (unimportant/non-critical loads) to flatten the consumption curve and avoid the power blackout due to overloading.

Electricity Billing

The traffic-light demand-side management uses a particular tariff for each colour. The implementation of a tariff-based approach has given this system the ability to be used for customer billing. The customers usually buy electricity in terms of units (measured in kWh). The units can be updated by adding them when more units have been bought and by deduction based on the power consumption and particular tariff. Fig. 43 explains how the billing is achieved.

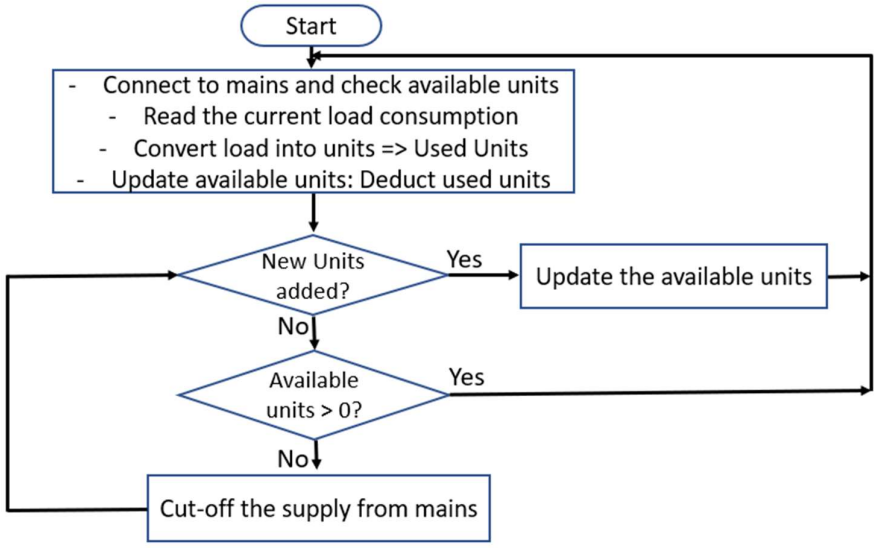

Fig. 43: Flowchart on the updating electric units and billing

3.3 Hardware Prototyping

The development prototype was done by connecting some development boards from manufacturers. Three separate circuits: solar energy harvesting circuit, high voltage circuit, and low voltage circuit boards were distantly isolated and connected through the breadboard and plug-in cable.

The solar energy harvesting circuit comprises an energy harvester (it can use either a solar PV cell or from a power line), PMIC, and Li-ion rechargeable battery. The high-voltage circuit consists of a relay switch, a current sensor, and a voltage sensor. Lastly, the low-voltage circuit includes an MCU and the LoRa module for wireless communication.

3.3.1 Circuit Building

LoRa Transceiver

Fig. 44 shows the circuit for the LoRa transceiver for data transmission and reception to the host computer. All the circuits in this research study were drawn using an Electronic Design Automation (EDA) – *Eagle Autodesk*.

This LoRa transceiver acts as a modem. It has Universal Serial Bus (USB) connector for serial data communication to and from a host computer. Communication between the microcontroller and a LoRa module occurs via the SPI interface.

The 5V-dc supply of the USB interface serves as the input voltage for the transceiver circuit. There is an LED to indicate when the transceiver is on and operating. An 8MHz crystal is added into the circuit as a clock source for the microcontroller.

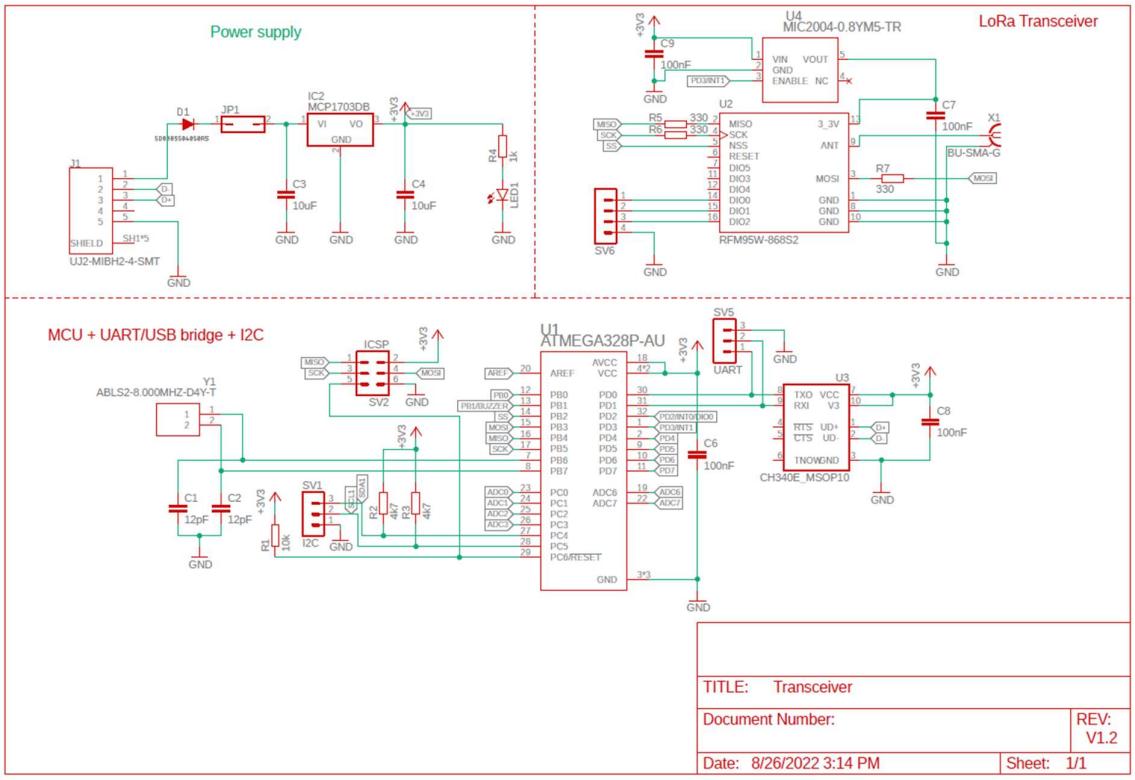

Fig. 44: Schematic circuit for LoRa transceiver

Consumer Module

The consumer module prototype was built and optimized in two independent circuits. One circuit is for control (a low-voltage circuit), and another circuit is for high-power measurement (for measuring the load connected to the supplies in the consumer modules).

A low-voltage circuit main consists of a microcontroller and a LoRa module. This circuit has some added features and components, including a visual display via 3 LEDs, sound output via a buzzer, and data transmission via USB. There is also an ISP/ICSP programming interface that can be accessed via a 2x3 connector strip. Moreover, there is an 8-pin connector available for connecting to the high-power circuit. Fig. 45 shows the circuit schematic diagram for the Control (low-voltage) Circuit. The list of components (with their circuitry nomenclatures and specific functions) is provided in appendices I and II.

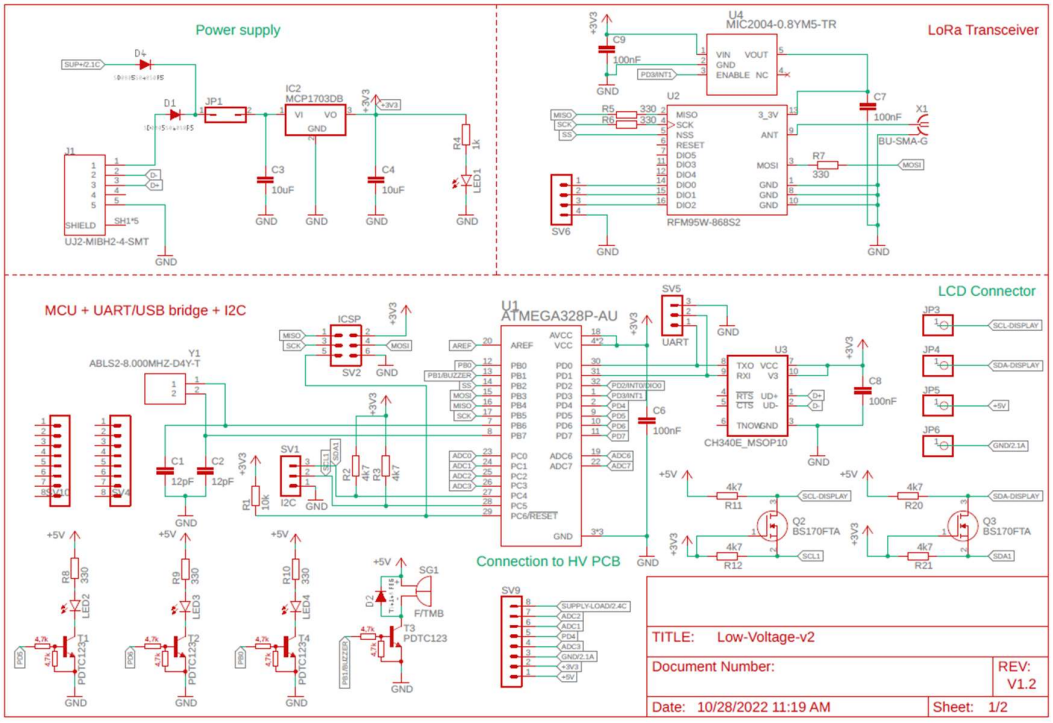

Fig. 45: Schematic circuit for the low-voltage control unit

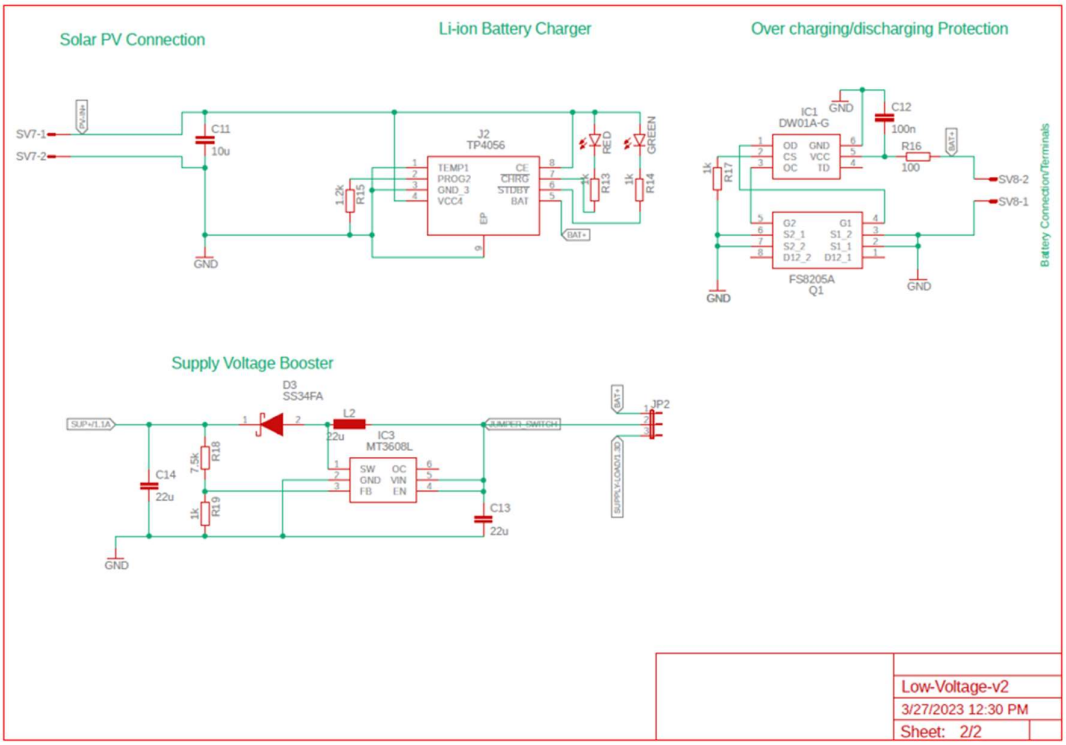

Fig. 46: Schematic circuit for the solar energy harvester and power supply

In addition, the power supply circuit was built and linked to the low-voltage circuit. The solar energy harvester and power supply circuit are given in Fig. 46. It includes the connections to the solar energy harvester's PV panel, rechargeable batteries, and 5V from any other regulated source (using a 3-connector jumper, JP2). The circuit includes a Li-ion battery charger with overcharging and over-discharging protection. There is also a voltage booster which ensures the final supply voltage is always regulated to 5V regardless of whether it is supplied from the PV panel, battery, or from mains.

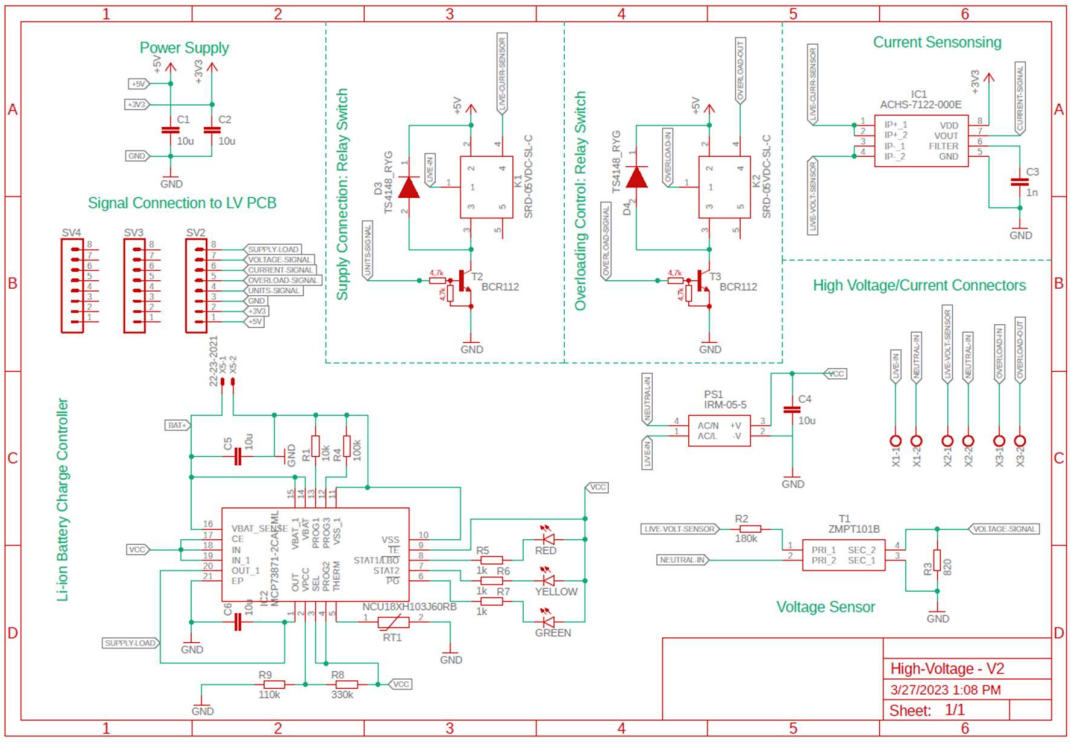

Fig. 47: Schematic circuit for the high-voltage connection

A high-voltage circuit is shown in Fig. 47 above. It is mainly made up of current and voltage sensors for AC mains. These sensors are used for measuring the amount of power consumed by the consumer load. The circuit also consists of the high-voltage relay switches used for load shedding when executing the load control for consumers with overload. In addition, the AC-DC converter is also available to provide the entire circuit with 5V dc power supply as well as charge the batteries; this is an alternative power supply to the PV-panel-based energy harvester.

3.3.2 PCB Layout

All the circuits explained in section 3.3.1 above were converted into Printed Circuit Board (PCB) layouts. These layouts were prepared for the preparations of the circuit boards to be used for mounting all components (including sensors, microcontroller, and LoRa modules), explained in section 3.2 of this dissertation. The PCB layouts for the LoRa transceiver, low-voltage circuit, and high-voltage circuit (for a consumer module) are given in Fig. 48 to Fig. 50.

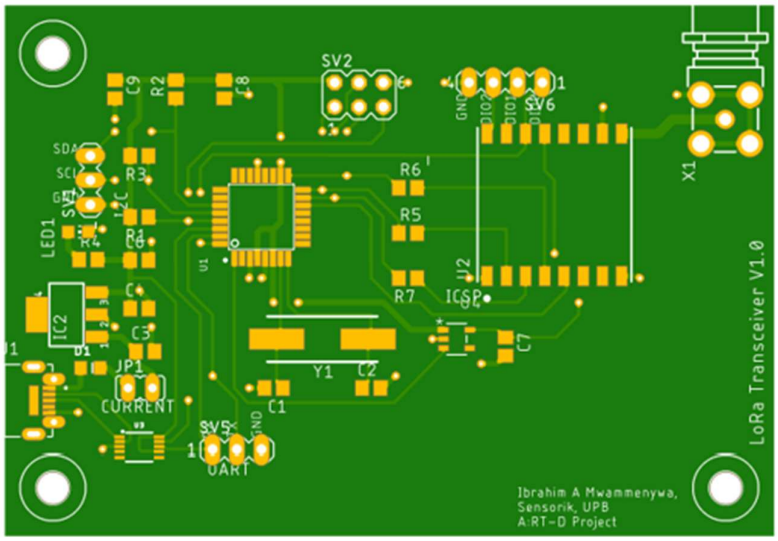

Fig. 48: PCB layout for the LoRa transceiver

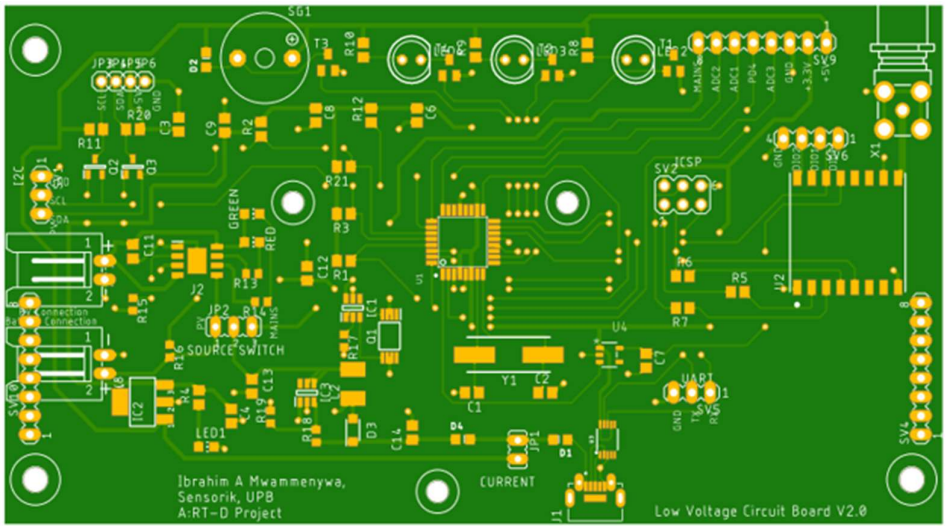

Fig. 49: PCB layout for the low-voltage control unit and solar energy harvester circuits

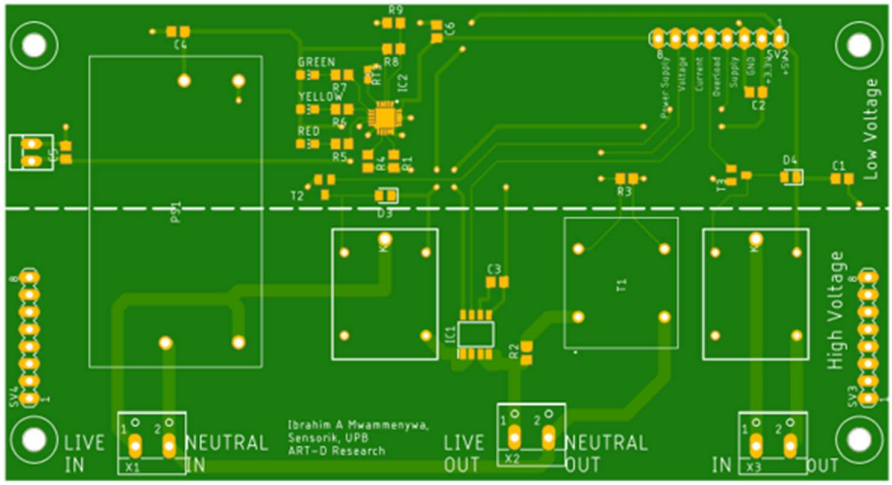

Fig. 50: PCB layout for the high-voltage circuit

In the PCB layouts shown in Fig. 48 to Fig. 50 above, the conductive lines to be printed or etched vary in width and depth depending on the calculated maximum current expected. It was considered to avoid the over-heating and consequently burning of the PCBs (especially the high-voltage PCB).

3.3.3 PCB Implementation

Two pieces of transceivers and five consumer modules were fabricated. The implementation involved soldering SMT and THT components based on the specification and design of the circuit. These devices were used to test their intended functionalities' accuracy and performance.

After corrections and improvements on the designs and layouts, four pieces of transceivers and 65 pieces of consumer modules were fabricated based on the PCB layouts given in section 3.3.2 above. Fig. 51 to Fig. 53 show the completely soldered PCBs for a transceiver and a consumer module.

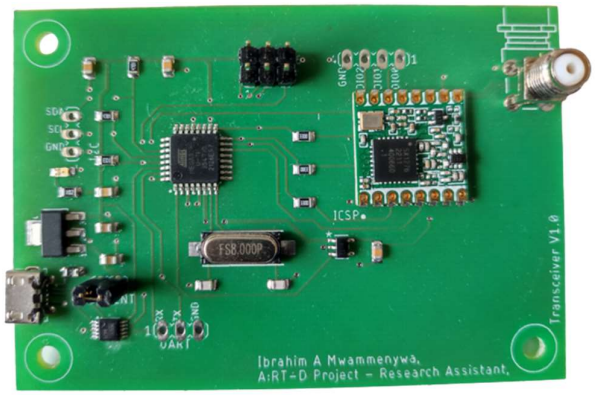

Fig. 51: Soldered/mounted PCB for the LoRa transceiver

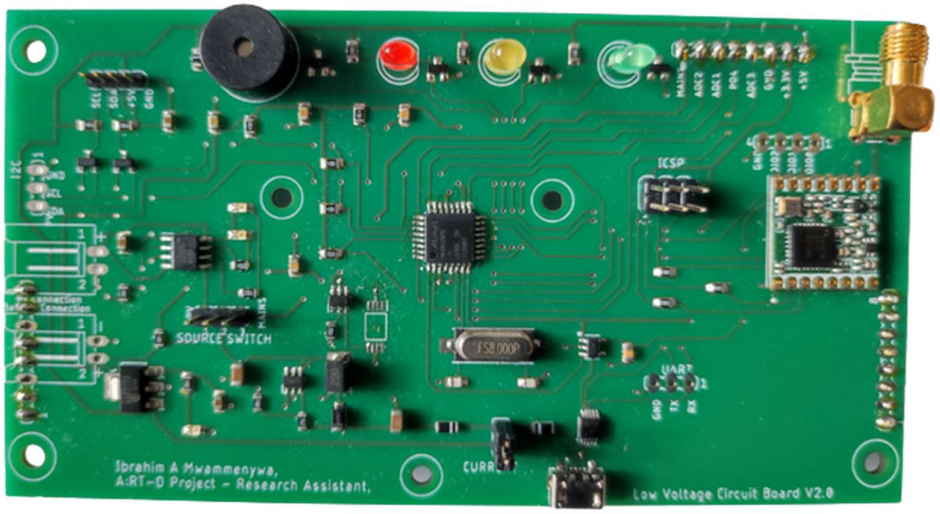

Fig. 52: Soldered/mounted PCB for the low-voltage circuit

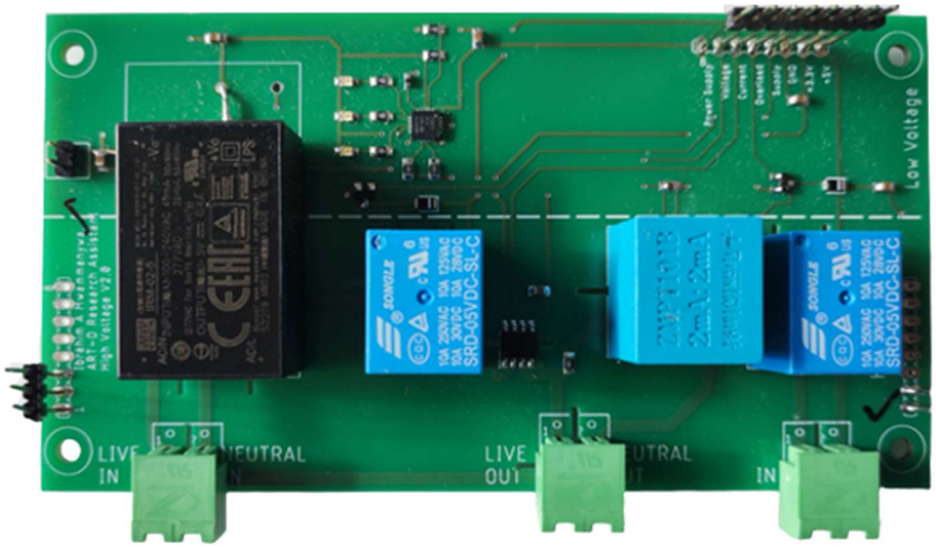

Fig. 53: Soldered/mounted PCB for the high-voltage circuit

The fitting of low-voltage and high-voltage PCBs is so that there is a 10 mm spacing between the two PCBs. The air gap in between acts as an insulation gap, as observed in Fig. 54(b).

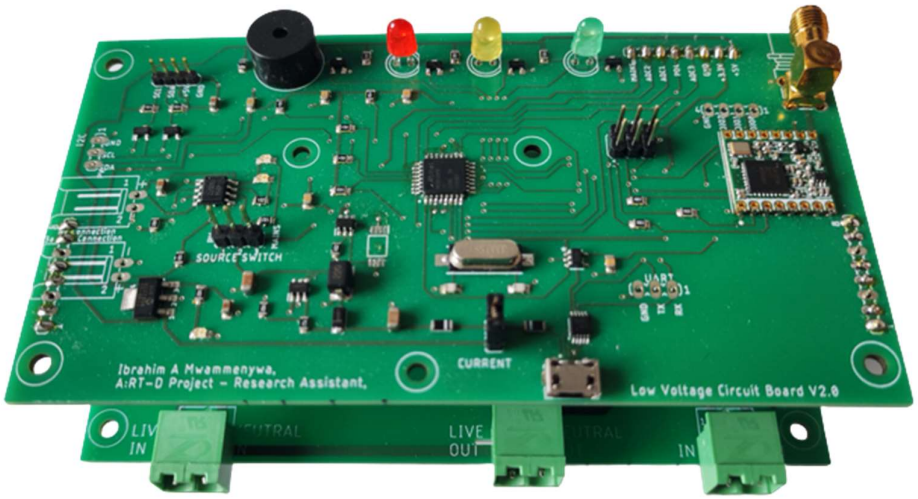

(a)

(b)

Fig. 54: Fitting of the low-voltage on the high-voltage PCBs

These fabricated and soldered PCBs were assembled and fitted in electrical enclosures of GAINTA model G265CMF. These enclosures are made of polycarbonate material with a tightness of IP65 which ensures the protection of the PCBs from water and dust [151]. The transparent lid allows consumers to have a clear view of the traffic lights of the consumer modules and ensures safety for the users.

The implementation of this prototype costed 30 € for each LoRa transceiver and 55 € for each consumer module. This cost is based on the list of the electronics components provided in appendices I and II, and the IP65 enclosure for each module.

Fig. 55: Soldered PCBs inside fitted inside enclosures

3.3.4 Prototype Testing

The developed prototypes of the LoRa transceivers and consumer modules were tested for their intended functionalities. Different functionalities were performed, and the performance was analysed. The current and the voltage sensors (of the consumer module) were performed at different voltage and current values, as shown in Tables 7 and 8, respectively. Voltage and current sensor readings were compared to an accurate and precision laboratory standard multimeter, Keysight model U124B. The developed sensors gave an absolute error of about less than 5% and 0.3% for current between 0 – 5A and voltage readings between 210 – 240V respectively, the standard AC line voltage for different consumers connected in the microgrid.

Table 7: Voltage readings compared between standard multi-meter and developed consumer module

True Value (V)	Sensor Reading (V)	Absolute Error (%)
200	199.11	0.44
210	209.40	0.29
220	219.70	0.14
230	230.3	0.13
240	240.30	0.13
250	247.16	0.92
260	257.46	0.98
270	267.76	0.83

Table 8: Current readings compared between standard multi-meter and developed consumer module

True Value (A)	Sensor Reading (A)	Absolute Error (%)
0	0.007	Offset
1	0.97	3
2	2.02	1
3	2.98	0.67
5	5.21	4.2
7	7.46	6.67
10	10.82	8.2

The high-voltage PCBs were subjected to the rated current, 10 A maximum RMS current, and the heating effect was observed. With this high current, a temperature of about 70°C to 90°C was observed. An improved version using wider traces and connecting cables acting as external shunt resistors on the back of the board was implemented. Fig. 56 shows improved PCBs that did not dispatch heat that could burn it and lead to any safety concerns for the users (when installed in consumer households).

Fig. 56: The thermal test of PCB to the maximum rated current of the current sensor

Furthermore, the RoLa transceiver was tested for transmission range by using different values of SF and BW for each range measurement. During the testing, 225 data sets, each with a 4-byte payload, were sent at 20 dB output amplification. Table 9 shows the range measurement results of the transmission time, SF, and BW. As the results of the multiple measurements show, selecting the longest possible transmission duration via the parameters SF and BW is prudent to achieve the greatest possible transmission range. For this study, it is possible to cover the range of 1 km to 2 km (typical radius of rural villages) in suburban and rural areas with a BW of 62.5 kHz, SF of 12, and 20dB of transmitted power.

Table 9: Range measurement results [113]

Range [m]	BW [kHz]	SF	Transmission Time [ms]	Packet Received [%]	Received Signal Strength [dBm]
200	62.5	12	1654.78	100	-126
		10	413.69	100	-125
		8	123.9	100	-120
	125	12	827.39	100	-123
		10	206.84	100	-124
		8	61.95	100	-121
400	62.5	12	1654.78	100	-132
		10	413.69	92	-137
		8	123.9	100	-131
	125	12	827.39	100	-132
		10	206.84	100	-131
		8	61.95	92	-132
600	62.5	12	1654.78	100	-134
		10	413.69	100	-133
		8	123.9	100	-136
	125	12	827.39	100	-136
		10	206.84	100	-132
		8	61.95	100	-132
800	62.5	12	1654.78	100	-137
		10	413.69	100	-137
		8	123.9	100	-134
	125	12	827.39	100	-138
		10	206.84	100	-137
		8	61.95	8	-133
1000	62.5	12	1654.78	100	-138
		10	413.69	100	-139
		8	123.9	24	-136
	125	12	827.39	0	-
		10	206.84	0	-
		8	61.95	0	-

3.4 Host Computer

Fig. 57 shows that every consumer module wirelessly communicates to the host computer using LoRa technology. Among the tasks of the host computer in this design is to receive power consumption data from the consumer module, PV power generation data, and the State of Charge (SoC) of the battery in real time. The received data are processed using FLC in the host computer, and the host computer issues the power-controlling signal that is wirelessly transmitted to the consumer modules.

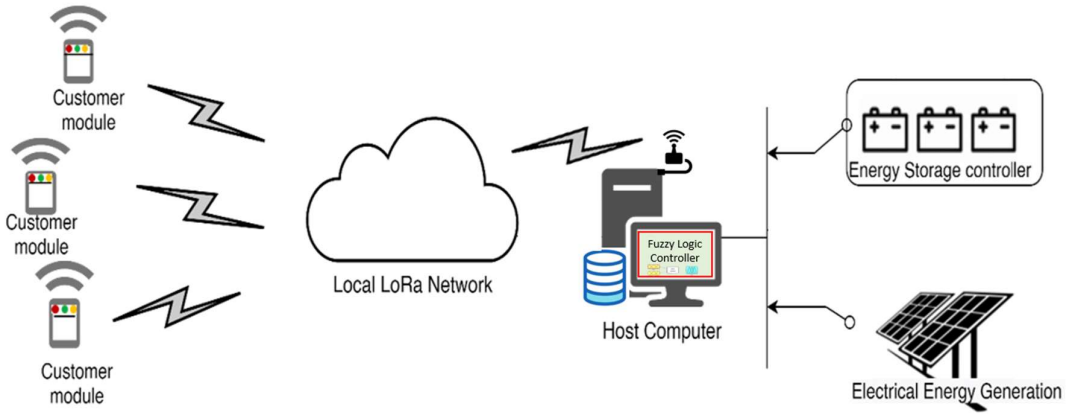

Fig. 57: Host Computer as the brain of the model

The optimum specifications of the host computer are given in Table 10 below. The host computer is connected to a LoRa transceiver to enable the LoRa wireless bidirectional communication with consumer modules. Moreover, this computer is configured with the database (explained in chapter four - section 4.3.2) to store all data from consumer modules, PV generation, and battery's SoC measurements. Moreover, the computer will be equipped with an FLC application that provides real-time load control signals (explained in chapter four - section 4.3.3). Real-time load control signals will be wirelessly sent to consumer modules.

Table 10: Optimum specifications of the host computer

Specification	Value
RAM	12 GB
Storage (HDD)	> 1 TB
Processor	> Intel core i5 > 6th Generation processor of 4 cores with minimum clock speed of 2.4 GHz
Operating System	Windows 10 or above

3.5 Chapter Summary

In this chapter, the LoRa-based transceiver and consumer modules prototypes development have been presented in detail. The process of a prototype implementation, starting from conceptual designing, circuit building, components selection, and final prototyping and testing, has been elaborated. This chapter only concentrated on the hardware building of the prototype. The software (firmware and application) running in these prototypes is discussed in the next chapter of this dissertation.

CHAPTER FOUR

FIRMWARE AND PC SOFTWARE DEVELOPMENT

4.1 Introduction

In the previous chapter, the hardware prototypes of the LoRa-based transceiver and consumer modules were developed and tested. In this chapter, the firmware running in the consumer module and the PC software in the local server (or a computer) are elaborated.

4.2 Firmware Development

The firmware development started with coding in an Arduino Integrated Development Environment (IDE). Arduino IDE provides easy access to some libraries to get started with the ATmega328P on the Arduino development board, such as the Dragino Arduino LoRa shield shown in Fig. 58, was used in this project.

Fig. 58: Dragino's arduino LoRa shield

In expanding the functions of the developed module and including other components such as sensors, the firmware development was shifted to Atmel Studio 7 IDE and coded using the C++ programming language. An AVRDUDE software was first integrated to use the pre-installed boot loader in Arduino [152]. An Atmel AVRISP MKII USB-ISP programmer, shown in Fig. 59, was used to load the developed firmware on the prototype [153].

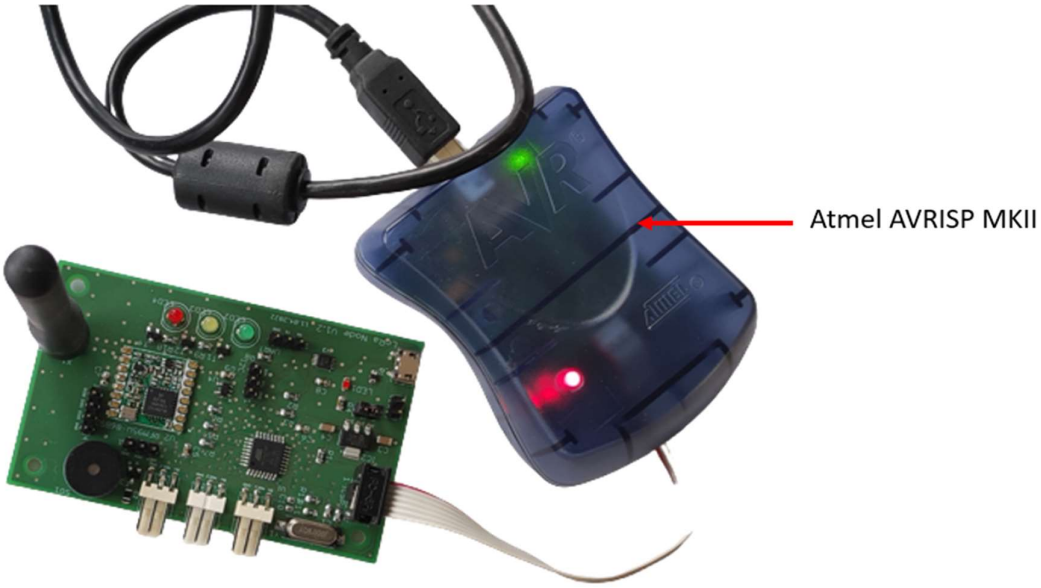

Fig. 59: An Atmel AVRISP MKII USB-ISP programmer

Different code files and functions were developed in the development of this firmware. The functions were also linked with various existing libraries of Arduino and the RFM95 LoRa module. The program code files and functions are explained below in detail;

4.2.1 ACS712.cpp

ACS712.cpp is the file containing the code for the MCU to process the readings from the current sensor and provide the root-mean-square (RMS) of the current value. This file contains the following functions;

ACS712(ACS712_type type, uint8_t _pin)

This function takes in two arguments: the current sensor type (ACS712 type) and the MCU pin number connected to it. With the type of the current sensor, the MCU is programmed to use a pre-defined current sensitivity of the sensor reading. Furthermore, the current sensitivity can be manually defined to increase its accuracy if the developer has standard meters and an oscilloscope.

int calibrate()

This function reads the analogue input value from the current sensor. It maps the voltage signal from the current sensor to an integer value between 0 and 1023 for a 10-bit ADC in ATmega328P used in this research.

float getCurrentDC()

This function calibrates the current sensor's DC current offset from the integer value returned by the function *int calibrate()*. This value is helpful in removing the offset error in the measurement. It is executed before the function *float getCurrentAC(uint16_t frequency)*.

float getCurrentAC(uint16_t frequency)

The function gives the final AC current value read by the current sensor. It uses the frequency argument for sampling and the *float getCurrentDC()* to remove the DC offset value and return the RMS current value.

4.2.2 ZMPT101B.cpp

ZMPT101B.cpp is a C++ code file containing the MCU code to process the readings from the voltage sensor and provide the respective root-mean-square (RMS) of the voltage value. It includes functions: *int calibrate(), float getVoltageDC(),* and *float getVoltageAC(uint16_t frequency)* with similar functions to the respective function in the ACS712.cpp file explained in section 5.2.1 above.

4.2.3 LoRa Module Programming Files

This study employs the RoLa module initially developed by Phillip Holle in Sensorik Lab [139]. Some of the code files in the firmware of the used RoLa transceiver module were used as the libraries during the development of the firmware for the wireless sensory system for monitoring the microgrid. Code file such as rfm95w.c, spi_atmega328p.c, and uart_atmega328p.c are referenced to provide different LoRa transceiver module

functionalities, as explained in [139]. However, some functions in those files were manipulated and improved with different suitable configurations in the main file of this firmware, sketch.cpp which is explained in section 4.2.4 below.

4.2.4 Sketch.cpp

Sketch.cpp is the main file for this firmware. It contains all the program sequences for initializing and using the functions of the wireless sensory system for monitoring the microgrid, as explained in chapter three – section 3.2. This file can be used as the stepping foundation for further improvement of this prototype. Furthermore, this file allows the definitions of several parameters linked to other files and libraries without going to those particular code files. This file contains some crucial functions, as explained below;

```
void setup()
```

In this function, all the important parameters are defined. The MCU's input and output pins are clearly set, and their states are defined within this function. Moreover, in this file, the serial clock sequence is set, and the LoRa transceiver operations are initiated by invoking the functions `void Rfm95PowerOn(True)` and `void SpiInitMaster(),` which are in files *rfm95w.c* and *spi_atmega328p.c* respectively.

```
void loop()
```

This is a function that runs the main program sequence. The main program sequence is made up of small sequences which were programmed in different functions for programming simplicity and easy debugging. Table 11 below explains the different micro functions in the main function `void loop()`.

Table 11: Functions within main program file and their tasks

Function Name	Details
`void loading()`	It enables the current and voltage sensors to start sensing electric current and voltage respectively
`void mainsOn()`	It enables the relay to switch on and allow the electricity connection from mains to the consumer
`void loadControlOn()`	It enables the relay to switch on and supply the non-critical load with electricity
`float currentRead()`	It invokes the MCU to read an instant electric current value from the current sensor and returns RMS current value
`float voltageRead()`	It invokes the MCU to read an instant electric voltage value from the current sensor and returns RMS voltage value
`float loadCalculator (float I, float V)`	It computes the total power consumption of the connected load
`void Rfm95ChangeCarFreq (float carFreq)`	It allows to change the carrier frequency as different frequencies are used for uplink and downlink.
`void dataTransfer(float *data, uint8_t sizeOfData)`	It allows the LoRa transceiver to send a specified data array of up to 127 bytes
`void dataReceiver(float *firstElementOfData, uint8_t *lengthOfData)`	It allows the LoRa transceiver to receive a specified data array of up to 127 bytes
`int setAlert(float load, float powerLimit)`	It compares the consumer's load to the limit value received from central server and sets up the tariff level
`float notification (int alert)`	It enables MCU to send the notification signal (demand-response based on the traffic light and buzzer to catch the consumer attention on the change of tariff)
`void loadControl (int redTotalTime)`	It enables the MCU to disconnect non-essential loads if a consumer is overloading the microgrid over the allowed time
`float unitsCalculator (int id, float newPowerUnits, float consumedUnits, float index)`	It computes the available units by adding new units (if any) and subtracting the consumed units over the time
`void mainsControl (double availableUnits)`	It checks the available units. If there is no available unit, it cuts off the electricity supply
`void lcdDisplay(double availableUnits, int alert)`	It prints the values of the remaining/available units and the current type of tariff in use on the LCD screen

4.3 PC Interface and Control Application Development

4.3.1 Data Reception and Transmission Application

A desktop application was developed based on the Python programming language. This application allows the data to flow between the host computer and the LoRa transceiver to. A transceiver is physically connected to the host computer using the Universal Serial Bus (USB) connector.

This application was developed based on three interrelated Python files were created, namely *global.yml*, *MySQLConnector.py* and *DataReceiverTransmitter.py.*

- In *global.yml,* the COM ports and Database connection credentials are defined.
- In *MySQLConnector.py*, the Structured Query Language (SQL) related queries and logic are defined. SQL is used for writing data to the database, retrieving data from a database, and manipulating the data to get the desired information that can be used by the FLC (detailed in section 4.3.3).
- DataReceiverTransmitter.py has a logical control of transmitting data from a host computer to a transceiver and receiving data from a transceiver. The data flow is serially in both directions.

A batch file, *LoRaTranceiver.bat* was created. It contains the executable commands to sequentially run the codes and commands which are in the three Python files explained above. The *LoRaTranceiver.bat* is in the start-up folder of the kernel (operating system of the host computer), in a way that when the host computer starts up, the PC application for the LoRa transceiver also starts up immediately. This batch file in the OS's kernel start-up folder automates routine data transmission and reception tasks without requiring user input or intervention. When the PC application is up and running, it can send the data via the transceiver or write the data received by the transceiver into the database.

4.3.2 Database Implementation

MySQL database has been implemented in this study. MySQL is the Relational Database Management System (RDBMS), which operates in and is named after Structured Query Language (SQL) - the programming language it's written in. It is an open-source DBMS that

supports SQL standards and other additional features such as complex queries, foreign keys, triggers, updatable views, transactional integrity, and multi-version concurrency control.

phpMyAdmin is a Graphical User Interface (GUI) for administrating and managing MySQL database, which was used in this research study. This open-source tool provides graphical administrative support and built-in functions of MySQL. XAMPP has been used as the local host for this database. Different JSON and PHP scripts were used in linking the database with the PC application to allow smooth and consistent data manipulation (including data insertion, updating, retrieval, and deletion). This database contains different schemas, as shown in Fig. 60.

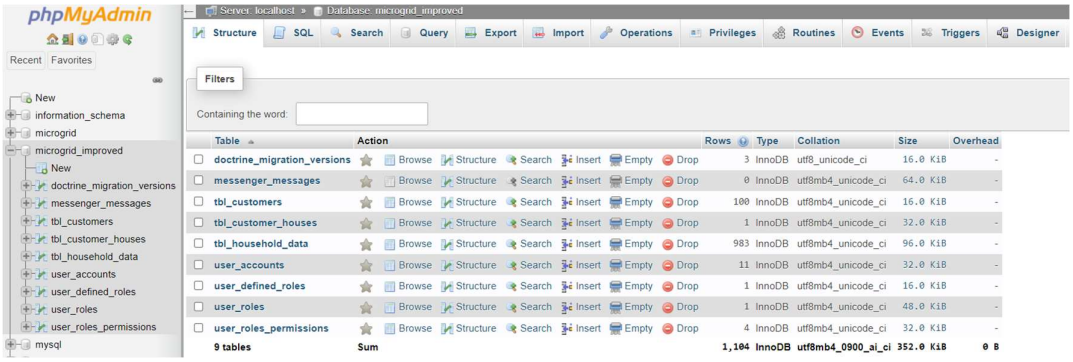

Fig. 60: Developed MySQL database with its schemas

4.3.3 Fuzzy Logic Controller: Program Implementation

The FLC was implemented within the PC application on the host computer. It was implemented using the *Simpful* software running on the *Python 3* programming language environment. It takes inputs in a human-readable FIS representation, comprising a group of fuzzy sets defined by membership functions, linguistic variables, fuzzy rules, and resulting outputs (defined as crisp values, arbitrary functions, or fuzzy sets), as shown in Fig. 61.

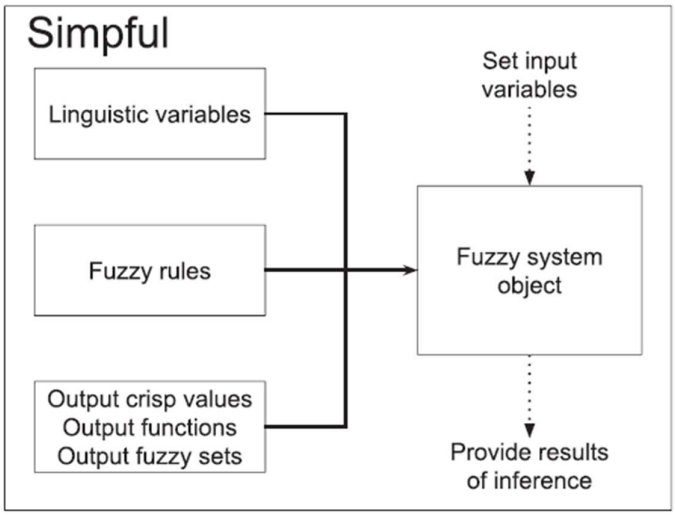

Fig. 61: Graphical representation of the Fuzzy System Object in Simpful [79].

The following are the basic requirements needed to design an FLC-based artificial intelligent system that achieves the objective of real-time load control [154].

- *FLC Model:* In this study, the load control signal is produced from the FIS, which takes in a real-time SoC of the battery and PV power generation, as shown in Fig. 62. In this study, a load control FIS is modelled by using a Takagi–Sugeno model.

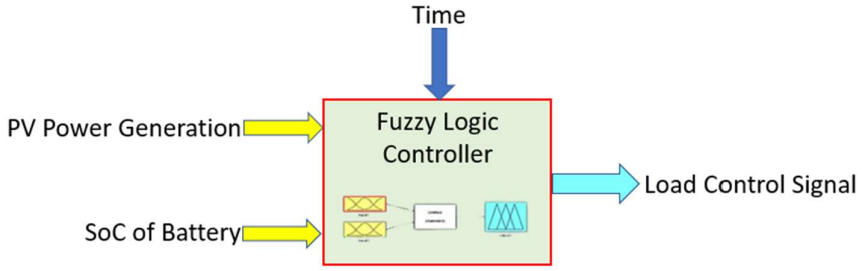

Fig. 62: Model of Load Control Signal using FIS

- *Fuzzy Membership Functions:* The inputs, PV power generation, SoC of the battery (which is proportional to the terminal voltage of the battery [155]), and time are implemented as Trapezoidal, Sigmoidal, and Trapezoidal membership functions, respectively. These inputs were sized based on the preliminary study, and data were collected from December 2022 to March 2023, as detailed in chapter five. The resulting membership functions with a degree of membership are graphically stipulated in Fig. 63, with the logical output membership function in Fig. 63(d).

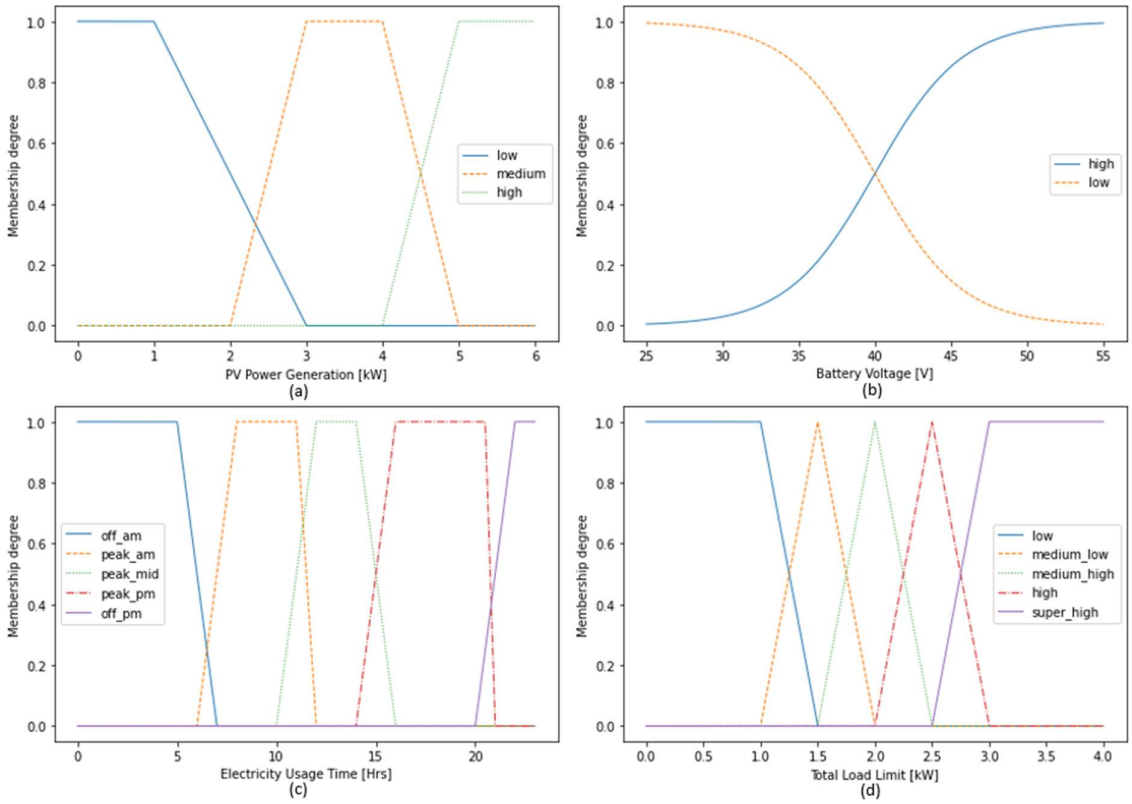

Fig. 63: Membership functions for load control FIS

- *Fuzzy Rules:* The input and output membership functions in FIS are governed by the set of the following rules:
  - *IF (Generation IS low) AND (Battery IS low) THEN (Limit IS low)*
  - *IF (Generation IS low) AND (Battery IS high) THEN (Limit IS low)*
  - *IF (Generation IS medium) AND (Battery IS low) THEN (Limit IS medium_low)*
  - *IF (Generation IS medium) AND (Battery IS high) THEN (Limit IS high)*
  - *IF (Generation IS high) AND (Battery IS low) THEN (Limit IS medium_high)*
  - *IF (Generation IS high) AND (Battery IS high) THEN (Limit IS super_high)*
  - *IF (UsageTime IS peak_pm) THEN (Limit IS medium_high)*

  The rules were simulated to produce the graphical relationship between fuzzy inputs and outputs, as illustrated in Fig. 64. The total allowed load is maximum high when there is a maximum PV power generation and batteries are charged to the nominal capacity. Subsequently, the allowable load is at the minimum when there is no PV generation and batteries are running low.

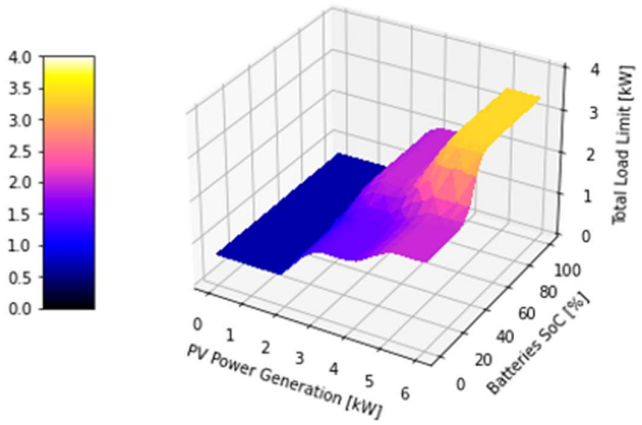

Fig. 64: Relationship between inputs (PV Power generation and SoC of Battery) and output (Total Load Limit)

4.4 Chapter Summary

In this chapter, the software (firmware and application) running in LoRa-based transceiver and consumer modules and the host computer have been elaborated on in detail. Different software development environments and programming languages have been employed. Moreover, this chapter also explained how load monitoring and control with FLC is achieved from the logical and programming point of view.

CHAPTER FIVE

DATA ACQUISITION, ANALYSIS AND FINDINGS

5.1 Introduction

This chapter discusses the process of field data collection and analysis. It explains the field study area, the types of data gathered, and the analysis methods used for this research study. It also presents an in-depth discussion of findings obtained from the data analysis. Finally, this chapter shows how the field-study findings correspond to implementing the proposed load monitoring and demand-side management system based on FLC and LoRa wireless communication in microgrids.

5.2 Study Area

This research study was conducted in Silale village, located in the Kongwa district in the Dodoma region. The region is situated in the central part of Tanzania. Silale village is located in a rural region with no reliable connection to the national electric grid.

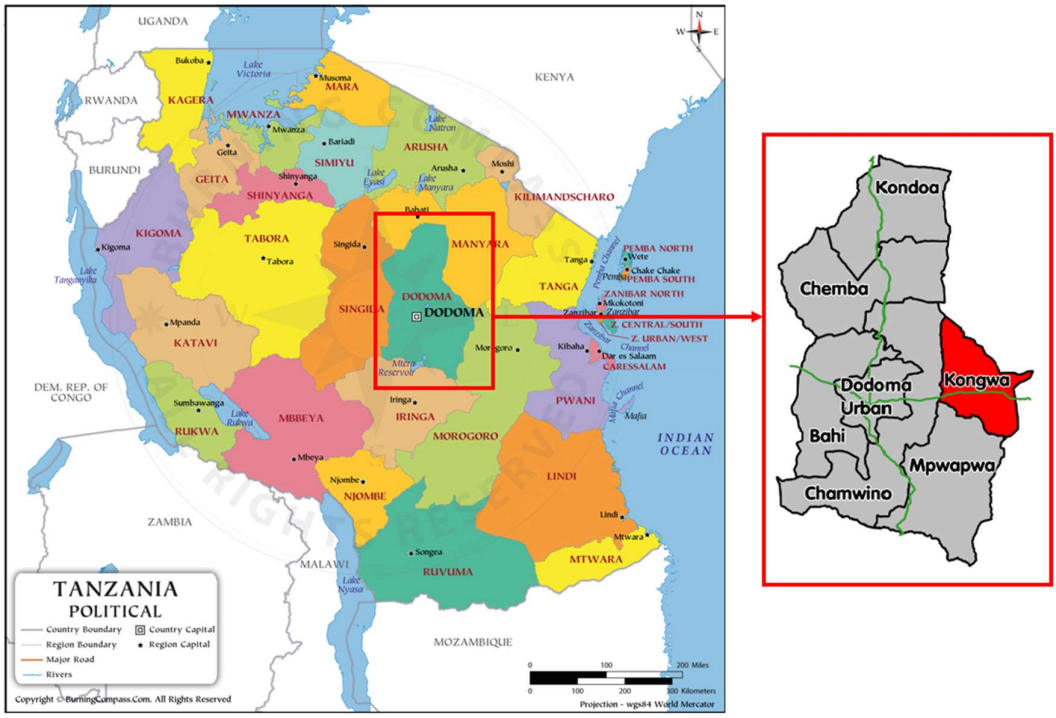

Fig. 65: Kongwa district pointed from Tanzanian map [156, 157]

In order to access clean energy, specifically electric energy, Silale Village is connected to a community-owned Solar PV Microgrid. The microgrid is situated at the village's centre. It serves about 60 households and shops, spanning a radius of about 1 km from the microgrid, as shown in Fig. 66. Moreover, a primary school and a church are also connected to the microgrid.

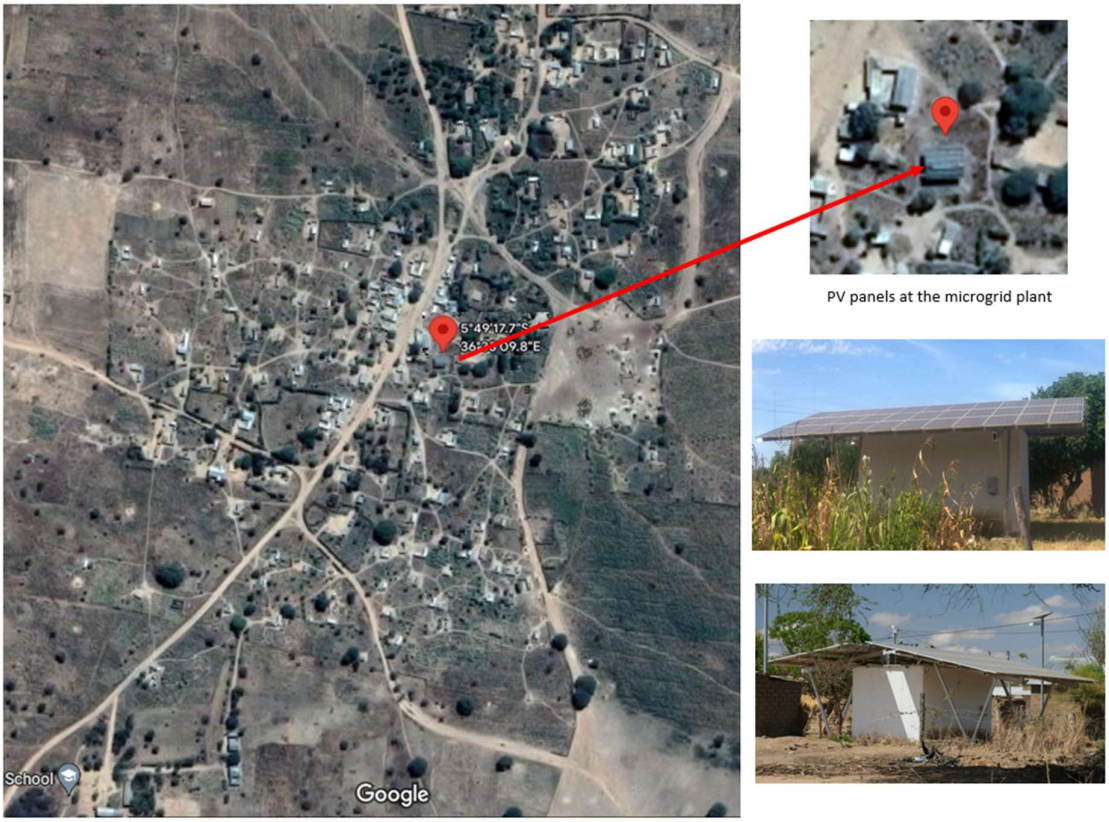

Fig. 66: Solar microgrid at the centre of Silale village (source google maps)

The Solar PV microgrid at Silale is rated at 13.75 kWp generated by a total of 55 solar PV panels of 250 Wp each. The panels are arranged in a series of 2 arrays, with the first array of 33 PV panels facing east and another array of 22 PV panels facing west. Some of the panels are damaged/broken. The panel arrays feed a Maximum-Power-Point-Tracking (MPPT) connected with an SMA triphase charger controller. Furthermore, three SMA inverters are working in master-slave mode. The microgrid has 24 rechargeable - 2V energy storages, 1236 Ah lead acid dry cells, and a total output of 48 V-dc.

Fig. 67: Microgrid equipment at Silale: (a) SMA triphase charger controller, (b) Inverters, and (c) Battery Pack

Fig. 68 shows the schematic diagram of the Silale community microgrid. The microgrid has three single-phase distribution lines, each distributed to households, except one line distributed to homes and shops in the village centre. Each consumer is charged at the flat-rate payment of TZS 3,000/= (equivalent to USD 1.3) per month.

Silale community microgrid was selected as a case study for this research, as it is an established microgrid that has been operating for more than five years. Moreover, they don't have any load monitoring and control mechanisms up to this project. Thus, the output of this research study will contribute to the operability and sustainability of the Silale community microgrid project.

In genesis, the Silale community microgrid was developed to provide a clean energy for village members especially electricity primarly for lighting at night and low load demanding devices such as radios, mobile phones and televisions shown in Table 12. In addition, the microgrid could provide electricity for economic activites such as restaurants during the day when there is more PV generation.

Table 12: Common loads in Silale community microgrid

Load Name	Power Rating [W]	Average Operation Hours/day	Remarks
Light	8 – 13	8-12	Each household has between 2 and 5 lights
Radio	10	8	Few households have radios
Sub-woofer	40	4	Few households, restaurants and a pub have subwoofers
Television	100	4	Few households, restaurants, and a pub people have radios
Mobile phone	5	2	Each household has at least 1 mobile phone
Refrigerator/Freezer	130	4	One in a restaurant and in a pub

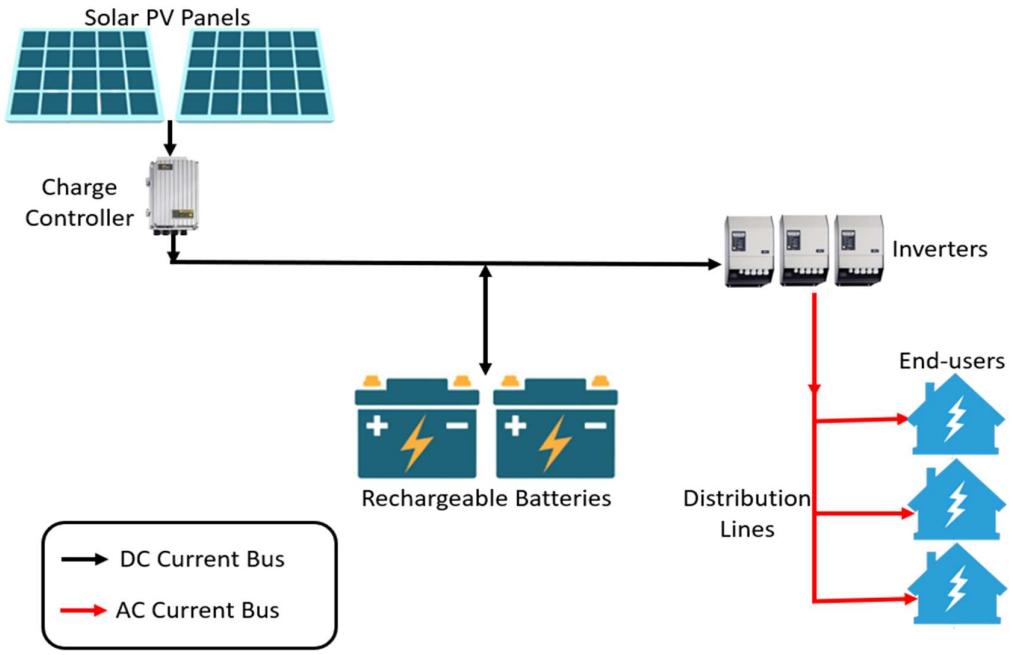

Fig. 68: Silale community microgrid schematic diagram

5.3 Data Collection

During this study, the load monitoring and control devices developed (in chapter three) were installed on each consumer connected to the microgrid, as illustrated in Fig. 69. These devices were used for collecting data such as load, voltage variations, and consumed current from the users. The collected data were wirelessly transmitted to the host computer. The host computer uses a database to record and save the data as they were received.

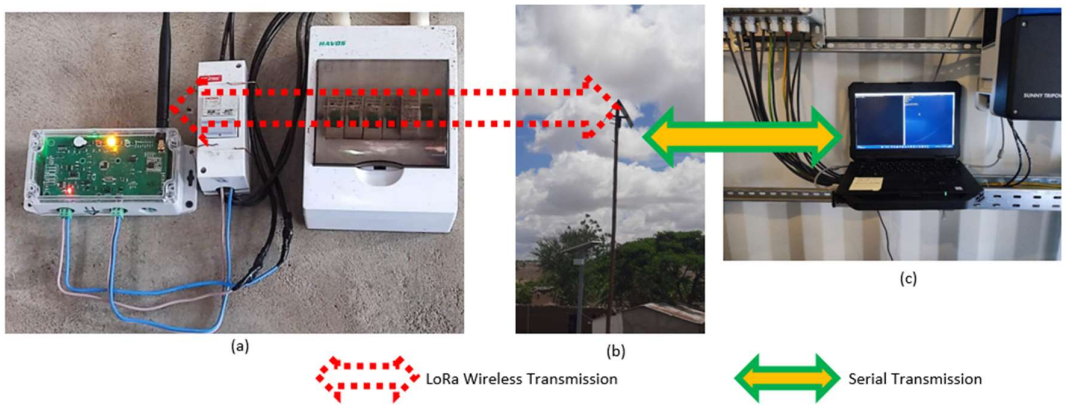

Fig. 69: Data transmission from (a) installed load monitoring module to (b) LoRa transceiver, then to (c) host computer

Fig. 70 illustrates the new schematic diagram for the Silale community microgrid after installing the load monitoring and control system, i.e. installation of consumer modules and the host computer for data collection and load control signal computation.

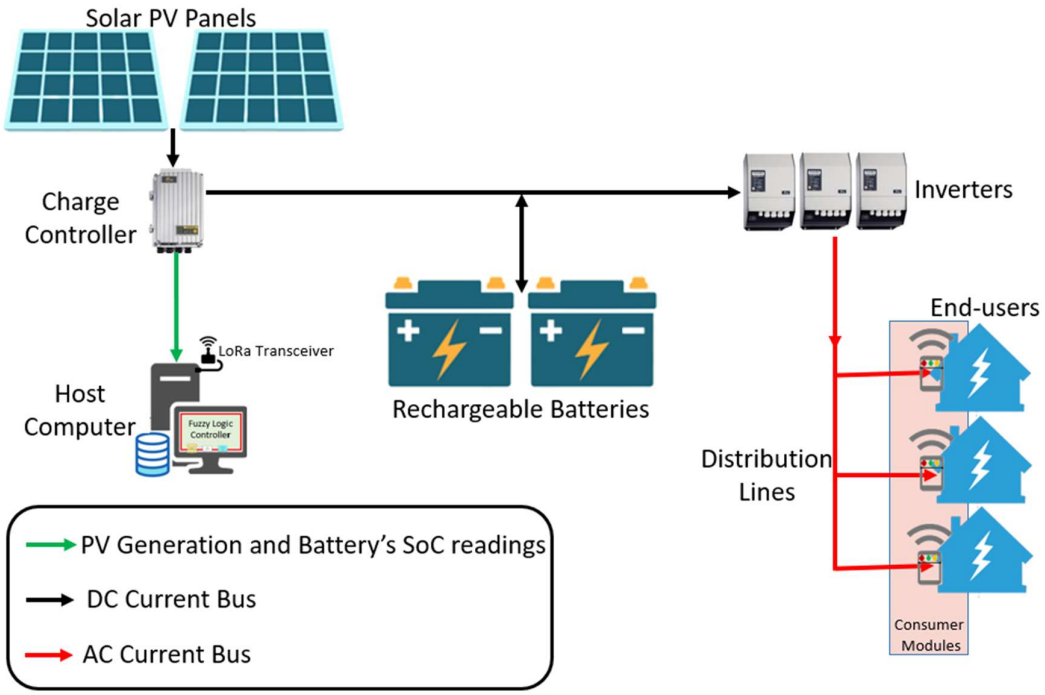

Fig. 70: Newly implemented schematic diagram of Silale community microgrid

The data from the consumer modules were received by the LoRa transceivers connected to the host computer at the microgrid station. The LoRa transceiver is the central node of the star topology of the LoRa network implemented, as shown in Fig. 71. LoRa transceiver sends and receives data packets in sequence. To avoid a collision from different nodes, the central node

(LoRa transceiver) acts as the master, and other nodes (consumer modules) operate as slaves. The consumer modules only send one at a time when it receives a request packet that matches its unique node identification number (node ID). Fig. 72 shows the flowchart of how the requests and responses are negotiated between the central LoRa transceiver and consumer modules.

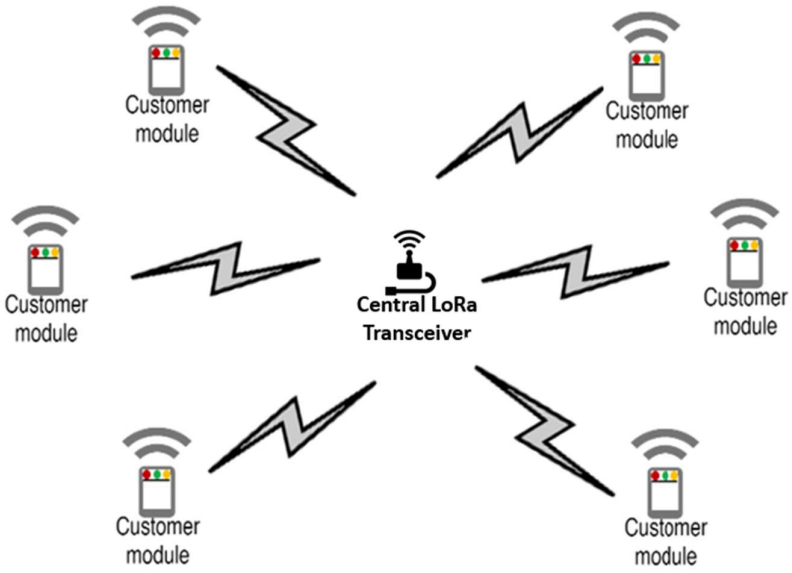

Fig. 71: Star Topology configuration for the LoRa network implemented

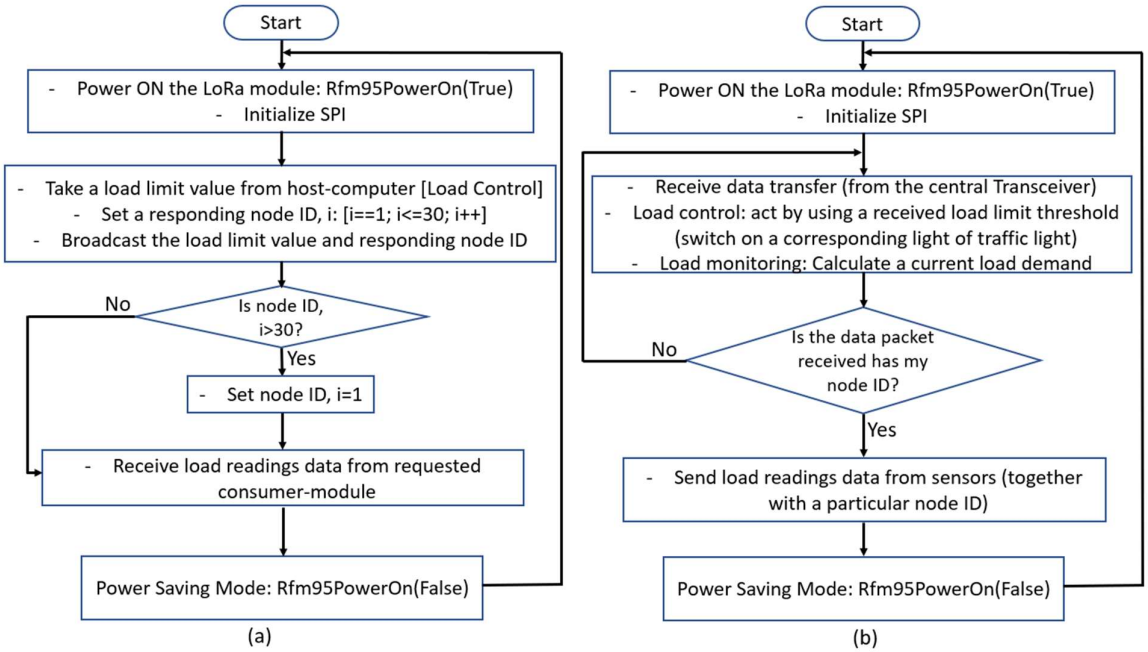

Fig. 72: Flowcharts for (a) Central LoRa transceiver; (b) Consumer module

This study uses two central LoRa transceivers, each serving 30 consumer modules. With two main transceivers, the network size is halved, and the time resolution of a particular consumer module to send its reading is also split. To avoid interference, the two set of central LoRa transceivers and their corresponding consumer modules operate at different main frequencies of 885.8 MHz and 886.1 MHz, each with a bandwidth of 62.5 kHz. The gap between two main frequencies is larger than 1.5 times the channel bandwidth recommended for the LoRa communication system [144]. The central transceivers were raised to about 7 meters using poles to improve the data reception. The received data were stored in the database using a Python script, as shown in Fig. 73.

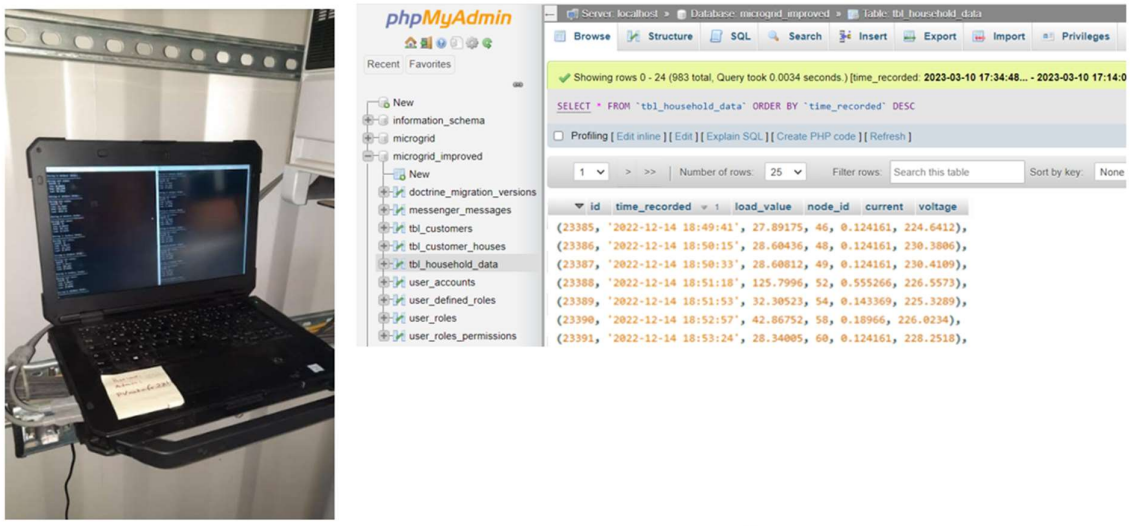

(a) (b)

Fig. 73: (a) The host computer running a script to write data into the database; (b) The data installed in the MySQL database

5.4 Data Analysis

Initially, the load demand (power consumption) data from December 2022 to March 2023 were recorded and analyzed. The data were carefully checked using the specialized statistical data analysis packages for the Python programming language. The statistical packages used were Pandas for simplified data processing, extraction, and manipulation. Matplotlib was taken for data visualization [158]. Before the statistical analysis of the microgrid's historical data, specific incomplete data points (at different particular times) were filtered out. Gaps in those particular data often were caused by loss of LoRa wireless communication between a consumer module and the LoRa transceiver at the microgrid centre or the host computer switched off during a prolonged blackout in the microgrid.

5.5 Findings: Results and Discussions

The collected data carried different information. When all the data were analyzed, information such as load profiles, power generation profiles, and state-of-charge of batteries was calculated and illustrated graphically.

5.5.1 Mean Load Profiles

As indicated before, the Silale community microgrid provided clean energy for lighting at night and low-load demanding devices such as radios, mobile phones and televisions. In addition, the microgrid could provide power for a limited number of economic activities, such as restaurants during the day with more PV generation.

Fig. 74 shows the mean daily load profile at the Silale community microgrid, contrary to the original purpose of establishing this microgrid. The profile indicates that consumers can only enjoy access to electricity during the daytime when there is sunshine. The load peaks when most people return from their daily farm and agricultural activities. The power demand peaks at a mean value of around 3 kW. This peak demand is due to most restaurants switching on radios, subwoofers and fridges to sell cold drinks. However, even before the sun goes down in the evening, the consumers start using a high amount of electricity from the storage battery. Since there is no load control mechanism, the electricity supply goes off around 7 pm to 9 pm (blackouts start), and batteries are entirely discharged by that time. This unmanaged and uncontrolled load puts the village in darkness at night, contrasting the microgrid's original goal. The following day, electricity power demand sharply increases from 6 am to 8 am as the PV panels restart to generate electrical energy. The power is used to power the lights that were not switched off the previous night when the blackout occurred. The load demand steadily increases going to mid-day as people open shops, charge their phones and switch on their radios.

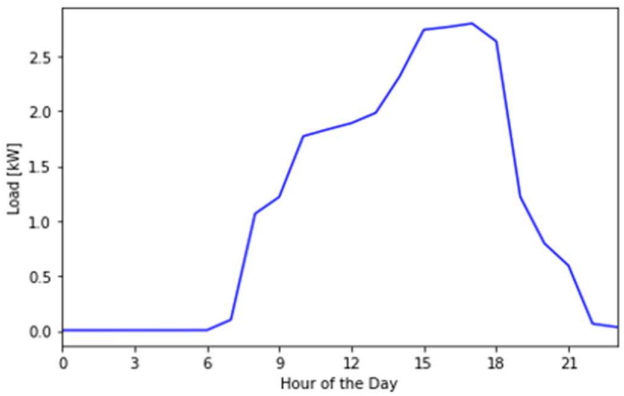

Fig. 74: Mean daily load profile at Silale community microgrid

Moreover, further analysis of the general daily profile shows a slight difference between days of the week, as illustrated in Fig. 75. The total electric power consumption significantly depends on the day, whether a weekend or a weekday. On weekends, people typically don't go to work on their farms, and students don't go to schools. The peak load demand from mid-day to around 6 pm is significantly different. The demand is higher on weekends than weekdays because more people are at home. On weekends, there is a considerable difference from around 3 pm to 6 pm as many people go to sports bars to watch soccer games. Consequently, around 7 pm, the load curve drops sharply as the grid switches off automatically, with all the energy stored in the batteries usually finished.

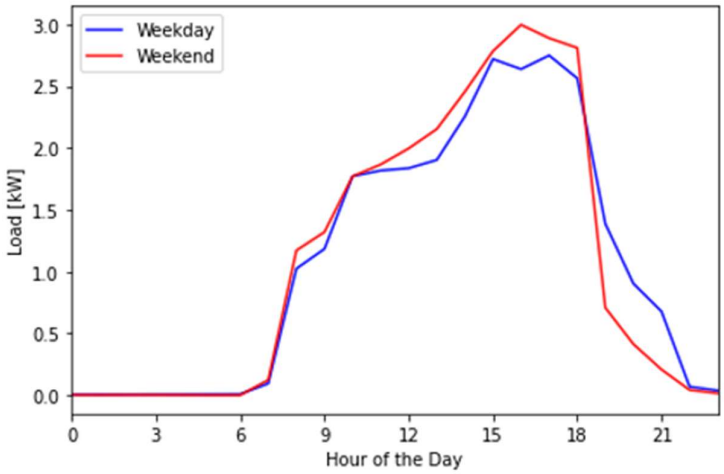

Fig. 75: Comparison in mean daily load profiles between a typical weekday and weekend

5.5.2 Solar PV Power Generation

In this microgrid, there are a total of 55 PV panels with 22 PV panels facing the western side compared to 33 PV panels facing the eastern side of the compass; among them, 13 PV panels are broken. Fig. 76 shows the mean installed and estimated daily power generated from the solar PVs at the microgrid plant. The installed PV generation curve represents the generation profile of how all 55 PV panels would have generated, while an estimated PV generation curve represents a generation without 13 broken PV panels. The installed and estimated PV power generation were computed using the solar irradiance power data of Silale village provided by NASA from 2018 to 2022, using the formula in equation (16). Usually, the PV generation starts at around 6 am and peaks at around 11.30 am to midday, which is the typical solar irradiation characteristic of the tropical region around the equator [76, 159].

$$PV\ Generation\ [W] = P_r\ x\ r\ x\ I\ x\ A \quad (16)$$

P_r $-$ $PV\ Performance\ ratio\ (equivalent\ to\ 0.75\ in\ SSA)$

r $-$ $PV\ panel\ efficiency\ (given\ as\ 16\%)$

I $-$ $Solar\ irradiation\ power\ [W/m^2]$

A $-$ $Total\ surface\ area\ of\ the\ PV\ panels\ [m^2]$

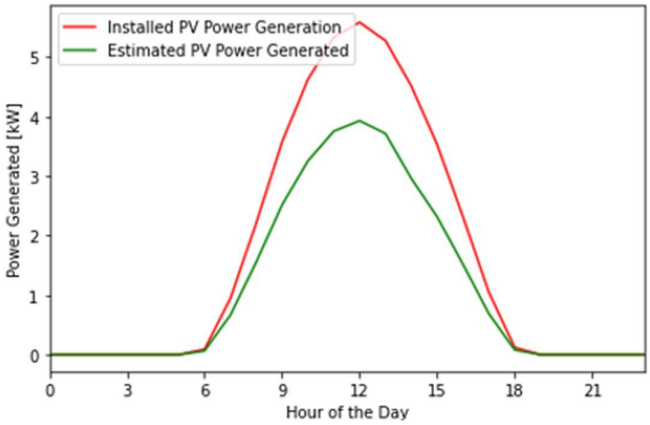

Fig. 76: Installed and estimated mean daily solar PV power generation

Moreover, the estimated power generated by the PV panels was compared to the mean daily load profile in the Silale community microgrid, as shown in Fig. 77. From 6 am to 2 pm, the generated power surpasses the load demand. The excess energy is used to charge the batteries until 11 am when they are fully charged. The peak load is relatively lower compared to the peak power generated daily. However, the peak load occurs around 3 pm, close to sunset, when the PV power generation is already low. It is a typical behaviour of solar microgrids as no power generation is in the evening and at night. Still, more energy is needed for lights and other appliances in households and businesses [159]. Consequently, the power stored in the batteries usually supplies this peak load.

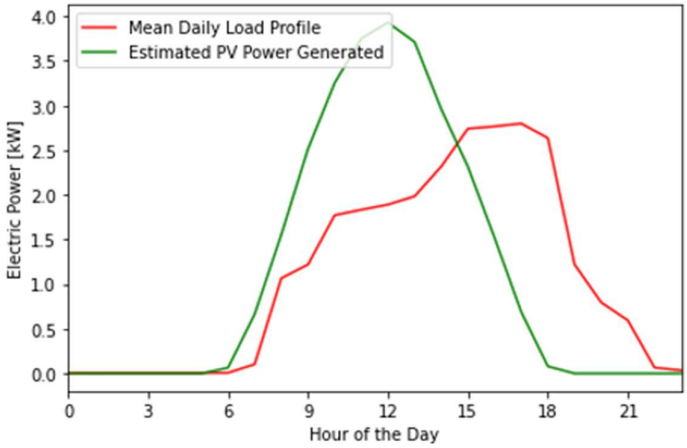

Fig. 77: The relationship between mean daily estimated PV power generation and load profiles

5.5.3 Determination of State of Charge using Battery Voltage

In estimating the State of Charge (SoC) of the battery, different methods can be used such as the Coulombs Counting (CC) over time (also known as Ampere-hour counting), concentration of battery acid and Open Circuit Voltage (OCV) reading [160, 161]. Among them, the commonly applied method by battery system manufacturers is ampere-hour counting. Its accuracy relies mainly on precise calibration before counting. Another practically-used technique is estimating the SoC based on the battery terminal voltage, the OCV.

The State of Charge S_{OC} is defined as the remaining charge capacity in the battery and is given by the equation (18). Inversely, the Depth of Discharge D_{OD} shows the amount in percentages of drained charges from the fully charged battery.

$$D_{OD} = \left(\frac{Q_d}{Q_{max}}\right) \text{X } 100\% \tag{17}$$

$$S_{OC} = \left(\frac{Q_r}{Q_{max}}\right) \text{X } 100\% = \left(\frac{Q_{max} - Q_d}{Q_{max}}\right) \text{X } 100\% = 100\% - D_{OD} \tag{18}$$

$Q_r = remaining\ charges;$

$Q_d = drained\ or\ used\ charges;$

$Q_{max} = full\ rated\ charge\ capacity;$

Fig. 78 shows an equivalent circuit of a battery. The OCV of the battery is given by the equation (19).

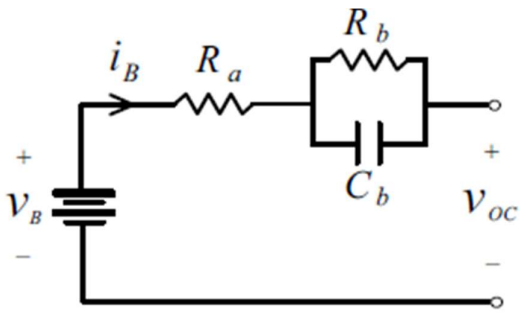

Fig. 78: Equivalent circuit of a battery

$$V_{OC} = V_B - V_{Co}.e^{\left(\frac{-t}{R_b C_b}\right)} \tag{19}$$

$V_{OC} = open\ circuit\ voltage;$

$V_B = internal\ battery\ voltage;$

$V_{Co} = initial\ voltage\ in\ lumped\ capacitance\ of\ cell\ plate\ C_b;$

$R_a = resistance\ due\ cell\ conections;$

$R_b = charge\ transfer\ resistance;$

When the battery is not connected to the load, the open circuit voltage V_{OC} is assumed to be equal to the battery internal voltage V_B. V_B can be obtained in equation (19) by using a coefficient relationship between time-varying parameters and V_B as shown in equation (20) [162].

$$V_{OC} = V_B - \left[a_2 {V_B}^2 + a_1 V_B + a_0\right] . e^{\{-t\left[b_2 {V_B}^2 + b_1 V_B + b_0\right]\}} \quad (20)$$

Different studies show that there is an approximately proportional between S_{OC} and V_B as illustrated in equation (21) [163].

$$S_{OC} = \alpha_1 V_B + \alpha_2 \quad (21)$$

Combining equations (20) and (21), the S_{OC} can be approximately shown by the polynomial relationship to V_{OC} at a time instant in minutes, as shown in equation (22).

$$S_{OC} = c_4 {V_{OC}}^2 + c_3 t^2 + c_2 V_{OC} + c_1 t + c_0 \quad (22)$$

The relationship between S_{OC} and V_{OC} in equation (22) has been used in several studies [162, 163] for Pb-acid batteries with a cell voltage of 2V. The case study, Silale community microgrid has a similar battery system of Pb-acid, with 24 batteries each rated at 2V, though 2 of them were removed for being faulty as shown by the measurements taken on May 19, 2023; in Table 13.

Table 13: State of health of batteries in Silale Community Microgrid

Silale Batteries State [V]		
Battery No	Before Charging	After Charging
1	2.10	2.14
2	2.10	2.14
3	2.09	2.14
4	2.11	2.15
5	2.11	2.15
6	2.10	2.14
7	2.09	2.14
8	1.05	2.13
9	0.84	2.13
10	2.10	2.14
11	2.10	2.15
12	2.11	2.15
13	0.15	0.00
14	1.75	2.12
15	0.00	0.00
16	2.10	2.14
17	2.08	2.12
18	2.10	2.15
19	2.10	2.15
20	1.41	2.13
21	2.10	2.15
22	2.10	2.15
23	2.10	2.15
24	0.62	2.11

In this study, initially, the SoC of the battery system was determined using the OCV method, due to its simplicity and based on the case study at Silale community microgrid. This was done by observing and recording the voltage of the battery system during charging and discharging of the battery as recommended in [160], at the time interval of 60 minutes. The determination of the SoC employed the coefficient parameters provided in Table 14. These coefficients have been adopted from similar studies [162, 163] and bounded in the observed SoC limits at Silale community grid which were 30% (load cut-off) and 99.9% for 41V and 52V respectively. Fig. 79 shows the corresponding SoC of the battery determined from the battery voltages read in Silale microgrid community.

Table 14: Coefficients for SoC estimation equation (22)

Symbol	Coefficient
c_4	170.0947
c_3	-0.0013
c_2	-579.2584
c_1	0.23
c_0	509.63

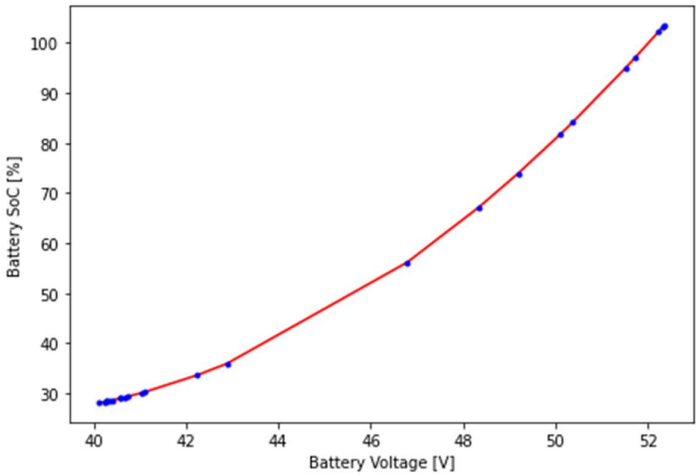

Fig. 79: Relationship of the SoC and battery voltage

Moreover, the effect of the temperature was neglected as it was insignificant to the voltage changes during charging and discharging. This was due to the rate of cell voltage drop being approximately 2.8 mV/°C during the temperature changes of 25°C – 32°C during the days of measurements. The effect of cell voltage drop is surpassed by the effect of the voltage changes due to changes in charge capacity. Fig. 80 shows the relationship between cell voltage and temperature as given in the datasheet [164].

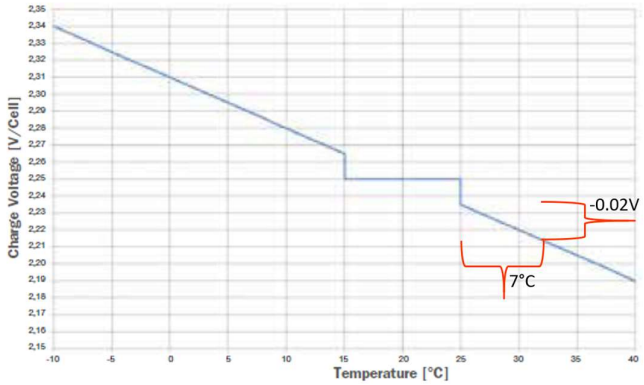

Fig. 80: Temperature related float charge voltage adjustment [164]

Fig. 81 shows SoC of the battery changes during the day due to the charging and discharging of the battery in the microgrid. From 3 pm, the load is supplied with electrical energy from the batteries to around 9 pm when the batteries are entirely off-charge and microgrid blackouts. Without a load control, the microgrid cannot even supply energy for lights in the village during night hours.

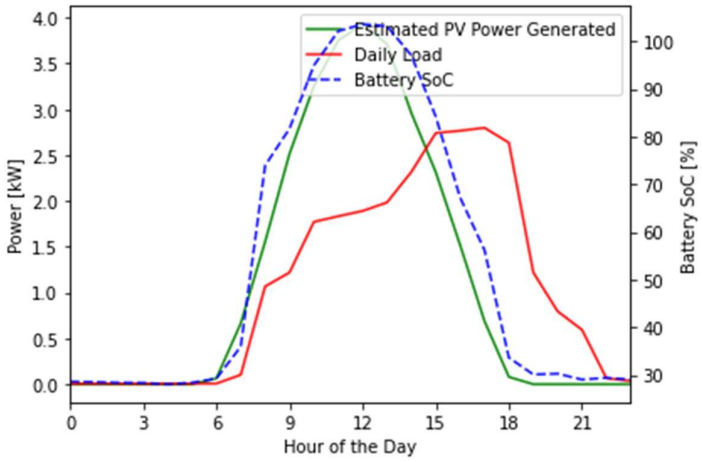

Fig. 81: Relationship between mean load profile, estimated PV power generation and SoC of Battery

Therefore, this research study implemented the FLC-based system to control the load during critical times, especially during the evening when there is no PV generation and the microgrid only depends on energy stored in batteries.

5.5.4 Load Control: Simulated Results

The data analysed in sections 5.5.1 to 5.5.3 above were simulated with the proposed FLC system implemented in this research study. Estimated PV power generation data and battery voltages of uncontrolled load profile at that particular time, as shown in Fig. 81 were used to

assess the microgrid's operation at the minimum possible limit for load control. It is assumed to be the worst case, as it shows the battery system could not provide any power after 10 pm. However, in the real-case implementation, the FLC-based system developed in this study would have a spontaneous effect on the battery capacity due to real-time load control. Thus the battery charge capacity would not decrease at a rate such as that shown in Fig. 81.

Fig. 82 shows the controlled (green curve) and uncontrolled (red curve) load profiles. With the FLC system implemented in this study, the high load demand from 3 pm to 7 pm, which would consume all the stored energy from the batteries, has been flattened. That extra load might be shifted to the time between 9 am and midday, where the PV power generation usually peaks, as shown in Fig. 83. The green curve (controlled load profile) shows that it is possible for the batteries to power the village for the whole night if the load is adequately controlled in the afternoon and evening hours, especially from 12 am to 7 pm. Moreover, the simulation results show that without load control, the loads consume a total energy of about 18.5 kWh from 12 am to 10 pm when the batteries are entirely discharged. In contrast, the FLC-controlled load consumes 13.6 kWh from 12 am to 10 pm, equivalent to 73.5% of the energy stored in the batteries. In addition, the FLC-controlled load consumes 18.3 kWh of battery energy from 12 am to 6 am the following day, when the batteries recharge. This is equivalent to using only 98.9% of battery energy while maintaining the availability of electricity for the core service, such as lights for the whole night.

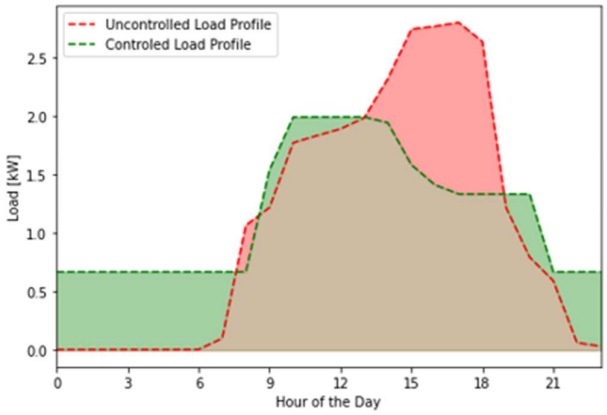

Fig. 82: Comparison between the mean controlled and uncontrolled load profiles

Fig. 83 shows that the controlled load profile allows the discharged batteries to be charged to a minimum acceptable charge level first by limiting the load between 6 am and 8 am. This regulation satisfies the microgrid system's condition of having batteries with a minimum required energy before it starts supplying power to other loads, as shown in Fig 81. Moreover, the controlled load profile shows that the estimated PV-generated power can supply all loads

directly until 4 pm while charging the batteries. Compared to the uncontrolled load profile, the load starts to consume the energy stored in the battery from 3 pm at the peak demand.

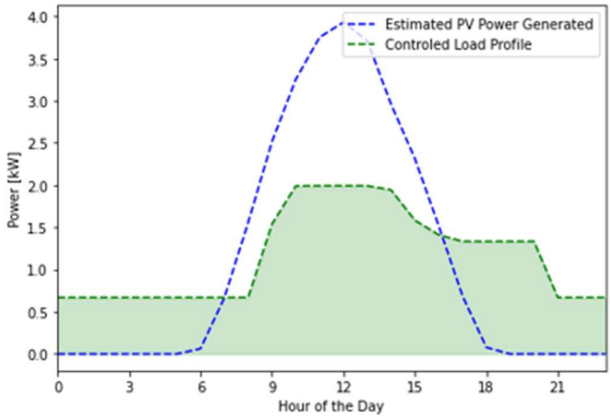

Fig. 83: The fitting of the mean daily controlled load profile to the mean PV power generation

5.5.5 Load Control: Real Measurements

The FLC-based traffic light system described earlier in chapter four, section 4.3.3, was installed in the microgrid system from August to October 2023. The measured field data for the PV generation and the SoC of the batteries were recorded and analysed. These data were measured and extracted from the SMA triphase charger controller connected to the PV panels and the battery pack. The measured data were found to be different from the estimated values used in sections 5.5.3 and 5.5.4 above.

Fig. 84 shows the difference between estimated and measured PV power generated. The difference can be caused by dust on the panel surfaces, damages, wear and tear of the PV panels. Additionally, there is poor orientation and distribution of the panels: fewer panels are facing west than east. According to the alignment of the solar cell, power generation is higher in the morning than in the evening, in contrast to the measured load profiles.

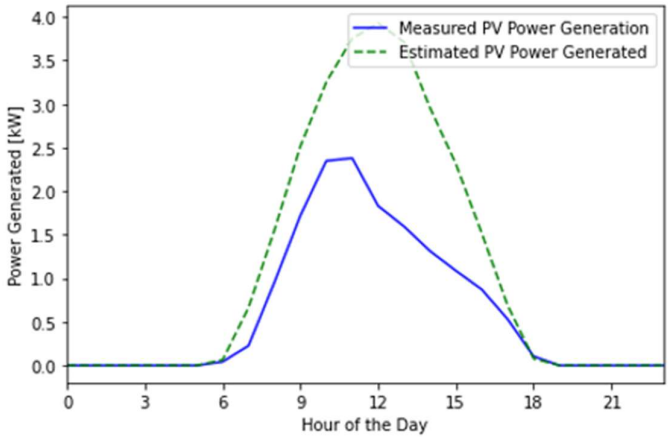

Fig. 84: Mean estimated and measured PV power generated

Fig. 85 shows the mean PV generation profile and the SoC of the batteries as recorded by the microgrid system at that time. It illustrates how the FLC's real-time load control (limit value) signal relates to the instantaneous PV generation value and batteries' SoC. The load limit goes down from 5 am to 8 am due to there is not only insufficient PV generation but also a significant drop in SoC at that time. From 8 am to midday, the load limit increases proportionally to increase in both PV generation and SoC of batteries. However, the load limit also decreases as the PV generation starts going down at midday. This regulation limits the load connected and allows the batteries to be fully charged for night consumption. The FLC system increases the load limit from 6 pm to 9 pm as it is usually a peak time for people to work, watch television programs and have family gatherings in their households. From 9 pm to 5 am, the load limit goes down to the amount sufficient for providing lights at night.

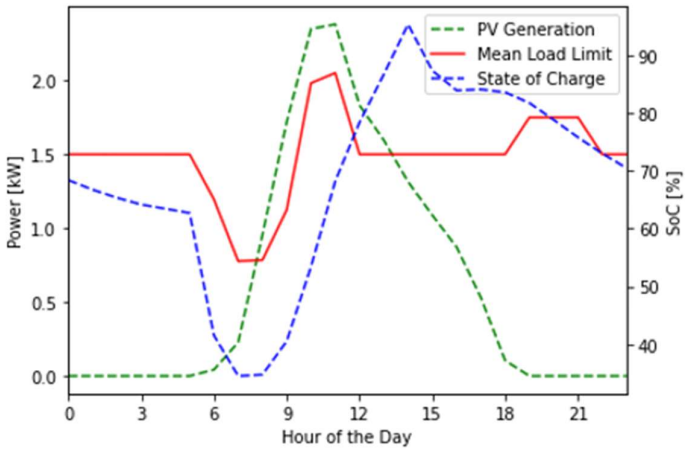

Fig. 85: Relationship of mean load limit produced by FLC concerning the corresponding PV generation and batteries' SoC

Mean Daily Load Profile

Fig. 86 shows the mean daily load profile at the Silale community microgrid under the load control introduced in this study. The profile indicates that consumers can enjoy access to electricity throughout the day and night. The controlled electrical load now peaks during the evening around 8 pm, when most people are at home or in local pubs and sports bars after their daily farm and agricultural activities. The power demand is maximum at a mean value of around 2 kW. This peak demand is due to almost all users having their lights on and some of them, including local pubs and restaurants, having televisions, radios and subwoofers switched on. This load is controlled between 6 pm to 9 pm to allow people to use electricity for other activities depending on the battery SoC, even though most people tend to use just above the limit (where the traffic lights usually give them yellow and even a red signal). However, from 9 pm, the load is forced to be reduced by the FLC based on the remaining SoC in the batteries. The control enables the system to supply electricity for lights to be on almost the whole night until around 5 am. The load drops from 5 am to 6 am as people wake up and switch off the lights as they go out for their daily activities.

Moreover, from 6 am to 9 am, the FLC sends signals to all meters to limit the load to a very low amount to prioritize charging the batteries to reach the minimum required charge capacity required by the system. From 9 am to midday, the FLC increases the load control limit proportionally to the increase in PV generation and the battery's SoC, as illustrated in Fig. 85. An increase in the load control limit would allow more load to be connected to the grid. However, during this time, most people are not effectively using electricity due to different reasons, including the nature of their main activity in the village as they are busy on their farms. From 2 pm to 6 pm, the load is controlled in such a way that it can only use what is generated by the PV; the batteries are not drained. Batteries are mainly used from 6 pm to around 6 am.

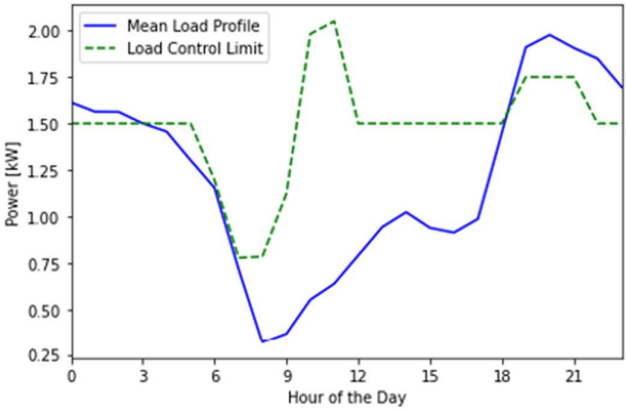

Fig. 86: Mean daily load profile after introduction of FLC-based traffic light load control

Fig. 87 compares the mean load profiles of the Silale community microgrid before and after the installation of the FLC-based traffic light load control system. The load control has effectively enforced that electricity users do not drain batteries' energy in the afternoon from 3 pm to 6 pm. This allows the batteries to store enough energy to supply electricity at night, at least for lights, which is the primary load of this microgrid. Previously, people unknowingly and uncontrolled used more electricity in the afternoon while not allowing the batteries to charge, and even drained the small energy stored in the batteries between 3 pm and 6 pm, resulting in blackouts at night. Furthermore, there is a considerable drop in electricity usage from 8 am to midday even though the limit is a little bit higher, as shown in Fig. 86. This change is due to different factors such as people switching off their lights in the morning. Before this, they did not switch off lights when the electricity went off at night. Subsequently, when electricity came back during the day, the lights went on while most people had already left their homes. Also, some people are currently not stressing on charging their rechargeable lamps as before, since now they have electric power at night, at least for lights.

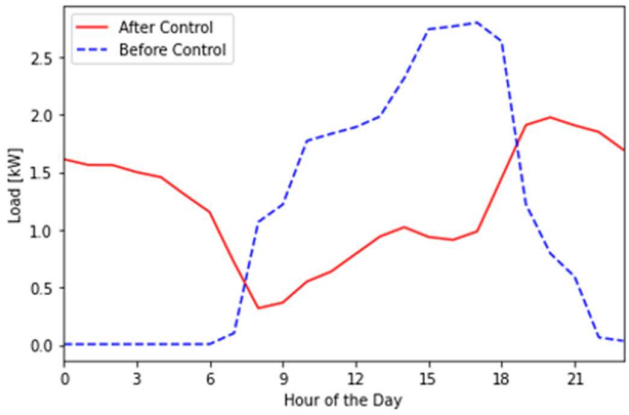

Fig. 87: Comparison of mean daily profiles before and after FLC-based traffic lights load control

Load Profiles of Electricity Users

During this study, the FLC and traffic light based load control were installed for data collection, as explained in section 5.3 of this dissertation. However, only a limited number of electricity users fully cooperated in this study. Some users were more eager to follow the traffic lights, and some were not interested and even tried to by-pass the meters or destroy them. Fig. 88 displays the contrasting conditions of the meters in different households based on how seriously they took care of the meters.

Fig. 88: Conditions of meters in different households

Fig. 89 shows the load profiles of each electricity user connected in Silale community microgrid. It shows 12 users have mean daily load profiles which are above the mean daily load limit and did not fully comply with the indication of the traffic lights on their electricity meters.

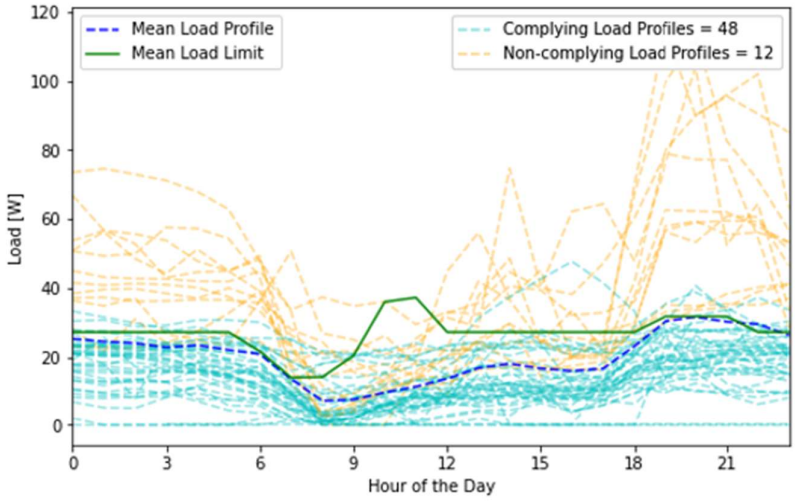

Fig. 89: Mean daily profile of every electricity user

The influence of the changes in traffic lights (changing signals among green, yellow and red lights) can be observed when comparing the load profiles to the control profiles. Red LED lights when the load is greater than the load limit, yellow LED lights when the load is 20% closer to the load limit, and green LED lights when the load is much lower compared to yellow LED threshold. The traffic light influence is shown in Fig. 90 and Fig. 91 with the respective colour shade.

Fig. 90 shows the mean load profile change for different businesses in the village before and after implementing the FLC-based traffic light load control in the microgrid. When the load profiles are compared, FLC-based traffic light system has encouraged and sometimes forced these businesses not to greedily use all the electricity in the afternoon and bring blackouts at night. Nevertheless, adherence to the traffic light has been a challenge especially during the peak hours of the evening, after 7 pm, for example, those operating a local pub and sports bar. When they had been using electricity at the red traffic light signal for over 30 minutes, the system switched off their loads and switched on again after 15 minutes, indicating a decrease in the load. On the contrary, the operator of a local restaurant always adhered to the traffic light signals and operated her loads within the limit.

Fig. 90: Mean load profile before and after load control for businesses in Silale village

Furthermore, the load profiles of some residential households were also analysed, as shown in Fig. 91. Some households were willing to follow the traffic light signals and act accordingly. Nevertheless, some households with high load demand, such as the teacher's household shown in Fig. 91, were unwilling. The meters switching off loads after 30 minutes and reconnecting power after 15 minutes caused the load profiles to be as a sharp zig-zag curve. This behaviour shows that such households are not sensitive to this DSM technique.

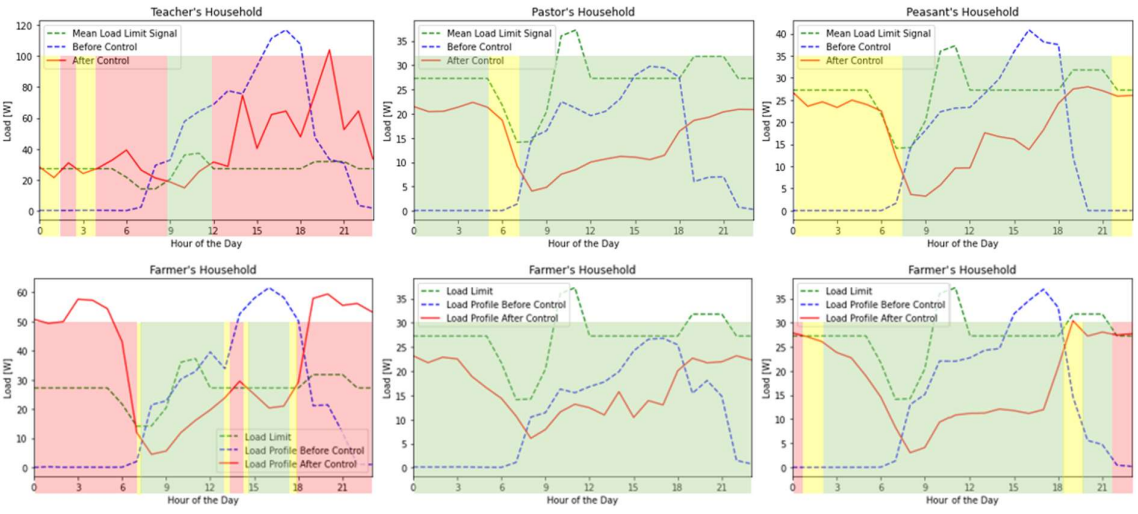

Fig. 91: Mean load profile before and after load control for some households in Silale village

5.5.6 Discussion

The findings explained in section 5.5.5 above have shown a change in load profiles with an improvement in the general load monitoring and control in Silale PV microgrid. However, on individual cases, there was very little influence of the traffic light system on some users' daily electric consumption behaviour. In Fig. 90 and 91, some users, especially strong electricity users, had red lights requesting them to decrease their loads, but in contrast, they did not willingly and positively react to it. The lack of response from some electric users was due to different reasons. Some electric users are connected to both the PV microgrid and also to the newly extended national grid. They do not care much if the PV grid goes off, since they could shift to the national grid when no power is available from the PV microgrid.

Fig. 92 shows the average estimated PV power generation of Silale community microgrid for an entire year using the solar irradiance power data of Silale village provided by NASA from 2018 to 2022 and the formula in equation (16). It shows the PV generation will be lower from April to July than the annual mean. Therefore, the power availability and reliability during these months greatly depend on all electricity users' compliance with the traffic light control. Non-compliance of some users to the traffic light control could result in blackouts during these months of low solar irradiance.

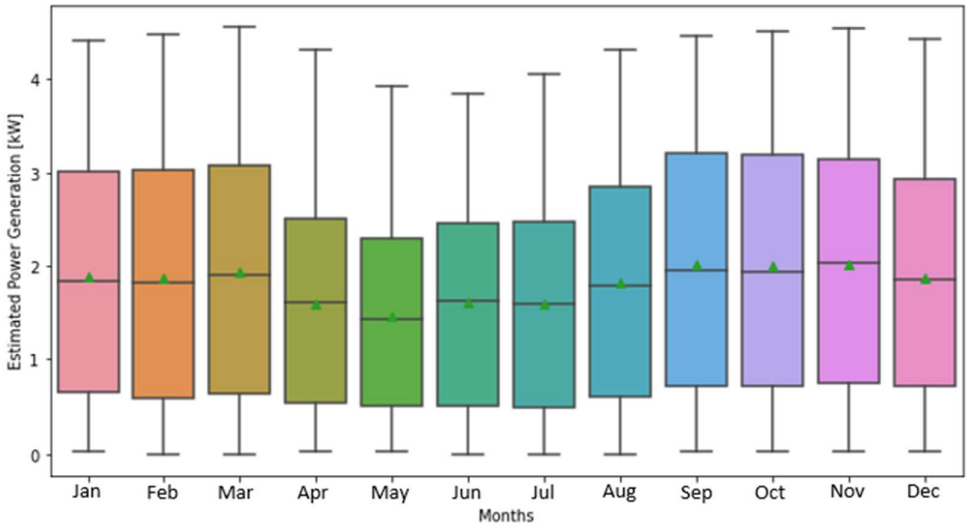

Fig. 92: Average estimated PV generation for Silale community microgrid

Additionally, since all electric users are paying the same monthly flat-rate, some consumers did not want to reduce their consumption as they thought that would benefit others and still pay the same monthly charge. Moreover, some people switched on their high-volume radios and subwoofers for the show-off and recognition and left even when traffic lights indicated the

need for load reduction. Furthermore, at night, some devices were switched on, users fell asleep and therefore, no response for any changes on the traffic lights will occur. With the load on and people not inside their houses, there is no response to the traffic lights' request for changing (especially reducing) load demand. The FLC system had to enforce load reduction by switching off some loads (except for lightning) when users had been using electricity at the red traffic light signal for over 30 minutes and switching on again after 15 minutes. However, this brought some challenges and complains that the system might damage their equipment and was not fully embraced by some users.

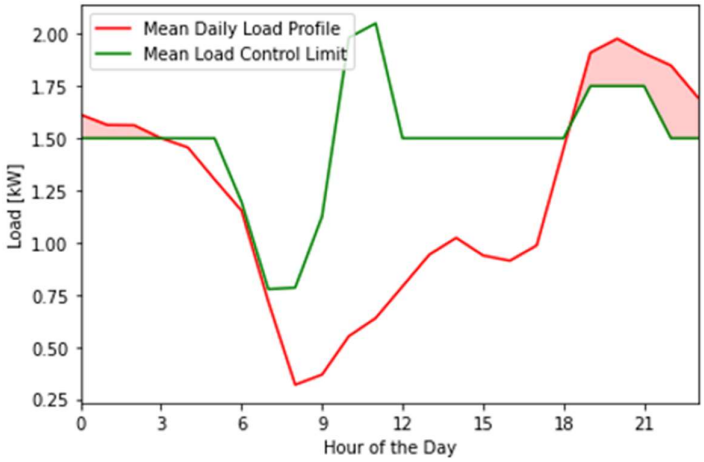

Fig. 93: Mean daily load profile and mean daily load limt profile

Fig. 93 above shows that from 6 pm to 4 am, the mean load profile exceeds the mean limit profile. The extra energy used is equivalent to 0.88 kWh per day. This study recommends that the village energy committee introduce a more expensive tariff for users who use electricity above the limit during the red traffic light. The maximum flat rate tariff is TZS 3,500/kWh for solar PV microgrids in Tanzania, as EWURA indicates [165]. If Silale microgrid imposes a TZS 3,500/kWh tariff for every usage above the limit, it will generate an extra income of TZS 92,400 per month. This additional income equals a 51.3% increase to a total of TZS 180,000 collected monthly. The extra income could be used for the maintenance of the microgrid.

Moreover, Fig. 93 shows that from 8 am to 6 pm, there is a very low loading to the microgrid, and about 7.24 kWh of energy is not utilized to the FLC-based load control limit. This energy can be used for socio-economical activities such as clean water pumping and improving the livelihood of the community. Also, users with high loads at night should be encouraged to shift some of their loads to this time.

Furthermore, The two central LoRa transceivers and 60 consumer modules installed in the Silale community microgrid cost 3,360 €. The same amount could buy 16 PV panels of a similar rating as those installed at the microgrid, each with an average market price of 200 €. Thes PV panels could either replace the broken panels or increase the PV generation capacity. However, buying the panels would only increase day-time PV generation. Still, it would not solve their electricity problems at night since it would require about 12,000 € to replace the battery system to attain its intended initial capacity [166]. With the FLC-based system developed in this study, the battery system's life cycles (life span) can be improved by controlling and limiting the Depth of Discharge (DoD) of the batteries. The life span (cycles) of a battery is inversely proportional to the DoD_{max} of the battery [167, 168]. This is expressed by equation (17). As shown in Fig. 82, the DoD_{max} has been improved from 100% (complete discharge of the battery) to 70% (normally the battery reaches morning with about 30% of its capacity remaining). This improvement can improve the life cycles of batteries by about 50%, assuming the charge capacity remains the same before and after, and k = 1.2. The improvement in the operational lifetime of the battery is the result of tightening the SoC limit using the FLC system.

$$Life\ cycle\ extension\ factor\ = [\frac{1}{DoD_{max}}]^{k} \quad (17)$$

$k - ranges\ between\ 1.1\ to\ 1.3\ for\ Pb - acid\ batteries$

DoD_{max} − Permitted usable capacity before recharging

5.6 Chapter Summary

This chapter discusses the process of field data collection and analysis. It provides a clear picture of the situation at the case-study microgrid, such as the load profiles, power generation curves, and SoC of the energy storage battery bank. The field study findings have shown that, to a certain extent, the FLC-based traffic light system can be used for load control to ensure a proper and real-time DSM to avoid overloading in the microgrids. However, this research has also shown that some people would not wilfully cooperate with this DSM technique. In future studies, the financial incentives and penalties should be added to this developed FLC-based traffic light DSM technique to make more people conscious of following and responding to the traffic light signals.

CHAPTER SIX

CONCLUSION AND RECOMMENDATIONS

6.1 Conclusion

This research study aimed to design and develop a robust, autonomous, low-cost wireless sensor system for loading and controlling power utilisation to ensure proper and real-time DSM to avoid overloading in distributed microgrids. A novel real-time load monitoring and control system which acts as an intelligent system of demand limiters has been successfully developed employing the FLC and LoRa wireless communication technology. This work has produced and installed 60 LoRa-based consumer modules in 60 Silale Village, Tanzania households. The consumer modules wirelessly transmit each household's load (power consumption) to the host computer. Consumer modules also wirelessly receive the control signal from the host computer for controlling power usage by using traffic-light system notification. The developed prototype provides a feasible, modern, and more reliable approach for load control in microgrids in rural SSA.

Simulation results based on the data collected before load control was enforced show that the FLC technique effectively levels the load profile and shapes it by the PV power generation curve. Results show that the system can maintain the availability of electricity for the core service, such as lights for the whole night without blackouts while saving about 1.1% of battery energy until the charging starts the following morning. After implementing the developed system in the microgrid, the field findings show that it is possible to use an FLC-based traffic light for the load control to ensure a proper and achieve real-time DSM, to avoid overloading in the microgrids.

Finally, it is noted that the cooperation of the connected consumers is essential for this system to deliver the intended load control function. This system can be very useful in a real-time pricing environment and/or with other financial incentives provided to consumers. The traffic light system may encourage them to change their power consumption pattern to ensure the microgrid's sustainability by reducing power consumption during peak demand and low generation hours. With proper awareness, understanding, and substantial gain, consumers may be motivated to adjust their lifestyles, especially their power consumption profile.

6.2 Recommendations

Real-time load monitoring and control are essential for the future of smart-grids and the sustainability of the present RES-based microgrids. Due to the intermittent nature of the RESs, load monitoring and control in RES-based microgrids is important for ensuring the microgrid's electric power availability, reliability, and sustainability. This research is an initiative to find techniques for attaining power availability and microgrid sustainability in RES-based microgrids in rural areas of SSA. This research work recommends the following points:

- Using load and power generation forecast techniques and load monitoring and control as DSM techniques to form a robust solution for a much more reliable electrical energy supply in microgrids. Microgrid owners and operators should employ a cheap and real-time solution like a LoRa-based load monitoring and control system presented in this dissertation.
- Consumers should be encouraged to change their electricity usage behaviour and promptly respond to the notification and load control signals for the sustainability of the microgrid. By using a traffic-light system such as the one presented in this dissertation, the consumers can simply observe the notifications on the consumer module and change their consumption patterns. When working with tariff or incentive schemes, the traffic-light system can be more effective in load control and sustainability of microgrids. Microgrid operators and community leaders should create awareness among electricity customers on the importance of DSM and the benefits they can get from it to encourage their participation in the program.
- Future research should work on other LPWAN technologies which can provide a shorter transmission time compared to 1600 ms, which was attained in this research. The system will increase accuracy if the data can be accurately transferred in long range at low power and even a shorter latency. Future research also can use other AI and Machine Learning (ML) techniques, such as ANN for load control over an LPWAN, and asses the general improvement in methodologies and results.
- In the future, similar work is recommended on microgrids operating on other power sources, such as biomass, wind, and geothermal energy, as an extension of this study, which has focused on the solar PV microgrid. Future works can consider other RESs and the complex configurations of microgrids, such as microgrids with diesel generators and other hybrid microgrids.
- Additional studies should be carried out on implementing the LoRa technique in an embedded system that may allow a receiver to send and receive concurrently. Likewise, an

antenna length beyond 1/4 of the wavelength (of the monopole antenna) can be considered in future developments to bring about further improvements in data transmission.

- Moreover, future research should also work on how we can employ the LPWAN and AI techniques such as FLC (employed in this study) for load monitoring and control of grid-tied microgrids and even extend it to cover the whole national grid. This work has used a distributed microgrid as a case study to provide the foundation for expanding this study to the network of microgrids in the future.

6.3 Outlook

The developed consumer module can be rated to measure currents up to 10A. However, if the hardware is adopted, this value can be increased by replacing the high-value relay switches and current sensors. For accurate measurements, this module is suitable only for AC voltage in the range of 200-240V RMS.

The developed LoRa transceiver is designed for data transmission in the ISM license-free band of 862 MHz to 1020 MHz. The frequency assignment should also consider other wireless applications or systems employing the ISM bands in that frequency range to avoid signal interference.

REFERENCES

[1] Andrae, A.S. and Edler, T., 2015. On global electricity usage of communication technology: trends to 2030. *Challenges*, 6(1), pp.117-157. https://doi.org/10.3390/challe6010117

[2] Brynjolfsson, E., Hofmann, P. and Jordan, J., 2010. Cloud computing and electricity: beyond the utility model. *Communications of the ACM*, 53(5), pp.32-34. DOI: http://doi.acm.org/10.1145/1735223.173523

[3] Daly, H., & Walton, M. A., 2017. Energy access outlook 2017: from poverty to prosperity. World Energy Outlook 2017, Special Report. Paris, France: *International Energy Agency (IEA)*.

[4] World Resources Institute, 2017. Report: Tanzania Mini-grid Sector Doubles with Bold Policy Approach. Retrieved on April 2, 2021 from https://www.wri.org/news/release-report-tanzania-mini-grid-sector-doubles-bold-policy-approach

[5] PwC, 2016. Electricity Beyond the Grid: Accelerating Access to Sustainable Power for All, Global Power & Utilities. Retrieved on September 12, 2021 from https://www.pwc.com/gx/en/energy-utilities-mining/pdf/electricity-beyond-grid.pdf

[6] General Assembly, 2015. Resolution adopted by the General Assembly on 11 September 2015. A/RES/69/315 15 September 2015. New York: United Nations. Retrieved on September 12, 2021 from https://archive.unescwa.org/sites/www.unescwa.org/files/un_resolutions/a_res_69_315_e.pdf

[7] Akinyele, D., Belikov, J., and Levron, Y., 2018. Challenges of Microgrids in Remote Communities: A STEEP Model Application. *Energies*, 11(2), 432. https://doi.org/10.3390/en11020432

[8] Berizzi, A., Delfanti, M., Falabretti, D., Mandelli, S. and Merlo, M., 2019. Electrification processes in developing countries: grid expansion, microgrids, and regulatory framework. *Proceedings of the IEEE*, 107(9), pp.1981-1994. DOI: 10.1109/JPROC.2019.2934866

[9] Hartvigsson, E., Ehnberg, J., Ahlgren, E. and Molander, S., 2015. Assessment of load profiles in minigrids: A case in Tanzania. In *2015 50th International Universities Power Engineering Conference (UPEC)* (pp. 1-5). IEEE. https://doi.org/10.1109/UPEC.2015.7339818.

[10] Lecaros, S. S., Ireri, B., Mentis, D., and Kaldjian, E., (2019). For the Millions of East Africans Who Need Electricity Most, Data Shows Renewable Energy Is a Viable – and Affordable – Solution. World Resources Institute. Retrieved on September 12, 2022 from https://www.wri.org/blog/2019/09/millions-east-africans-who-need-electricity-data-shows-renewable-energy-most-viable-affordable-solution

[11] Ministry of Energy, 2019. Wizara ya Nishati – Jamhuri ya Muungano ya Tanzania. Retrieved on February 7, 2021, from https://www.nishati.go.tz/ks/.

[12] Ahlborg, H., and Hamma, L., 2011. Drivers and barriers to rural electrification in Tanzania and Mozambique. *World Renewable Energy Congress*, 2493–2500. Retrieved on September 12, 2021 from https://ideas.repec.org/a/eee/renene/v61y2014icp117-124.html.

[13] Ministry of Energy and Minerals, 2015. *Tanzania's SE4ALL Action Agenda*. Dar es Salaam, Tanzania. Ministry of Energy and Minerals, the United Republic of Tanzania. Retrieved on September 20, 2021 https://www.seforall.org/sites/default/files/TANZANIA_AA-Final.pdf

[14] García Vera, Y.E., Dufo-López, R. and Bernal-Agustín, J.L., 2019. Energy management in microgrids with renewable energy sources: A literature review. *Applied Sciences,* 9(18), p.3854. DOI: 10.3390/app9183854.

[15] Khadar, A., Ahamed, J., Madanpalli, E., & Nagaraj, I. M., (2017). Research Advancements Towards in Existing Smart Metering over Smart Grid. *International Journal of Advanced Computer Science and Applications,* 5(8), 84-92. Retrieved on August 27, 2021 from https://pdfs.semanticscholar.org/af2c/d713c42203caf9c93c207a22a91b593636bb.pdf

[16] Omary, S. 2020. A Two-Way Electricity Usage Monitoring System for Decentralized Solar Mini-Grids in Tanzania. Masters Dissertation, NM-AIST. Retrieved on January 19, 2023 from https://dspace.nm-aist.ac.tz/handle/20.500.12479/915

[17] Mišák, S., Stuchlý, J., Platoš, J., and Krömer, P., 2015. A heuristic approach to active demand side management in off-grid systems operated in a smart-grid environment. *Energy and Buildings,* 96(272-284. doi: 10.1016/j.enbuild.2015.03.033.

[18] Ngowi, J. M., Bångens, L., and Ahlgren, E. O., 2019. Benefits and challenges to productive use of off-grid rural electrification: The case of mini-hydropower in Bulongwa-Tanzania. *Energy for Sustainable Development*, 53, 97-103. https://doi.org/10.1016/j.esd.2019.10.001

[19] Harper, M., 2014. Review of Strategies and Technologies for Demand-Side Management on Isolated Mini-Grids. *Lawrence Berkeley National Laboratory (LBNL)*, 3, 1–26. Retrieved on March 19, 2022 from https://escholarship.org/uc/item/0wc020br.

[20] Segatto, M. E. V., de Oliveira Rocha, H. R., Silva, J. A. L., Paiva, M. H. M., and do Rosário Santos, M. A., 2018. Telecommunication Technologies for Smart Grids: Total Cost Optimization. *Advances in Renewable Energies and Power Technologies,* 2, 451–478. https://doi.org/10.1016/B978-0-12-813185-5.00007-3.

[21] Lloret, J., Tomas, J., Canovas, A., and Parra, L., 2016. An Integrated IoT Architecture for Smart Metering. *IEEE Communications Magazine*, 54(12), 50–57. https://doi.org/10.1109/MCOM.2016.1600647CM.

[22] Sandelowski, M., Davis, D.H. and Harris, B.G., 1989. Artful design: Writing the proposal for research in the naturalist paradigm. *Research in Nursing & Health*, 12(2), pp.77-84. https://doi.org/10.1002/nur.4770120204

[23] Hevner, A. R., 2007. A Three-Cycle View of Design Science Research. *Scandinavian Journal of Information Systems*, 19(2), 4. Retrieved on March 19, 2022 from http://aisel.aisnet.org/sjis/vol19/iss2/4

[24] Sinde, R., Begum, F., Njau, K. and Kaijage, S., 2020. Refining network lifetime of wireless sensor network using energy-efficient clustering and DRL-based sleep scheduling. *Sensors*, 20(5), p.1540. https://doi.org/10.3390/s20051540

[25] El Brak, M., and Essaaidi, M., 2012. Wireless sensor network in smart grid technology: Challenges and opportunities. *2012 6th International Conference on Sciences of Electronics, Technologies of Information and Telecommunications*, 578–583. https://doi.org/10.1109/SETIT.2012.6481976.

[26] Barman, B. K., Yadav, S. N., Kumar, S., and Gope, S., 2018. Energy Utilization in Smart Grid. *2018 2nd International Conference on Power, Energy and Environment: Towards Smart Technology*, 2–4. DOI: 10.1109/EPETSG.2018.8658501.

[27] Vine, D., Buys, L., and Morris, P., 2015. The Effectiveness of Energy Feedback for Conservation and Peak Demand: A Literature Review. *Open Journal of Energy Efficiency,* 02(01), 7–15. https://doi.org/10.4236/ojee.2013.21002.

[28] Alahakoon, D., and Yu, X., 2016. Smart Electricity Meter Data Intelligence for Future Energy Systems: A Survey. *IEEE Transactions on Industrial Informatics*, 12(1), 425–436. https://doi.org/10.1109/TII.2015.2414355.

[29] Beigh, N. T., 2019. Review on Smart Electric Metering System Based on GSM/IOT. *Asian Journal of Electrical Sciences*, 8(1), 1-6. Retrieved on March 29, 2022 from https://www.researchgate.net/ publication/330358185

[30] Ton, D. T., and Smith, M. A,. 2012. The US department of energy's microgrid initiative. *The Electricity Journal*, 25(8), 84-94. https://doi.org/10.1016/j.tej.2012.09.013

[31] Ackermann, T., Andersson, G., and Söder, L., 2001. Distributed Generation: A Definition. *Electric Power Systems Research*, 57(3), 195-204. https://doi.org/10.1016/S0378-7796(01)00101-8

[32] Poullikkas, A., 2007. Implementation of Distributed Generation Technologies in Isolated Power Systems. *Renewable and Sustainable Energy Reviews*, 11(1), 30-56. https://doi.org/10.1016/j.rser.2006.01.006

[33] Pedersen, M. B., 2016. Deconstructing the Concept of Renewable Energy-Based Mini-Grids for Rural Electrification in East Africa. *WIREs Energy Environment*, 5, 570-587. https://doi.org/10.1002/wene.205.

[34] Masenge, I. H., and Mwasilu, F., 2020. Modeling and Control of Solar PV with Battery Energy Storage for Rural Electrification. *Tanzania Journal of Engineering and Technology*, 39(1). Retrieved on March 11, 2021 from https://www.ajol.info/index.php/tjet/article/view/235965

[35] Akinyele, D. O., Nair, N. K. C., Rayudu, R. K., and Seah, W. K., 2014. Clean Development Mechanism Projects for Developing Countries: Potential for Carbon Emissions Mitigation and Sustainable Development. *In 2014 Eighteenth National Power Systems Conference (NPSC)* (pp. 1-6). IEEE. DOI: 10.1109/NPSC.2014.7103828

[36] Kainkwa, R. M. R., 2008. Survey of wind power potential for wind-based electricity at Makambako, Iringa Tanzania. *Tanzania Journal of Science*, 34. Retrieved on March 11, 2021 from https://www.ajol.info/index.php/tjs/article/view/44282

[37] Renewables, 2017. Global Status Report; Renewable Energy Policy Network for the 21st Century; Technical Report; Paris Cedex, France, 2017. Retrieved on March 11, 2021 from http://www.ren21.net/wp-content/uploads/2017/06/17-8399_GSR_2017_Full_Report_0621_Opt.pdf (accessed on 23 October 2017).

[38] Willcox, M., Pueyo, A., Waters, L., Hanna, R., Wanjiru, H., Palit, D., and Sharma, K. R., 2015. Utilising Electricity Access for Poverty Reduction. *Practical Actions*. Retrieved on February 21, 2022 http://cdn1.practicalaction.org/e/l/54c7a51f-312c-4f20-a8e7-177c0a0000be.pdf

[39] Yadoo, A. and Cruickshank, H., 2012. The role for low carbon electrification technologies in poverty reduction and climate change strategies: A focus on renewable energy mini-grids with case studies in Nepal, Peru and Kenya. Energy Policy, 42, pp.591-602. https://doi.org/10.1016/j.enpol.2011.12.029

[40] Venkataraman, S., Ziesler, C., Johnson, P., and Van Kempen, S., 2018. Integrated wind, solar, and energy storage: Designing plants with a better generation profile and lower overall cost. *IEEE Power and Energy Magazine*, 16(3), 74-83. DOI: 10.1109/MPE.2018.2793478

[41] Zaidi, A. A., Zia, T., and Kupzog, F., 2010. Automated demand side management in microgrids using load recognition: *2010 8th IEEE International Conference on Industrial Informatics*, 774-779. doi: 10.1109/INDIN.2010.5549646.

[42] Muralikrishna, M., and Lakshminarayana, V., 2008. Hybrid (solar and wind) energy systems for rural electrification. *ARPN Journal of Engineering and Applied Sciences*, 3(5), 50-58. Retrieved on February 21, 2022 https://citeseerx.ist.psu.edu/document?repid=rep1&type=pdf&doi=a740cfe7e120fae4d2a4a860d8669de67dddba01

[43] Bhaskara, S. N., and Chowdhury, B. H., 2012. Microgrids—A review of modeling, control, protection, simulation and future potential. *In 2012 IEEE Power and Energy Society General Meeting* (pp. 1-7). IEEE. DOI: 10.1109/PESGM.2012.6345694

[44] Ministry of Energy, 2020. Power System Master Plan 2020 Update. Retrieved on February 2, 2021, from https://www.nishati.go.tz/ks/.

[45] Aly, A., Moner-Girona, M., Szabó, S., Pedersen, A. B., and Jensen, S. S., 2019. Barriers to large-scale solar power in Tanzania. *Energy for Sustainable Development*, 48, 43-58. https://doi.org/10.1016/j.esd.2018.10.009

[46] Masenge, I., and Mwasilu, F., 2020. Hybrid Solar PV-Wind Generation System Coordination Control and Optimization of Battery Energy Storage System for Rural Electrification. *In 2020 IEEE PES/IAS PowerAfrica (pp. 1-5)*. IEEE. DOI: 10.1109/PowerAfrica49420.2020.9219890

[47] Teske, S., Morris, T., and Nagrath, K., 2017. 100% Renewable Energy for Tanzania–Access to renewable and affordable energy for all within one generation Retrieved on February 21, 2022 through https://opus.cloud.lib.uts.edu.au and http://hdl.handle.net/10453/118647

[48] EWURA, 2021. Electricity Infrastructure. Retrieved on January 12, 2021, from https://www.ewura.go.tz/electricity-infrastructure/

[49] Odarno, L., Sawe, E., Swai, M., Katyega, M. J. J., and Lee, A., 2017. Accelerating Mini- Grid Deployment in Sub-Saharan Africa. Retrieved on February 21, 2021 from https://www.wri.org/ publication/tanzania-mini-grids.

[50] Freeman, R., 2005. Managing energy: Reducing peak load and managing risk with demand response and demand side management. Refocus, 6(5), pp.53-55. https://doi.org/10.1016/S1471-0846(05)70462-5.

[51] Ngondya, D. J., and Mwangoka, J. W., 2017. Token-based scheduling for access guarantee in deregulated electricity markets' smart grids. *Cogent Engineering*, 4(1), 1394417. https://doi.org/10.1080/23311916.2017.1394417

[52] Jabir, H. J., Teh, J., Ishak, D. and Abunima, H., 2018. Impacts of demand-side management on electrical power systems: A review. *Energies*, 11(5), p.1050. https://doi.org/10.3390/en11051050

[53] Lewis, N. S., and Nocera, D. G., 2006. Powering the planet: Chemical challenges in solar energy utilization. *Proceedings of the National Academy of Sciences*, 103(43), 15729-15735. doi: 10.1073/pnas.0603395103.

[54] Logenthiran, T., Srinivasan, D., and Shun, T. Z., 2012. Demand side management in smart grid using heuristic optimization. *IEEE transactions on Smart Grid*, 3(3), 1244-1252. doi: 10.1109/TSG.2012.2195686.

[55] Lampropoulos, I., Kling, W.L., Ribeiro, P.F. and van den Berg, J., 2013. History of demand side management and classification of demand response control schemes, *IEEE Power & Energy Society General Meeting*. (pp. 1-5). IEEE. DOI: 10.1109/PESMG.2013.6672716

[56] Panda, S., Rout, P.K. and Sahu, B.K., 2021, January. Residential sector demand side management: A review. *In 2021 1st Odisha International Conference on Electrical Power Engineering, Communication and Computing Technology (ODICON)* (pp. 1-6). IEEE. DOI: 10.1109/ODICON50556.2021.9428960

[57] Albadi, M. H., and El-Saadany, E. F., 2007. Demand response in electricity markets: An overview. *Power Engineering Society General Meeting, 2007*. IEEE, 1-5. doi: 10.1109/PES.2007.385728.

[58] Torriti, J., Hassan, M. G., and Leach, M., 2010. Demand response experience in Europe: Policies, programmes and implementation. *Energy,* 35(4), 1575-1583. doi: 10.1016/j.energy.2009.05.021.

[59] York, D. and Kushler, M., 2005, March. Exploring the relationship between demand response and energy efficiency: A review of experience and discussion of key issues. Washington, DC, USA: American Council for an Energy-Efficient Economy.1-88. Retrieved on February 21, 2021 from https://www.dret-ca.com/wp-content/uploads/2021/03/ACEEE-EE-and-DR-York_Kushler-2005.pdf

[60] Aalami, H.A., Moghaddam, M.P. and Yousefi, G.R., 2010. Demand response modeling considering interruptible/curtailable loads and capacity market programs. *Applied Energy*, 87(1), pp.243-250. https://doi.org/10.1016/j.apenergy.2009.05.041

[61] Hussain, M., and Gao, Y., 2018. A review of demand response in an efficient smart grid environment. *The Electricity Journal*, 31(5), 55-63. doi: 10.1016/j.tej.2018.06.003.

[62] Ngondya, D. J. 2018. Demand-Side Management Framework for Deregulated Electricity Markets, NM-AIST. Retrieved on January 19, 2023 from https://dspace.nm-aist.ac.tz/handle/20.500.12479/301

[63] Philipo, G.H., Chande Jande, Y.A. and Kivevele, T., 2020. Demand-side management of solar microgrid operation: Effect of time-of-use pricing and incentives. *Journal of Renewable Energy*, 2020. https://doi.org/10.1155/2020/6956214

[64] Philipo, G.H., Chande Jande, Y.A. and Kivevele, T., 2021. Clustering and fuzzy logic-based demand-side management for solar microgrid operation: case study of Ngurudoto microgrid, Arusha, Tanzania. *Advances in Fuzzy Systems*, 2021, pp.1-13. https://doi.org/10.1155/2021/6614129

[65] Gudi, N., Wang, L., and Devabhaktuni, V., 2012. A demand side management based simulation platform incorporating heuristic optimization for management of household appliances. *International Journal of Electrical Power & Energy Systems*, 43(1), 185-193. doi: 10.1016/j.ijepes.2012.05.023

[66] Billinton, R. and Huang, D., 2006, May. Peaking unit considerations in generating capacity adequacy assessment. In *2006 Canadian Conference on Electrical and Computer Engineering* (pp. 386-389). IEEE. DOI: 10.1109/CCECE.2006.277661

[67] Kundur, P., Paserba, J., Ajjarapu, V., Andersson, G., Bose, A., Canizares, C., Hatziargyriou, N., Hill, D., Stankovic, A., Taylor, C. and Van Cutsem, T., 2004. Definition and classification of power system stability IEEE/CIGRE joint task force on stability terms and definitions. *IEEE transactions on Power Systems*, 19(3), pp.1387-1401. DOI: 10.1109/TPWRS.2004.825981

[68] Babahajiani, P., Shafiee, Q. and Bevrani, H., 2016. Intelligent demand response contribution in frequency control of multi-area power systems. *IEEE Transactions on Smart Grid*, 9(2), pp.1282-1291. DOI: 10.1109/TSG.2016.2582804

[69] Aghajani, G.R., Shayanfar, H.A. and Shayeghi, H., 2017. Demand side management in a smart micro-grid in the presence of renewable generation and demand response. *Energy*, 126, pp.622-637. https://doi.org/10.1016/j.energy.2017.03.051

[70] Zunnurain, I., Maruf, M.N.I., Rahman, M.M. and Shafiullah, G.M., 2018. Implementation of advanced demand side management for microgrid incorporating demand response and home energy management system. *Infrastructures*, 3(4), p.50. https://doi.org/10.3390/infrastructures3040050

[71] Prasad, J., Jain, T., Sinha, N. and Rai, S., 2020, July. Load Shifting Based DSM Strategy for Peak Demand Reduction in a Microgrid. *In 2020 International Conference on Emerging Frontiers in Electrical and Electronic Technologies (ICEFEET)* (pp. 1-6). IEEE. DOI: 10.1109/ICEFEET49149.2020.9186983

[72] Zhu, L., Yan, Z., Lee, W.J., Yang, X., Fu, Y. and Cao, W., 2015. Direct load control in microgrids to enhance the performance of integrated resources planning. *IEEE Transactions on Industry Applications*, 51(5), pp.3553-3560. DOI: 10.1109/TIA.2015.2413960

[73] De Christo, T. M., Perron, S., Fardin, J. F., Simonetti, D. S. L., and de Alvarez, C. E., 2019. Demand-side energy management by cooperative combination of plans: A multi-objective method applicable to isolated communities. *Applied Energy*, 240, 453-472. doi: 10.1016/j.apenergy.2019.02.011

[74] Jordehi, A. R., 2019. Optimisation of demand response in electric power systems, a review. *Renewable and Sustainable Energy Reviews*, 103, 308-319. doi: 10.1016/j.rser.2018.12.054

[75] Yamchi, H. B., Shahsavari, H., Kalantari, N. T., Safari, A., and Farrokhifar, M., 2019. A cost-efficient application of different battery energy storage technologies in microgrids considering load uncertainty. *Journal of Energy Storage*, 22, 17-26. doi: 10.1016/j.est.2019.01.023

[76] Philipo, G.H., Kakande, J.N. and Krauter, S., 2022. Neural Network-Based Demand-Side Management in a Stand-Alone Solar PV-Battery Microgrid Using Load-Shifting and Peak-Clipping. *Energies*, 15(14), p.5215. https://doi.org/10.3390/en15145215

[77] Zadeh, L. A., 1999. From computing with numbers to computing with words. From manipulation of measurements to manipulation of perceptions. *IEEE Transactions on circuits and systems I: fundamental theory and applications,* 46(1), 105-119. DOI: 10.1109/81.739259

[78] Klir, G., and Yuan, B., 1995. *Fuzzy sets and fuzzy logic* (Vol. 4, pp. 1-12). New Jersey: Prentice hall.

[79] Spolaor, S., Fuchs, C., Cazzaniga, P., Kaymak, U., Besozzi, D., and Nobile, M. S., 2020. Simpful: a user-friendly Python library for fuzzy logic. *International Journal of Computational Intelligence Systems,* 13(1), 1687-1698. 10.2991/ijcis.d.201012.002

[80] Rathaiah, M., Reddy, P.R.K.K. and Sujatha, P., 2018. Adaptive Fuzzy Controller Design for Solar and Wind Based Hybrid System. *Int. J. Eng. Technol*, 7, p.283

[81] Anthony, M., Prasad, V., Kannadasan, R., Mekhilef, S., Alsharif, M.H., Kim, M.K., Jahid, A. and Aly, A.A., 2021. Autonomous fuzzy controller design for the utilization of hybrid PV-wind energy resources in demand side management environment. *Electronics,* 10(14), p.1618. https://doi.org/10.3390/electronics10141618

[82] Rohmanuddin, M., The, H.L., Ahmad, A.S. and Nazaruddin, Y.Y., 2000, October. Simplifying fuzzy rule base of multiple input multiple output systems by constructing multi-layer fuzzy controller. *In Smc 2000 conference proceedings. 2000 ieee international conference on systems, man and cybernetics.'cybernetics evolving to systems, humans, organizations, and their complex interactions*'(cat. no. 0 (Vol. 5, pp. 3728-3733). IEEE. DOI: 10.1109/ICSMC.2000.886590.

[83] Rajendhar, P. and Jeyaraj, B.E., 2019. Application of DR and co-simulation approach for renewable integrated HEMS: a review. *IET Generation, Transmission & Distribution*, 13(16), pp.3501-3512. https://doi.org/10.1049/iet-gtd.2018.5791

[84] Zobaa, A.F. and Vaccaro, A. eds., 2014. *Computational intelligence applications in smart grids: enabling methodologies for proactive and self-organizing power systems*. World Scientific.

[85] Nehrir, M., LaMeres, B., and Gerez, V., 1999. A customer-interactive electric water heater demand-side management strategy using fuzzy logic: *IEEE Power Engineering Society. Winter Meeting,* 433-436. doi: 10.1109/PESW.1999.747494

[86] Xu, L., Wang, Z., Liu, Y. and Xing, L., 2021. Energy allocation strategy based on fuzzy control considering optimal decision boundaries of standalone hybrid energy systems. *Journal of Cleaner Production*, 279, p.123810. https://doi.org/10.1016/j.jclepro.2020.123810

[87] Rahman, M. M., Hettiwatte, S., and Gyamfi, S., 2014. An intelligent approach of achieving demand response by fuzzy logic based domestic load management: *In 2014 Australasian Universities Power Engineering Conference,* 1-6. IEEE. DOI: 10.1109/AUPEC.2014.6966610

[88] Ravibabu, P., Praveen, A., Chandra, C. V., Reddy, P. R., and Teja, M. K. R., 2009. An approach of DSM techniques for domestic load management using fuzzy logic. *In 2009 IEEE International Conference on Fuzzy Systems*, 1303-1307. doi: 10.1109/FUZZY.2009.5277401

[89] Kandris, D., Nakas, C., Vomvas, D. and Koulouras, G., 2020. Applications of wireless sensor networks: an up-to-date survey. *Applied System Innovation*, 3(1), p.14. https://doi.org/10.3390/asi3010014

[90] Zhang, S. and Zhang, H., 2012. A review of wireless sensor networks and its applications. *In 2012 IEEE international conference on automation and logistics* (pp. 386-389). IEEE. DOI: 10.1109/ICAL.2012.6308240

[91] Olakanmi, O.O., Pamela, A. and Ashraf, A., 2017. A review on secure routing protocols for wireless sensor networks. *International Journal of Sensors Wireless Communications and Control*, 7(2), pp.79-92. DOI: https://doi.org/10.2174/2210327907666170906144322

[92] Verma, S., Sood, N., and Sharma, A. K., 2018. Design of a novel routing architecture for harsh environment monitoring in heterogeneous WSN. *IET Wireless Sensor Systems,* 8(6), 284–294. https://doi.org/10.1049/iet-wss.2018.5025

[93] Tchakonte, D. T., Simeu, E., and Tchuente, M., 2020. Lifetime Optimization of Wireless Sensor Networks with Sleep Mode Energy Consumption of Sensor Nodes. *Wireless Networks*, 26(1), 91-100. https://doi.org/10.1007/s11276-018-1783-3

[94] Halawani, S., and Khan, A. W., 2010. Sensors Lifetime Enhancement Techniques in Wireless Sensor Networks - A Survey. *Journal of Computing*, 2(5), 34–47. https://doi.org/10.48550/arXiv.1005.4013.

[95] Kosunalp, S., and Cihan, A., 2017. Harvesting Solar Energy for Limited-Energy Problem in Wireless Sensor Networks. *2017 25th Signal Processing and Communications Applications Conference, SIU 2017*. https://doi.org/10.1109/SIU.2017.7960535

[96] Sheikhi, M., Kashi, S. S., and Samaee, Z., 2019. Energy Provisioning in Wireless Rechargeable Sensor Networks with Limited Knowledge. *Wireless Networks*, 25(6), 3531–3544. https://doi.org/10.1007/s11276-019-01948-1

[97] Yue, X., Kauer, M., Bellanger, M., Beard, O., Brownlow, M., Gibson, D., Clark, C., MacGregor, C. and Song, S., 2017. Development of an indoor photovoltaic energy harvesting module for autonomous sensors in building air quality applications. *IEEE Internet of Things Journal*, 4(6), pp.2092-2103. DOI: 10.1109/JIOT.2017.2754981

[98] Zeadally, S., Shaikh, F.K., Talpur, A. and Sheng, Q.Z., 2020. Design architectures for energy harvesting in the Internet of Things. *Renewable and Sustainable Energy Reviews*, 128, p.109901. https://doi.org/10.1016/j.rser.2020.109901

[99] Kuzlu, M., Pipattanasomporn, M., and Rahman, S., 2014. Communication network requirements for major smart grid applications in HAN, NAN and WAN. *Computer Networks,* 67, 74–88. https://doi.org/10.1016/j.comnet.2014.03.029

[100] Philip, M.S. and Singh, P., 2020. Review of energy harvesting in lora based wireless sensor network. In *2020 2nd International Conference on Advances in Computing, Communication Control and Networking (ICACCCN)* (pp. 338-341). IEEE. DOI: 10.1109/ICACCCN51052.2020.9362892

[101] Jawad, H.M., Nordin, R., Gharghan, S.K., Jawad, A.M. and Ismail, M., 2017. Energy-efficient wireless sensor networks for precision agriculture: A review. *Sensors*, 17(8), p.1781. https://doi.org/10.3390/s17081781

[102] Porret, A. S., Melly, T., Enz, C. C., and Vittoz, E. A., 2000. A low-power low-voltage transceiver architecture suitable for wireless distributed sensors network. In *2000 IEEE International Symposium on Circuits and Systems (ISCAS)* (Vol. 1, pp. 56-59). IEEE. DOI: 10.1109/ISCAS.2000.857025

[103] Takriti, M., Boussaada, Z., Sansa, I., Curea, O. and Bellaaj, N.M., 2020, September. Wireless sensors networks applications for micro-grids management: State of art. In *2020 6th IEEE International Energy Conference (ENERGYCon)* (pp. 1058-1061). IEEE. DOI: 10.1109/ENERGYCon48941.2020.9236519

[104] Mekki, K., Bajic, E., Chaxel, F., and Meyer, F., 2019. A comparative study of LPWAN technologies for large-scale IoT deployment. *ICT Express*, 5(1), 1–7. https://doi.org/ 10.1016/j.icte.2017.12.005

[105] Siddique, A., Prabhu, B., Chaskar, A. and Pathak, R., 2019. A review on intelligent agriculture service platform with lora based wireless sensor network. *Life, 100*, p.7000. e-ISSN: 2395-0056

[106] Kumbhar, A., 2017. Overview of ISM bands and Software-defined Radio Experimentation. *Wireless Personal Communications*, 97(3), pp.3743-3756. https://doi.org/10.1007/s11277-017-4696-z

[107] Cattani, M., Boano, C. A., and Römer, K., 2017. An Experimental Evaluation of The Reliability of LoRa Long-Range Low-Power Wireless Communication. *Journal of Sensor and Actuator Networks,* 6(2). https://doi.org/10.3390/jsan6020007

[108] Gill, K., Yang, S. H., Yao, F., and Lu, X., 2009. A ZigBee-based Home Automation System. *IEEE Transactions on consumer Electronics,* 55(2), 422-430. DOI: 10.1109/TCE.2009.5174403

[109] LoRa Alliance, "RP002-1.0.3 LoRaWAN® Regional Parameters," [Online]. Available: https://lora-alliance.org/wpcontent/uploads/2021/05/RP002-1.0.3-FINAL-1.pdf. [Accessed Dec 1, 2021].

[110] Semtech "LoRa™ Modulation Basics," Datasheet AN1200.22, 2020. [Online]. Available: https://www.frugalprototype.com/ wpcontent/uploads/2016/08/an1200.22.pdf [Accessed Dec 1, 2021]

[111] Almuhaya, M. A., Jabbar, W. A., Sulaiman, N. and Abdulmalek, S., 2022. A survey on Lorawan technology: Recent trends, opportunities, simulation tools and future directions. *Electronics*, 11(1), p.164. https://doi.org/10.3390/electronics11010164

[112] Khutsoane, O., Isong, B. and Abu-Mahfouz, A. M., 2017. IoT devices and applications based on LoRa/LoRaWAN. In *IECON 2017-43rd Annual Conference of the IEEE Industrial Electronics Society* (pp. 6107-6112). IEEE. DOI: 10.1109/IECON.2017.8217061

[113] Mwammenywa, I., Petrov, D., Holle, P. and Hilleringmann, U., 2022. LoRa Transceiver for Load Monitoring and Control System in Microgrids. In *2022 International Conference on Engineering and Emerging Technologies (ICEET)* (pp. 1-5). IEEE, doi: 10.1109/ICEET56468.2022.10007274

[114] LoRa®. What are LoRa® and LoRaWAN®? Available online: https://lora-developers.semtech.com/documentation/tech-papersand-guides/lora-and-lorawan [accessed on 04 October 2022].

[115] Idris, S., Karunathilake, T. and Förster, A., 2022. Survey and Comparative Study of LoRa-Enabled Simulators for Internet of Things and Wireless Sensor Networks. *Sensors*, 22(15), p.5546. https://doi.org/10.3390/s22155546

[116] Bor, M.C., Roedig, U., Voigt, T. and Alonso, J.M., 2016. Do LoRa low-power wide-area networks scale? In *Proceedings of the 19th ACM International Conference on Modeling, Analysis and Simulation of Wireless and Mobile Systems* (pp. 59-67). https://doi.org/10.1145/2988287.2989163

[117] Fayadh, R.A., Malek, F. and Fadhil, H.A., 2014. Enhancement of a Three Combining Techniques Rake Receiver Using Adaptive Filter of M-Max Partial Update RLS Algorithm for DS-UWB Systems. *Journal of Next Generation Information Technology*, 5(4), p.93

[118] Semtech Corporation. AN1200.22 LoRa® Modulation Basics; Semtech: Camarillo, CA, USA, 2015. Available online: http://wiki.lahoud.fr/lib/exe/fetch.php?media=an1200.22.pdf [accessed on 29 September 2022].

[119] Bor, M. and Roedig, U., 2017. LoRa transmission parameter selection. In *2017 13th International Conference on Distributed Computing in Sensor Systems (DCOSS)* (pp. 27-34). IEEE. DOI: 10.1109/DCOSS.2017.10

[120] Mohassel, R.R., Fung, A., Mohammadi, F. and Raahemifar, K., 2014. Application of advanced metering infrastructure in smart grids. In *22nd Mediterranean Conference on Control and Automation* (pp. 822-828). IEEE. DOI: 10.1109/MED.2014.6961475

[121] Ghosal, A. and Conti, M., 2019. Key management systems for smart grid advanced metering infrastructure: A survey. *IEEE Communications Surveys & Tutorials*, 21(3), pp.2831-2848. DOI: 10.1109/COMST.2019.2907650

[122] Albayati, A., Abdullah, N.F., Abu-Samah, A., Mutlag, A.H. and Nordin, R., 2020. A serverless advanced metering infrastructure based on fog-edge computing for a smart grid: a comparison study for energy sector in Iraq. *Energies*, 13(20), p.5460. https://doi.org/10.3390/en13205460

[123] Beard, C. Smart Metering for Dummies. JohnWiley and Sons, Ltd.: Chichester, UK, 2010; Available online: https://www.smartme.co.uk/documents/smart_metering_for_dummies.pdf [accessed on 5 November 2021].

[124] Saputro, N., Akkaya, K. and Uludag, S., 2012. A survey of routing protocols for smart grid communications. *Computer Networks*, 56(11), pp.2742-2771. https://doi.org/10.1016/j.comnet.2012.03.027

[125] European Union, 2009. Directive 2009/72/EC of the European parliament and of the council of 13 July 2009 concerning common rules for the internal market in electricity and repealing directive 2003/54/EC. *Official J. Eur. Union*, vol. 52, pp. 55–93.

[126] Joshi, D. S. A., Kolvekar, S., Raj, Y. R., and Singh, S. S., 2017. IoT Based Smart Energy Meter. *Bonfring International Journal of Research in Communication Engineering*, 6, 89–91. https://doi.org/10.9756/bijrce.8209

[127] Ugonna, E. E., Ademola, A. K., and Olusegun, A. T., 2018. Design and construction of a smart electric metering system for smart grid applications: Nigeria as a case study. *International Journal of Scientific & Engineering Research,* 4(7), 800–804.

[128] Ashna, K. and George, S.N., 2013. GSM based automatic energy meter reading system with instant billing. In *2013 International Mutli-Conference on Automation, Computing, Communication, Control and Compressed Sensing (iMac4s)* (pp. 65-72). IEEE. DOI: 10.1109/iMac4s.2013.6526385

[129] Mir, S. H., Ashruf, S., Bhat, Y., and Beigh, N., 2019. Review on Smart Electric Metering System Based on GSM/IOT. *Asian Journal of Electrical Sciences*, 8(1), 1-6.

[130] Wu, H., and Shahidehpour, M., 2016. Applications of wireless sensor networks for area coverage in microgrids. *IEEE Transactions on Smart Grid*, 9(3), 1590-1598. DOI: 10.1109/TSG.2016.2594203

[131] Omary, S. and Sam, A., 2020. Performance Evaluation LoRa-GPRS Integrated Electricity usage Monitoring System for Decentralized Mini-Grids. *International Journal of Advanced Computer Science and Applications*, 11 (2), 438-445.

[132] Ghiasimonfared, A., Righini, D., Marcuzzi, F. and Tonello, A.M., 2017. Development of a hybrid LoRa/G3-PLC IoT sensing network: An application oriented approach. In *2017 IEEE International Conference on Smart Grid Communications (SmartGridComm)* (pp. 503-508). IEEE. DOI: 10.1109/SmartGridComm.2017.8340721

[133] Ghelli, A., Hagras, H. and Aldabbagh, G., 2015. A fuzzy logic-based retrofit system for enabling smart energy-efficient electric cookers. *IEEE Transactions on Fuzzy Systems,* 23(6), pp.1984-1997. DOI: 10.1109/TFUZZ.2015.2394781

[134] Hilleringmann, U., Petrov, D., Mwammenywa, I. and Kagarura, G.M., 2021. Local Power Control using Wireless Sensor System for Microgrids in Africa. In *2021 IEEE AFRICON* (pp. 1-5). IEEE. DOI: 10.1109/AFRICON51333.2021.9570970

[135] Ramsden, E., 2011. Hall-effect sensors: theory and application. Elsevier.

[136] Pololu Robotics and Electronics, 2022. https://www.pololu.com/product/4031 [Accessed 04/07/2022].

[137] Abubakar, I., Khalid, S. N., Mustafa, M. W., Shareef, H., and Mustapha, M., 2017. Calibration of ZMPT101B voltage sensor module using polynomial regression for accurate load monitoring. *ARPN Journal of Engineering and Applied Sciences*, 12(4), 1076–1084.

[138] Surtr Technology, 2019. Easy measure of AC Voltage using Arduino and ZMPT101B. Retrieved on April 10, 2021, from https://surtrtech.com/2019/01/21/easy-measure-of-ac-voltage-using-arduino-and-zmpt101b.

[139] Holle, P. 2022. Development of a LoRa-based data transmission system for use in micro-grids power plants [Master's Thesis]. Sensorik Department, Paderborn University

[140] Hackaday. 2018. Project Hackable CMWX1ZZABZ (LoRa) Devices. Retrieved on November 11, 2021, from https://hackaday.io/project/35169/logs.

[141] Philip, M. S. and Singh, P., 2020. Review of energy harvesting in lora based wireless sensor network. In *2020 2nd International Conference on Advances in Computing, Communication Control and Networking (ICACCCN)* (pp. 338-341). IEEE. DOI: 10.1109/ICACCCN51052.2020.9362892

[142] Shenzhen Hope Microelectronics Co., Ltd., "RFM95W Specification V2.0," [Online]. Retrieved on December 12, 2021, from https://www.hoperf.com/data/upload/portal/20190801/RFM95W-V2.0.pdf.

[143] Mwammenywa, I., Kagarura, G.M., Petrov, D., Holle, P. and Hilleringmann, U., 2021. LoRa-based Demand-side Load Monitoring and Management System for Microgrids in Africa. In *2021 International Conference on Electrical, Computer and Energy Technologies (ICECET)* (pp. 1-5). IEEE. DOI: 10.1109/ICECET52533.2021.9698506

[144] Semtech Corporation. AN1200.22 LoRa® Modulation Basics; Semtech: Camarillo, CA, USA, 2015. Available online: http://wiki.lahoud.fr/lib/exe/fetch.php?media=an1200.22.pdf [accessed on 29 September 2022].

[145] Qoitech AB. Otii Arc User Manual. [Online]. Available: https://www.qoitech.com/docs/user-manual/otii. [Accessed 05/17/2022].

[146] Lithium Battery Charger, 2022. https://www.aliexpress.com/item/33034500618.html [Accessed 04/07/2022].

[147] Vernet, A., Khayesi, J.N., George, V., George, G. and Bahaj, A.S., 2019. How does energy matter? Rural electrification, entrepreneurship, and community development in Kenya. *Energy Policy*, 126, pp.88-98. https://doi.org/10.1016/j.enpol.2018.11.012

[148] Wang, Z., Zhang, B., Yin, J., and Zhang, Y., 2011. Determinants and policy implications for household electricity-saving behaviour: evidence from Beijing, China. *Energy Policy*, 39(6), 3550-3557. doi: 10.1016/j.enpol.2011.03.055.

[149] Atmel Corporation, 2022. ATmega328P Manual. [Online]. Available: https://ww1.microchip.com/downloads/en/DeviceDoc/Atmel-7810-Automotive-Microcontrollers-ATmega328P_Datasheet.pdf. [Accessed 04/11/2022].

[150] Gainta Electrical Enclosures, 2022. https://www.gainta.com/en/g265cmf.html [Accessed 03/09/2022]

[151] Kumar, R., Roopa, A., and Sathiya, D. P., 2015. Arduino ATMEGA-328 microcontroller. *International Journal of Innovative Research in Electrical, Electronics, Instrumentation and Control Engineering*, 3(4), 27-29. doi: 10.17148/IJIREEICE.

[152] R. Hiestermann, "Setting up the Atmel Studio for programming abootloader," [Online]. Available: https://avr-programmierenrh.de/tutorials/atmel-studio-avrdude/. [Accessed 04/11/2022].

[153] Atmel Corporation. AVRISP mkII - USER GUIDE [Online]. Available: https://ww1.microchip.com/downloads/en/DeviceDoc/Atmel-42093-AVRISPmkII_UserGuide.pdf. [Accessed 07/21/2021]

[154] DeLima, P.G. and Yen, G.G., 2004. A truth space diagram temporal linguistic rule extraction procedure using multiple objective evolutionary algorithm. In *2004 IEEE International Conference on Fuzzy Systems (IEEE Cat. No. 04CH37542)* (Vol. 1, pp. 553-558). IEEE. DOI: 10.1109/FUZZY.2004.1375795

[155] Rubenbauer, H. and Henninger, S., 2017. Definitions and reference values for battery systems in electrical power grids. *Journal of Energy Storage*, 12, pp.87-107. https://doi.org/10.1016/j.est.2017.04.004

[156] Burning Compass, 2022. https://www.burningcompass.com/countries/tanzania/tanzania-region-map-hd.html [Accessed 09/21/2022]

[157] Wikipedia, 2022. https://en.wikipedia.org/wiki/Kongwa [Accessed 03/11/2022]

[158] Nelli, F., 2018. Python data analytics with Pandas, NumPy, and Matplotlib. Available online: https://link.springer.com/content/pdf/10.1007/978-1-4842-3913-1.pdf [Accessed 06/25/2022]

[159] Naamandadin, N.A., Ming, C.J. and Mustafa, W.A., 2018. Relationship between Solar Irradiance and Power Generated by Photovoltaic Panel: Case Study at UniCITI Alam Campus, Padang Besar, Malaysia. *Journal of Advanced Research in Engineering Knowledge*, 5(1), pp.16-20.

[160] Al Hadi, A.M.R., Ekaputri, C. and Reza, M., 2019, November. Estimating the state of charge on lead acid battery using the open circuit voltage method. In *Journal of Physics: Conference Series* (Vol. 1367, No. 1, p. 012077). IOP Publishing.

[161] Wu, G., Lu, R., Zhu, C. and Chan, C.C., 2010, September. An improved Ampere-hour method for battery state of charge estimation based on temperature, coulomb efficiency model and capacity loss model. In *2010 IEEE vehicle power and propulsion conference* (pp. 1-4). IEEE. DOI: 10.1109/VPPC.2010.5729017

[162] Moo, C.S., Ng, K.S., Chen, Y.P. and Hsieh, Y.C., 2007, April. State-of-charge estimation with open-circuit-voltage for lead-acid batteries. In *2007 Power Conversion Conference-Nagoya* (pp. 758-762). IEEE. DOI: 10.1109/PCCON.2007.373052

[163] Ng, K.S., Moo, C.S., Chen, Y.P. and Hsieh, Y.C., 2008, December. State-of-charge estimation for lead-acid batteries based on dynamic open-circuit voltage. In *2008 IEEE 2nd International Power and Energy Conference* (pp. 972-976). IEEE. DOI: 10.1109/PECON.2008.4762614

[164] Hoppecke, 2023. Installation, commissioning and operating instructions for valve-regulated stationary lead-acid batteries https://www.hoppecke.com/fileadmin/Redakteur/Hoppecke-Main/Products-Import/vrl_manual_en.pdf [Accessed 03/11/2023]

[165] Mottram, H., 2022. Injustices in rural electrification: Exploring equity concerns in privately owned minigrids in Tanzania. *Energy Research & Social Science,* 93, p.102829.

[166] Europe Solarstore, 2023. https://www.europe-solarstore.com/hoppecke-10-opzv-solar-power-1250-48v.html [Accessed 03/11/2023]

[167] Linden, D. (1994). Handbook of batteries (2nd ed.). McGraw-Hill.

[168] Mishra, P.P., Latif, A., Emmanuel, M., Shi, Y., McKenna, K., Smith, K. and Nagarajan, A., 2020. Analysis of degradation in residential battery energy storage systems for rate-based use-cases. *Applied Energy*, 264, p.114632. https://doi.org/10.1016/j.apenergy.2020.114632

APPENDICES

Appendix I: List of Components for Low-Voltage PCB

Low Voltage PCB		
Circuit Designation	**Function**	**No.**
U1	microcontroller	1
U2	LoRa module	1
U3	UART/USB converter	1
U4	circuit breaker	1
IC2	voltage regulator	1
Y1	quartz	1
X1	SMA connector (90°)	1
T1, T2, T3, T4	bipolar transistor	4
SG1	buzzer	1
J1	USB connector	1
D1, D4	diode	2
D2	diode	1
LED1, RED	LED SMD red	2
GREEN	LED SMD green	1
LED2	LED THD Green	1
LED3	LED THD yellow	1
LED4	LED THD red	1
R16	Resistor 100	1
R5, R6, R7, R8, R9, R10	Resistance 330	6
R4, R13, R14, R17, R19	resistance 1k	5
R15	resistance 1.2k	1
R2, R3, R11, R12, R20, R21	Resistor 4k7	6
R18	resistance 7.5k	1
R1	resistance 10k	1
C1, C2	Capacitor 12pF	2
C6, C7, C8, C9, C12	Capacitor 100nF	5
C3, C4, C11	Capacitor 10uF	3
C13, C14	Capacitor 22uF	2
-	868MHz antenna	1
SV9	8-Pin Connector	3
JP1, JP3	Jumper	2
JP1	Pin for Jumper	1
SV2	Pin headers 2X3	1
JP3-6	4-pin Connector	1
SV1, SV5	Pin headers 1X3	2
Q2, Q3	N-Channel MOSFET	2
	4-pin female patch - JST	1
	2-pin female patch - JST	6
SV7, SV8	2-pin Connector	2
J2	Li-ion Battery Charger	1
IC1	Li-ion Battery Protection IC	1
Q1	Dual N-Channel MOSFET	1
Q1	Dual N-Channel MOSFET	1
D3	Schottky Diodes	1
L2	Inductor 22uH	1
IC3	Voltage booster	1
SV6	4-pin Connector	1
JP3	2-way Jumper	1

Appendix II: List of Components for High-Voltage PCB

High Voltage PCB		
Circuit Designation	**Function**	**No.**
C1, C2, C4, C5, C6	Capacitor 10uF	5
SV2, SV3, SV4	3-pin Connector	3
R2	resistance 820k	1
X1, X2, X3 (X1, X2)	SCREW CLAMP	3
D3, D4	diode	2
T2, T3	bipolar transistor	2
K1, K2	relay switch	2
IC1	Current sensor	1
C3	Capacitor 1nF	1
T1	Voltage Sensor	2
R3	Resistor 100	1
C7	Capacitor 1u	2
R5, R6, R7,	Resistance 1k	3
R1, (R3)	resistance 10k	1
IC2	Dual Op-Amp	1
R4	Resistance 100k	1
R2	resistance 180K	1
R3	resistance 820	1
PS1	AC-DC Converter	1
RED	SMD LED	1
YELLOW	SMD LED	1
GREEN	SMD LED	1
RT1	NTC 10k resistor	1
IC2	Charger Controller	1
R9,	Resistance 110k	1
R8	Resistance 330k	1
X5	Battery Connector	1

RESEARCH OUTPUTS

Publications

L. D. Namujju, I. Mwammenywa, G. M. Kagarura, U. Hilleringmann and B. Hehenkamp, "Smart Metering and Choice Architecture in Demand-Side Management: A Power Resource-Constrained Perspective," *2024 IEEE 8th Energy Conference (ENERGYCON)*, Doha, Qatar, 2024, pp. 1-6, doi: 10.1109/ENERGYCON58629.2024.10488738.

J. S. Mwakijale, I. Mwammenywa and U. Hilleringmann, "LoRa-based Swarm Grid Implementation for Rural Electrification in Africa," *2023 IEEE PES/IAS PowerAfrica*, Marrakech, Morocco, 2023, pp. 1-4, doi: 10.1109/PowerAfrica57932.2023.10363319.

I. Mwammenywa, and U. Hilleringmann, "Analysis of Electricity Power Generation and Load Profiles in Solar PV Microgrids in Rural Villages of East Africa: Case of Mpale Village in Tanzania," in *2023 IEEE AFRICON*, Nairobi, Kenya, 2023, pp. 1-6, doi: 10.1109/AFRICON55910.2023.10293635.

I. Mwammenywa, D. Petrov, P. Holle and U. Hilleringmann, "LoRa Transceiver for Load Monitoring and Control System in Microgrids," *2022 International Conference on Engineering and Emerging Technologies (ICEET),* Kuala Lumpur, Malaysia, 2022, pp. 1-5, doi: 10.1109/ICEET56468.2022.10007274.

I. Mwammenywa, G. M. Kagarura, D. Petrov, P. Holle and U. Hilleringmann, "LoRa-based Demand-side Load Monitoring and Management System for Microgrids in Africa," *2021 International Conference on Electrical, Computer and Energy Technologies (ICECET),* Cape Town, South Africa, 2021, pp. 1-5, doi: 10.1109/ICECET52533.2021.9698506.

D. Petrov, K. Kroschewski, I. Mwammenywa, G. M. Kagarura and U. Hilleringmann, "Low-Cost NB-IoT Microgrid Power Quality Monitoring System," *2021 IEEE Sensors*, Sydney, Australia, 2021, pp. 1-4, doi: 10.1109/SENSORS47087.2021.9639641.

U. Hilleringmann, D. Petrov, I. Mwammenywa and G. M. Kagarura, "Local Power Control using Wireless Sensor System for Microgrids in Africa," *2021 IEEE AFRICON*, Arusha, Tanzania, 2021, pp. 1-5, doi: 10.1109/AFRICON51333.2021.9570970.